Supporting Information

Desymmetrization by Asymmetric Copper-Catalyzed Intramolecular C–H Insertion Reactions of α-Diazo-β-oxosulfones

Thomas A. Brouder,[†] Catherine N. Slattery,[†] Alan Ford,[†] U. B. Rao Khandavilli,[†] Eliška Skořepová,[†] Kevin S. Eccles,[†] Matteo Lusi,[‡] Simon E. Lawrence,[†] and Anita R. Maguire[*,§]

[†]School of Chemistry, Analytical and Biological Chemistry Research Facility, University College Cork, Cork T12 K8AF, Ireland

[‡]Department of Chemical & Environmental Sciences, University of Limerick, Limerick V94 T9PX, Ireland

[§]School of Chemistry and School of Pharmacy, Analytical and Biological Chemistry Research Facility, Synthesis and Solid State Pharmaceutical Centre, University College Cork, Cork T12 K8AF, Ireland

*Corresponding author e-mail: a.maguire@ucc.ie

Table of Contents

1. **Crystallographic data:** S3–S12
   - **1.1** Thermal Ellipsoid plots of compounds **29a**, **29b**, **31a**, **33a**, **33c**, **38a**, **38b**, **39a**: S3–S10
   - **1.2** Table S1: X-Ray Crystallographic Data: S11–S12
2. **HPLC data:** S13–S17
   - **2.1** Table S2: HPLC Conditions for the resolution of compounds **29**, **31**, **33**, **36**, **37**, **38** and **39**: S13–S15
   - **2.2** Representative HPLC Trace **29a** and **31a**: S16–S17
3. **Self-disproportionation of enantiomers (SDE):** S18
   - **3.1** Table S3: Self-disproportionation of enantiomers observed for **36a**: S18
4. **NMR Spectra:** (**14**–**39**) (All in $CDCl_3$): S19–S52

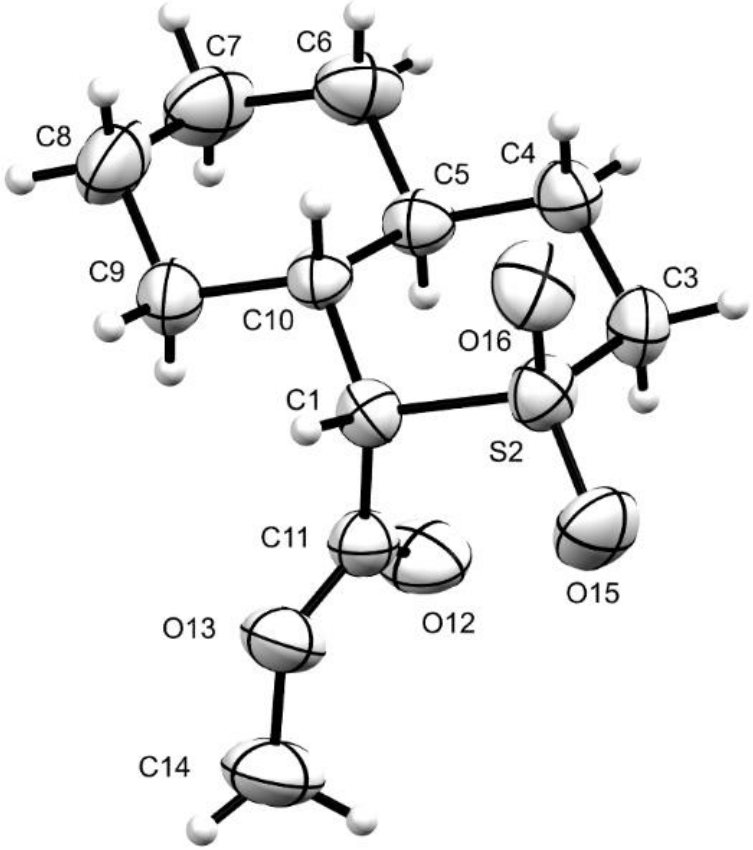

Figure S1: An ORTEP view of (1*S*,4a*S*,8a*R*)-**29a** showing the structure and relative stereochemistry. Anisotropic parameters are drawn at the 50% probability level. The single crystal of **29a** analysed was grown by slow evaporation over a number of weeks from a saturated solution of **29a** in ethanol in a small sample vial.

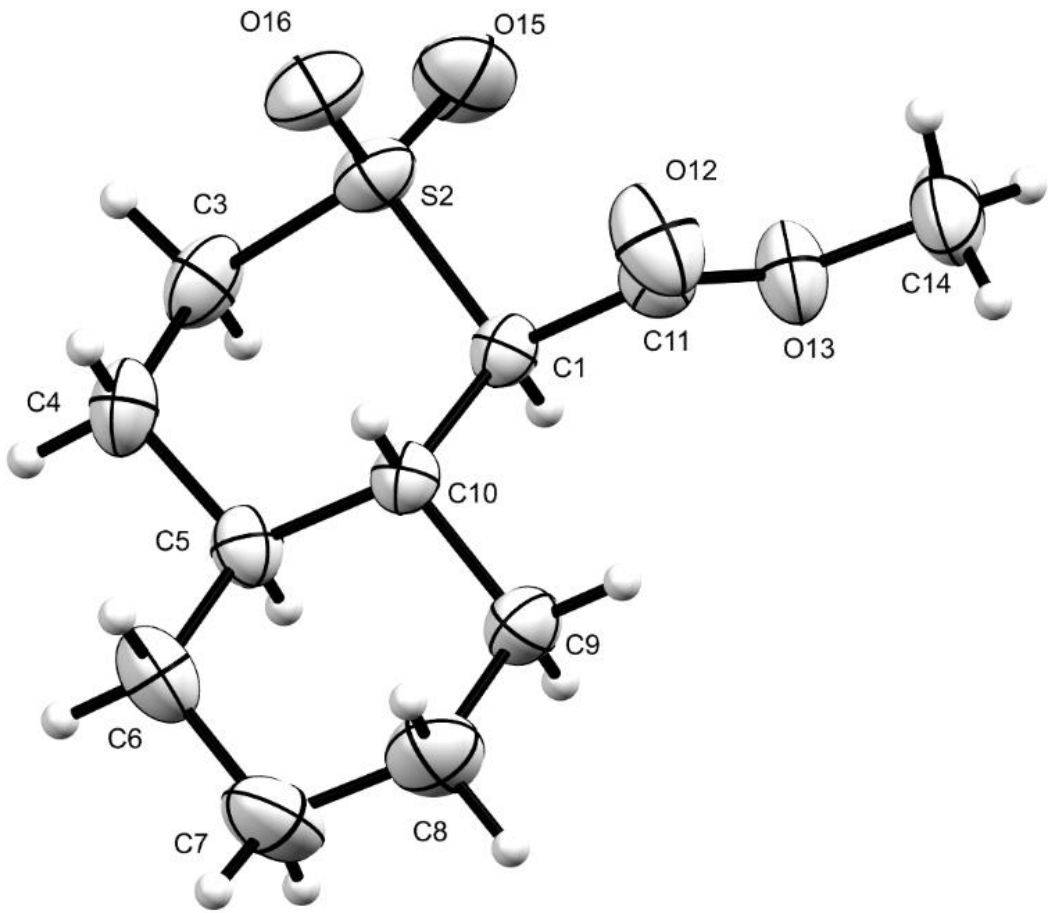

Figure S2: An ORTEP view of **29b** showing the structure and relative stereochemistry. Anisotropic parameters are drawn at the 50% probability level. The single crystal of **29b** analysed was grown by slow evaporation over a number of weeks from a saturated solution of **29b** in ethanol in a small sample vial.

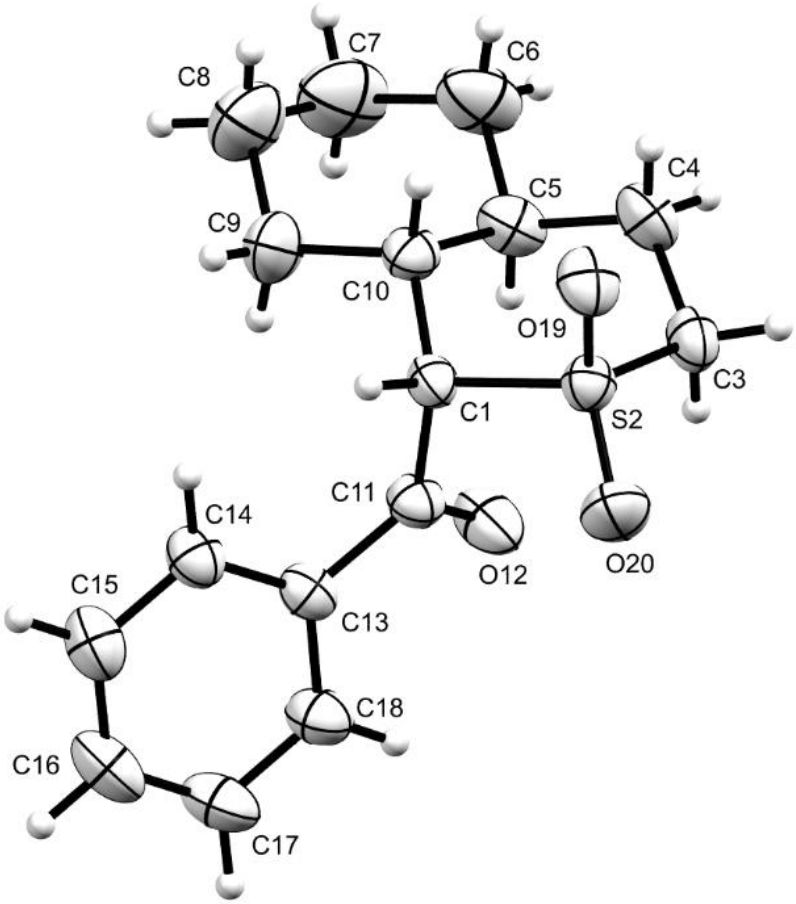

Figure S3: An ORTEP view of one of the crystallographically unique molecules in (1*S*,4a*S*,8a*R*)-**31a** showing the structure and relative stereochemistry. Anisotropic parameters are drawn at the 50% probability level. The single crystal of **31a** analysed was grown by slow evaporation over a number of weeks from a saturated solution of **31a** in ethanol in a small sample vial.

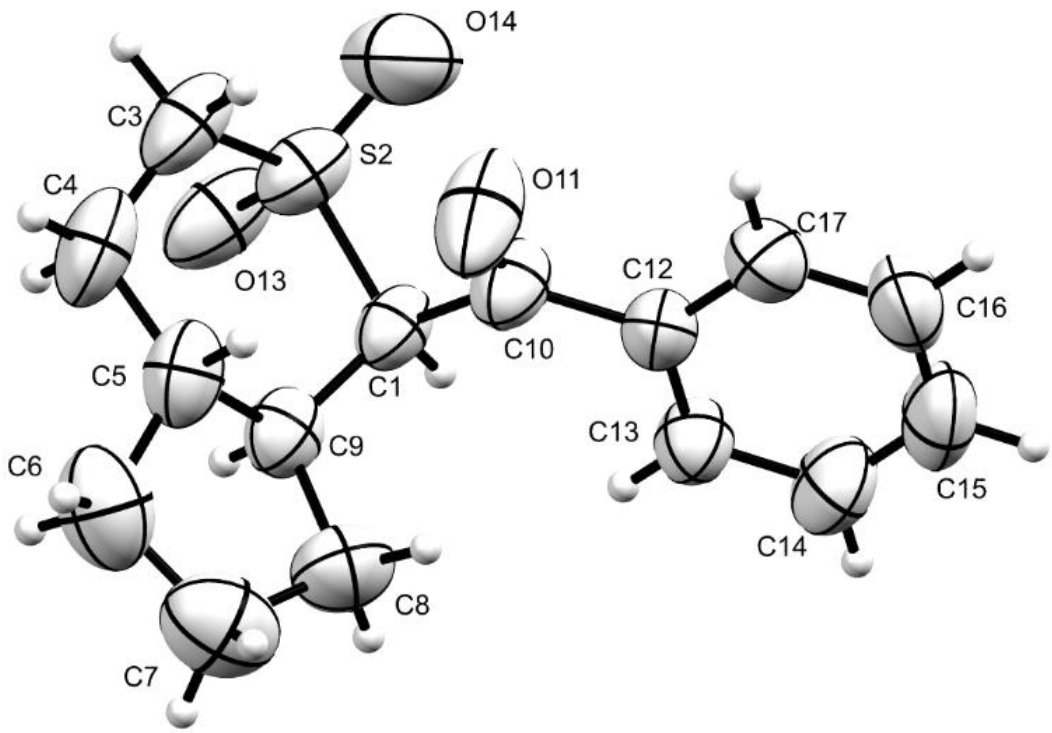

Figure S4: An ORTEP view of (1*R*,4a*R*,7a*S*)-**33a** showing the structure and relative stereochemistry. Anisotropic parameters are drawn at the 50% probability level. The single crystal of **33a** analysed was grown by slow evaporation over a number of weeks from a saturated solution of **33a** in ethanol in a small sample vial.

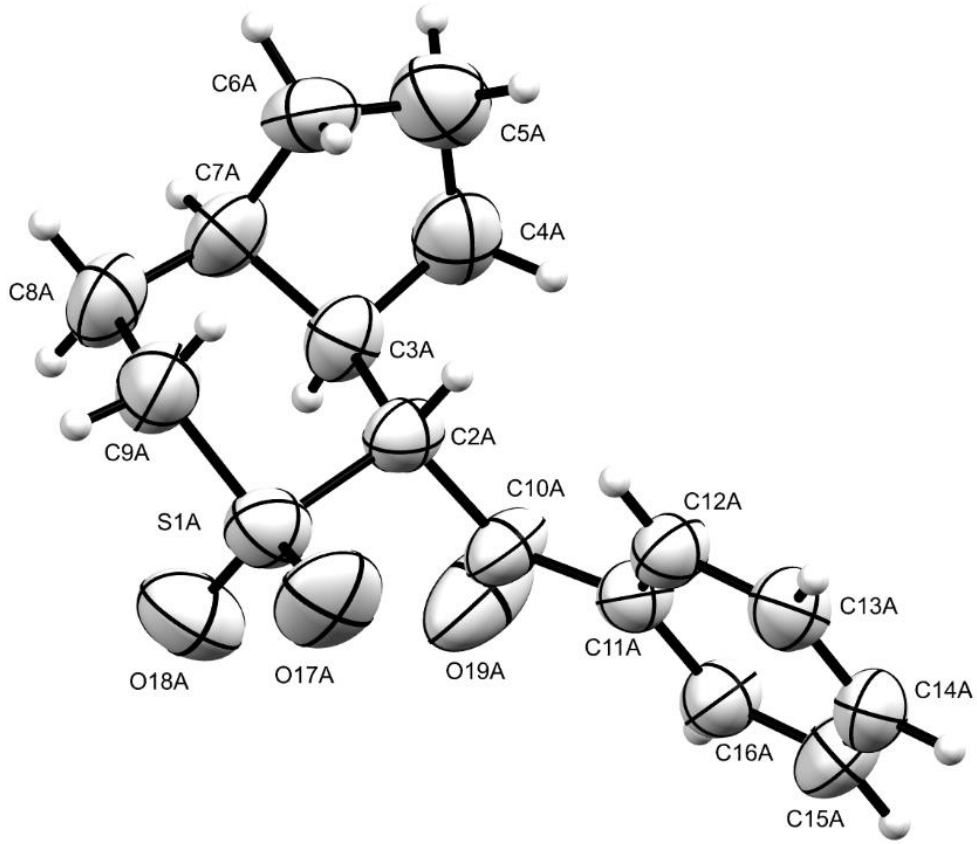

Figure S5: An ORTEP view of one of the crystallographically unique molecules in **33c** showing the structure and relative stereochemistry. Anisotropic parameters are drawn at the 50% probability level. The single crystal of **33c** analysed was grown by slow evaporation over a number of weeks from a saturated solution of **33c** in 2-propanol in a small sample vial.

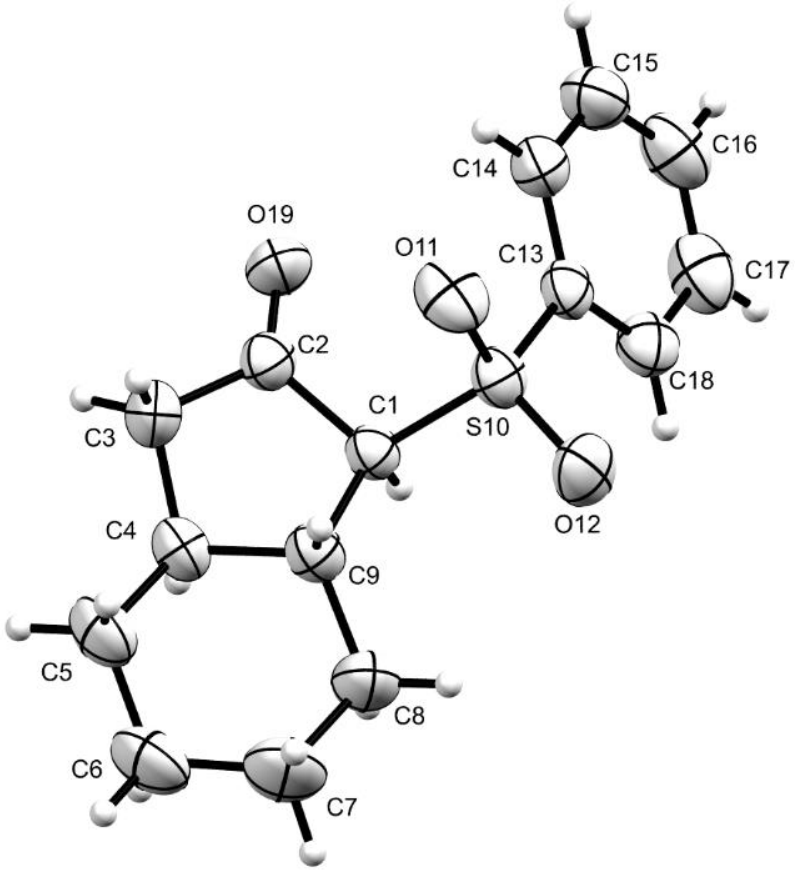

Figure S6: An ORTEP view of (1*S*,3a*S*,7a*R*)-**38a** showing the structure and relative stereochemistry. Anisotropic parameters are drawn at the 50% probability level. The single crystal of **38a** analysed was grown by slow evaporation over a number of weeks from a saturated solution of **38a** in ethanol in a small sample vial.

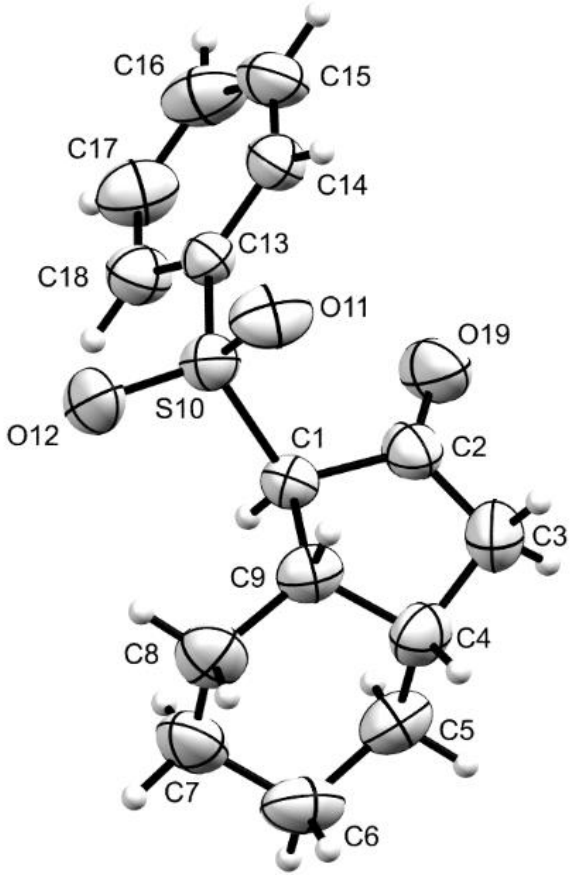

Figure S7: An ORTEP view of **38b** showing the structure and relative stereochemistry. Anisotropic parameters are drawn at the 50% probability level. The single crystal of **38b** analysed was grown by slow evaporation over a number of weeks from a saturated solution of **38b** in 2-propanol in a small sample vial.

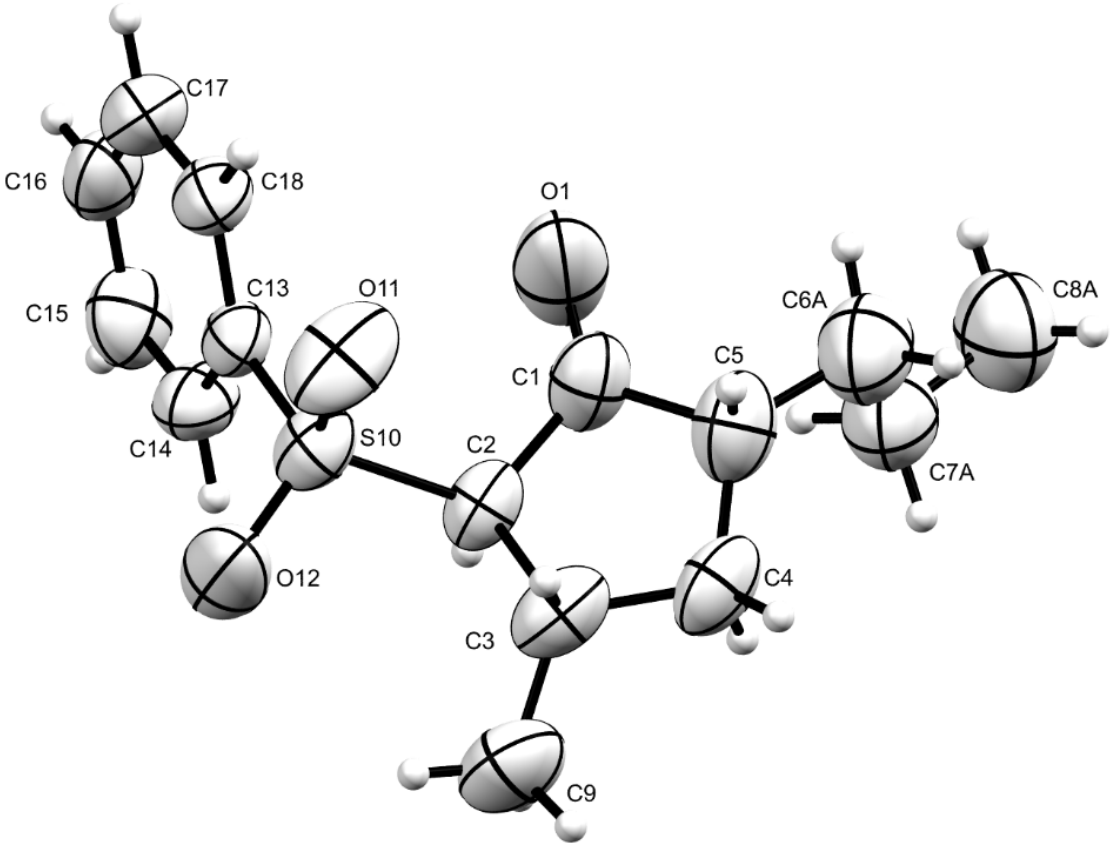

Figure S8: An ORTEP view of (2*R*,3*S*,5*R*)-**39a** showing the structure and relative stereochemistry, with the minor disordered propyl chain omitted for clarity. Anisotropic parameters are drawn at the 50% probability level. The single crystal of **39b** analysed was grown by slow evaporation over a number of weeks from a saturated solution of **39b** in ethanol in a small sample vial.

Table S1: Crystallographic Data

Compound No	**29a**	**29b**	**31a**	**33a**	**33c**
CCDC No.	1884349	1884356	1884355	1884353	1884351
Crystal System	Orthorhombic	Orthorhombic	Monoclinic	Hexagonal	Monoclinic
Space Group, Z	$P2_12_12_1$, 4	*Pbcn*, 8	$P2_1$, 6	$P6_5$, 6	$P2_1$, 4
Empirical Formula	$C_{11}H_{18}O_4S$	$C_{11}H_{18}O_4S$	$C_{16}H_{20}O_3S$	$C_{15}H_{18}O_3S$	$C_{15}H_{18}O_3S$
Formula Weight	246.31	246.31	292.38	278.35	278.35
Crystal size (mm)	0.33 x 0.30 x 0.22	0.30 x 0.25 x 0.10	0.45 x 0.33 x 0.23	0.60 x 0.40 x 0.21	0.20 x 0.01 x 0.01
Wavelength, λ (Å)	1.54178	1.54178	1.54178	1.54180	1.54178
Unit cell dimensions (Å)	a = 7.6248 (2) b = 10.4058 (3) c = 15.7850 (4)	a = 17.0380 (3) b = 10.0025 (2) c = 14.3181 (3)	a = 5.7060 (2) b = 26.0065 (9) c = 15.1667 (5) β = 96.6910(10)°	a = 18.398 (2) b = 18.398 (2) c = 7.8925 (10)	a =11.3456 (10) b = 5.7530 (5) c = 21.3395 (17) β = 90.003(6)°
Volume, V ($Å^3$)	1252.42(6)	2440.13(8)	2235.30(13)	2313.6(6)	1392.9(2)
Temperature (K)	296	296	296	296	296
Calculated Density, ($g \cdot cm^{-3}$)	1.306	1.341	1.303	1.199	1.327
μ (mm^{-1})	2.295	2.356	1.968	1.878	2.08
F(000)	528	1056	936	888	592
θ range	5.09 - 67.14	5.99 - 66.82	3.39 - 67.11	2.77 - 66.94	2.07 - 65.11
No. unique reflections	2067	2069	7265	2579	3761
No. observed reflections	2053	2024	7225	2475	2416
R_1 [I>2σ(I)]	0.0272	0.0348	0.0259	0.0348	0.0743
wR_2	0.0720	0.0967	0.0685	0.0952	0.2083
S (Goof)	1.078	1.051	1.077	1.037	1.018
Flack	0.075(8)	-	0.045(3)	0.100(10)	0.10(5)

Table S1: Crystallographic Data (cont.)

Compound No	**38a**	**38b**	**39a**
CCDC No.	1884350	1884354	1884352
Crystal System	Orthorhombic	Monoclinic	Orthorhombic
Space Group, Z	$P2_12_12_1$, 4	$P2_1/n$, 4	$P2_12_12_1$, 4
Empirical Formula	$C_{15}H_{18}O_3S$	$C_{15}H_{18}O_3S$	$C_{15}H_{20}O_3S$
Formula Weight	278.35	278.35	280.37
Crystal size (mm)	0.24 x 0.22 x 0.20	0.63 x 0.34 x 0.09	0.37 x 0.09 x 0.04
Wavelength, λ (Å)	1.54178	1.54178	0.71073
Unit cell dimensions (Å)	a = 5.7539 (2) b =12.6374 (3) c = 19.4407 (5)	a = 5.8882 (11) b =16.506 (3) c = 14.387 (3) β = 91.050(5)°	a = 5.7169(5) b = 15.0913(14) c = 17.6302(17)
Volume, V ($Å^3$)	1413.62(7)	1398.0(4)	1521.1(2)
Temperature (K)	296	296	296
Calculated Density, ($g \cdot cm^{-3}$)	1.308	1.322	1.224
μ (mm^{-1})	2.049	2.072	0.214
F(000)	592	592	600
θ range	7.68 - 67.09	5.36 - 67.34	1.78 - 26.43
No. unique reflections	2398	2386	3117
No. observed reflections	2385	2330	2295
R_1 [I>2σ(I)]	0.0237	0.0352	0.0486
wR_2	0.0649	0.0934	0.1404
S (Goof)	1.079	1.045	1.093
Flack	0.054(4)	-	0.02(4)

Table S2: HPLC Data

Compound	Compound Number	Column	λ max (cm^{-1})	Mobile Phase (Hexane: IPA)	Temp (°C)	Flow Rate (mL/min)	Retention Time	
							Enantiomer	Min
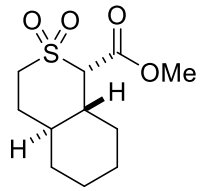	**29a**	Phenomenex Lux® 3μm Amylose-1	216	90 : 10	25	1.0	(−)-(1*R*, 4a*R*, 8a*S*)	11
							(+)-(1*S*, 4a*S*, 8a*R*)	14
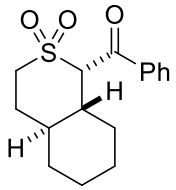	**31a**	Phenomenex Lux® 3μm Amylose-1	251	90 : 10	25	1.0	(−)-(1*R*, 4a*R*, 8a*S*)	16
							(+)-(1*S*, 4a*S*, 8a*R*)	26
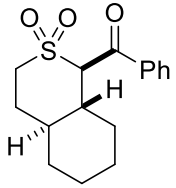	**31b**	Phenomenex Lux® 3μm Amylose-1	251	90 : 10	25	1.0	(+)	22
							(–)	33
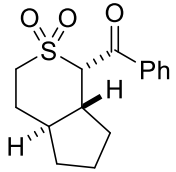	**33a**	Phenomenex Lux® 3μm Amylose-1	249.8	90 : 10	25	1.0	(−)-(1*R*, 4a*R*, 7a*S*)	20
							(+)-(1*S*, 4a*S*, 7a*R*)	25
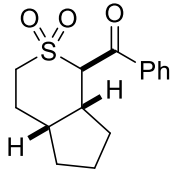	**33c**	Phenomenex Lux® 3μm Amylose-1	249.8	90 : 10	25	1.0	(−)	19
							(+)	22

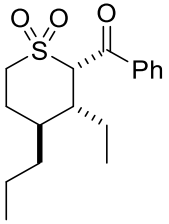	**36a**	Phenomenex Lux® 3μm Amylose-1	251	90 : 10	25	1.0	(−)-(2*R*, 3*S*, 4*R*)	10
							(+)-(2*S*, 3*R*, 4*S*)	14
		Chiralpak® AS-H	252.2	90 : 10	25	1.0	(+)-(2*S*, 3*R*, 4*S*)	12
							(−)-(2*R*, 3*S*, 4*R*)	14
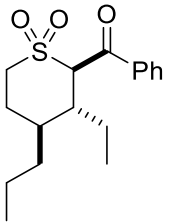	**36b**	Phenomenex Lux® 3μm Amylose-1	251	90 : 10	25	1.0	(+)	14
							(−)	16
		Chiralpak® AS-H	251	90 : 10	25	1.0	(−)	22
							(+)	37
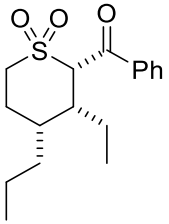	**36d**	Phenomenex Lux® 3μm Amylose-1	248.6	90 : 10	25	1.0	Not Confirmed	10
							Not Confirmed	12
		Chiralpak® AS-H	248.6	90 : 10	25	1.0	Not Confirmed	16
							Not Confirmed	26
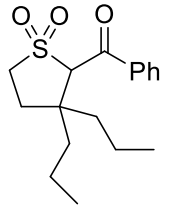	**37**	Phenomenex Lux® 3μm Amylose-1	249.8	90 : 10	25	1.0	(−)	9
							(+)	10
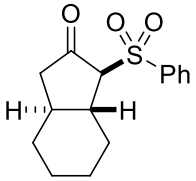	**38a**	Phenomenex Lux® 3μm Amylose-1	218	90 : 10	25	1.0	(−)-(1*R*,3a*R*,7a*S*)	21
							(+)-(1*S*,3a*S*,7a*R*)	26

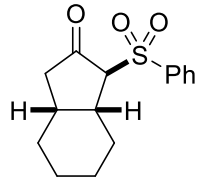	**38b**	Phenomenex Lux® 3μm Amylose-1	218	90 : 10	25	1.0	(+)	16
							(−)	21
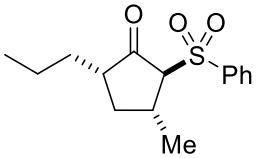	**39a**	Chiralcel® OJ-H	222	*gradient* **0 min:** 99.7 : 0.3 **340 min:** 98 : 2	25	0.5	(2*R*, 3*S*, 5*R*)	140
							(2*S*, 3*R*, 5*S*)	183
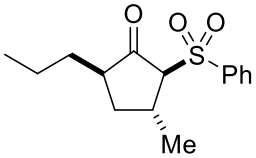	**39b**	Chiralcel® OJ-H	222	*gradient* **0 min:** 99.7 : 0.3 **100 min:** 99.7 : 0.3 **340 min:** 98 : 2	25	0.5	Not Confirmed	220
							Not Confirmed	232

Representative HPLC trace of 29a

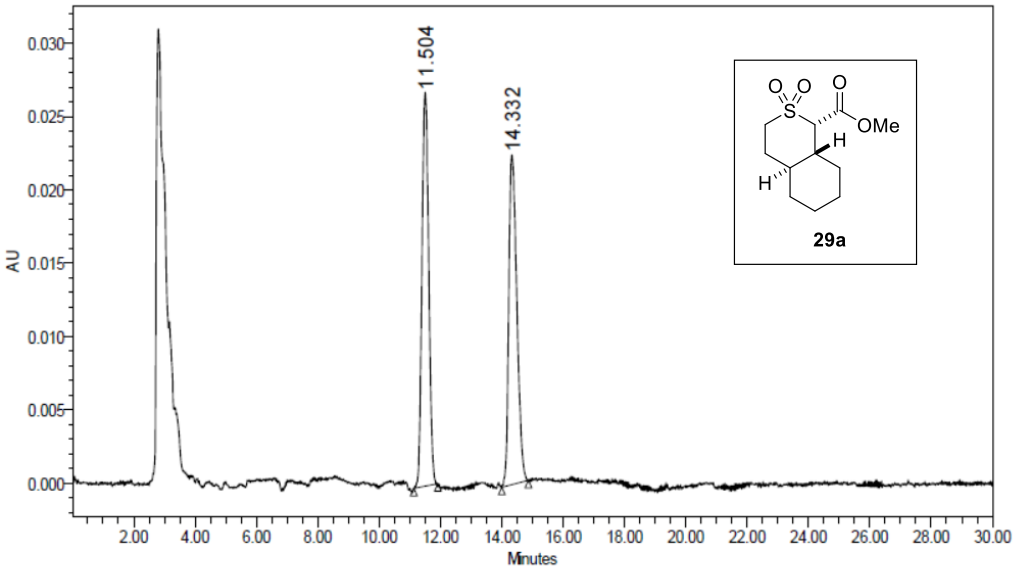

	RT	Area	% Area	Height
1	11.504	410618	50.00	26882
2	14.332	410682	50.00	22477

Figure S9: HPLC trace of 29a – racemic sample – 0% ee

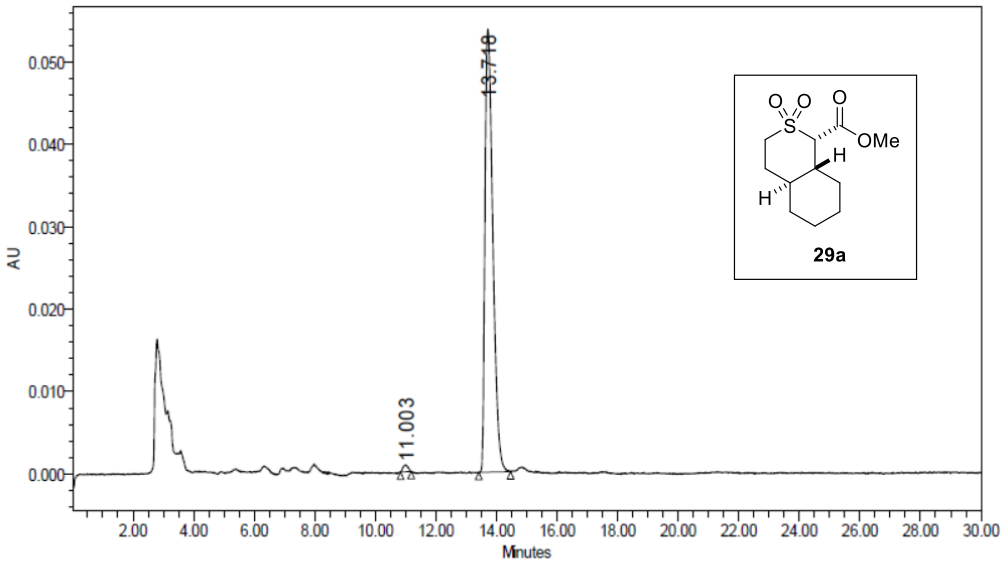

	RT	Area	% Area	Height
1	11.003	9617	0.98	818
2	13.718	972123	99.02	53787

Figure S10: HPLC trace of 29a – $CuCl_2$/NaBARF/(4R)-Ph – 98% ee

Representative HPLC trace of 31a

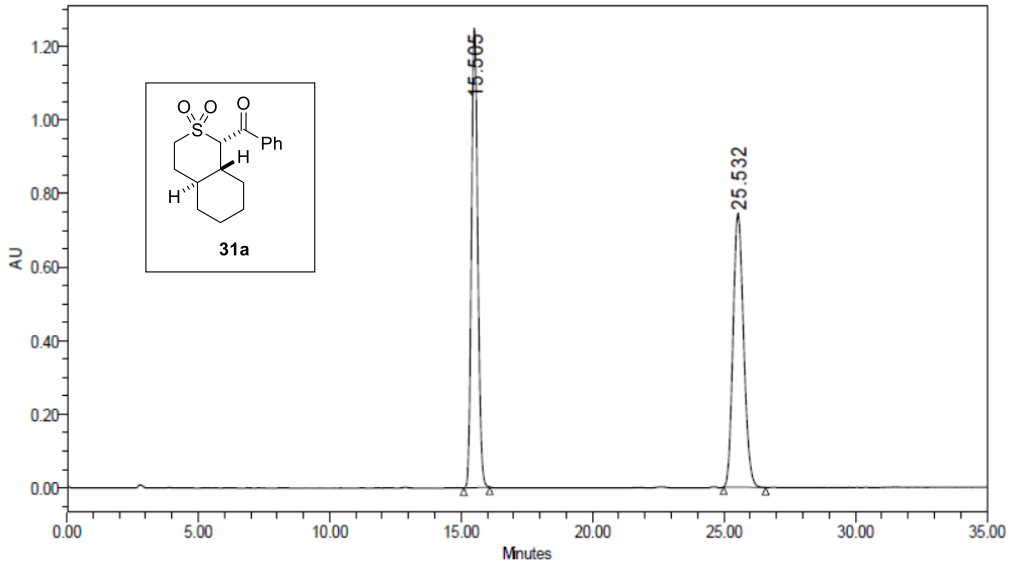

	RT	Area	% Area	Height
1	15.505	20798805	49.99	1250168
2	25.532	20804213	50.01	743881

Figure S11: HPLC trace of 31a – racemic sample – 0% ee

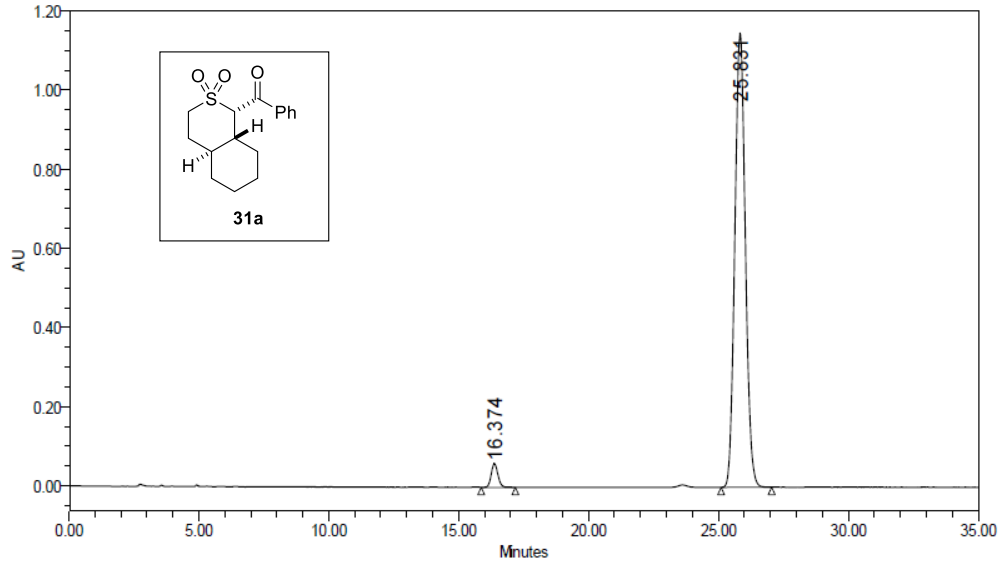

	RT	Area	% Area	Height
1	16.374	1066046	3.21	59724
2	25.831	32170631	96.79	1147925

Figure S12: HPLC trace of 31a – $CuCl_2$/NaBARF/(4R)-Ph – 94% ee

Table S3: Self-disproportionation of enantiomers (SDE) observed for 36a

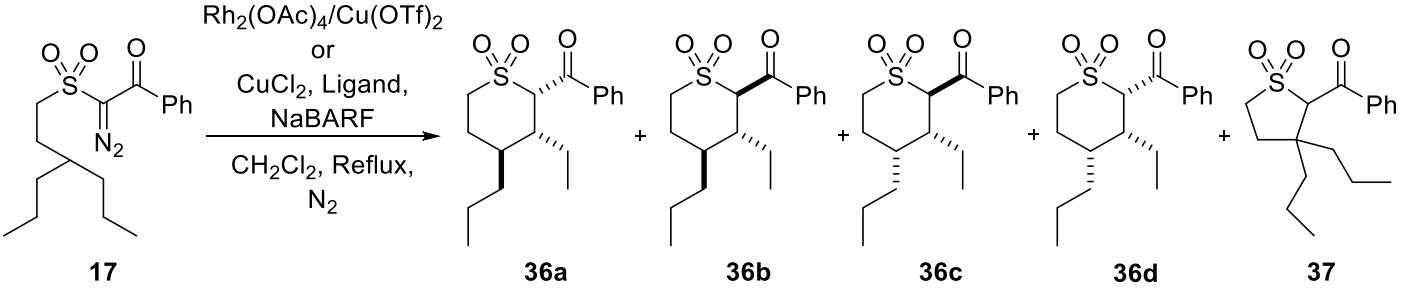

Entry	Ligand	Time (h)	36a : 36b : 36c : 36d : 37[a]	Fr 1: First 7 to 9 15 ml test tubes of 36a		Fr 2: Last 8 to 10 15ml test tubes of 36a		36a weighted average ee % [d]
				ee % [b]	Mass (mg) [c]	ee % [b]	Mass (mg) [c]	
1 [e]	**L1**	14	1 : 0.39 : 0.34 : 1.08 : 1.32	91	18	83	6	90
2 [f]	**L3**	5	1 : 0.61 : 0.43 : 1.17 : 1.36	89	9	83	6	87
3 [g]	**L4**	18	1 : 0.72 : 0.23 : 2.27 : 1.13	56	5	52	5	54
4 [h]	**L5**	62	1 : 0.57 : 0.60 : 2.15 : 1.94	84	6	73	3	80

[a]Ratios of products were calculated from signals in the crude ^{1}H NMR spectra. [b]The enantiomeric excess was measured by chiral phase HPLC analysis. [c]Isolated weight after chromatography. [d]The weighted average ee % for **36a** were calculated from the addition of the two isolated fractions enantiomeric excess values altered based on the contributing weight percentage of each fraction to the overall sample weight. [e]Data from Table 5, entry 3.[f]Data from Table 5, entry 5. [g]Data from Table 5, entry 6. [h]Data from Table 5, entry 7.

(Iodomethyl)cyclohexane (24)

^{1}H (300 MHz, $CDCl_3$)

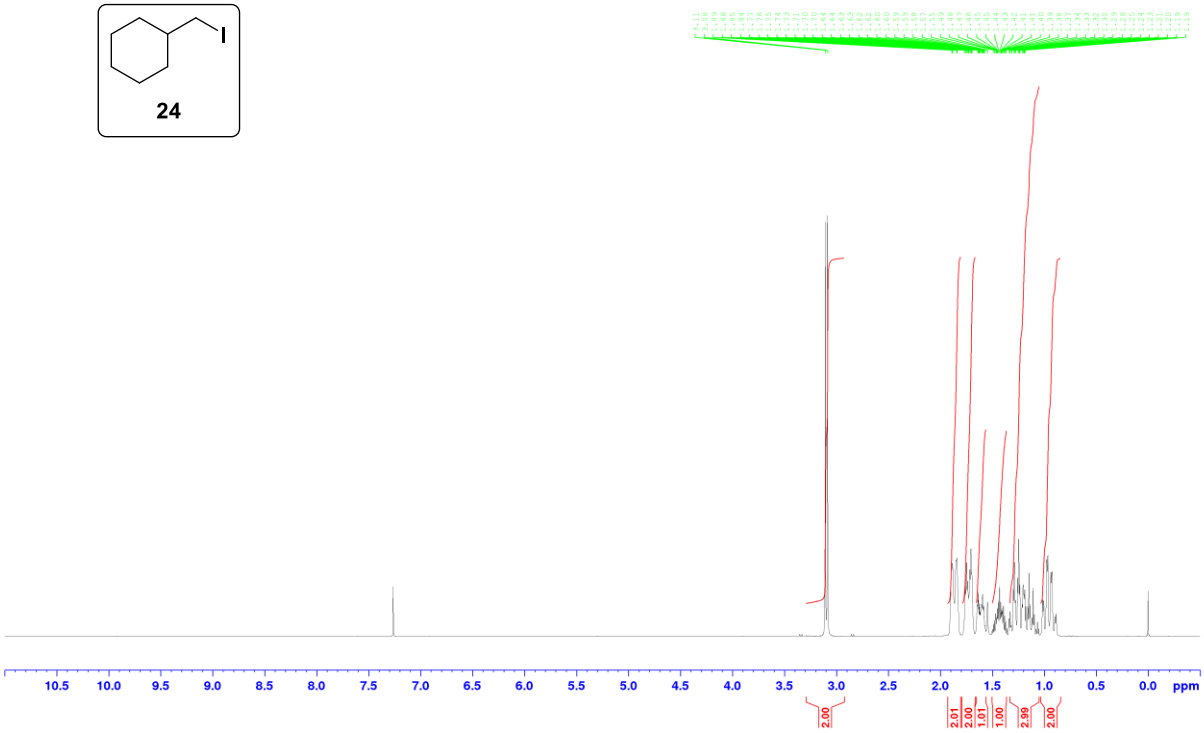

^{13}C (75.5 MHz, $CDCl_3$)

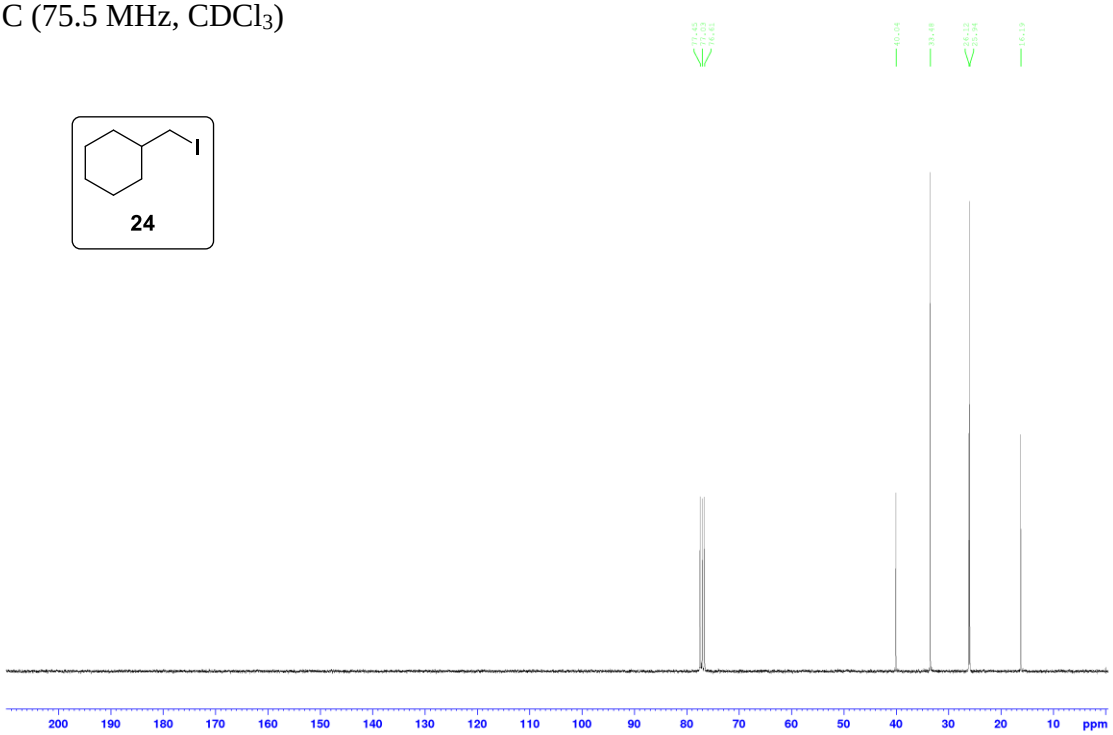

(Iodomethyl)cylopentane 25

^{1}H (300 MHz, $CDCl_3$)

25

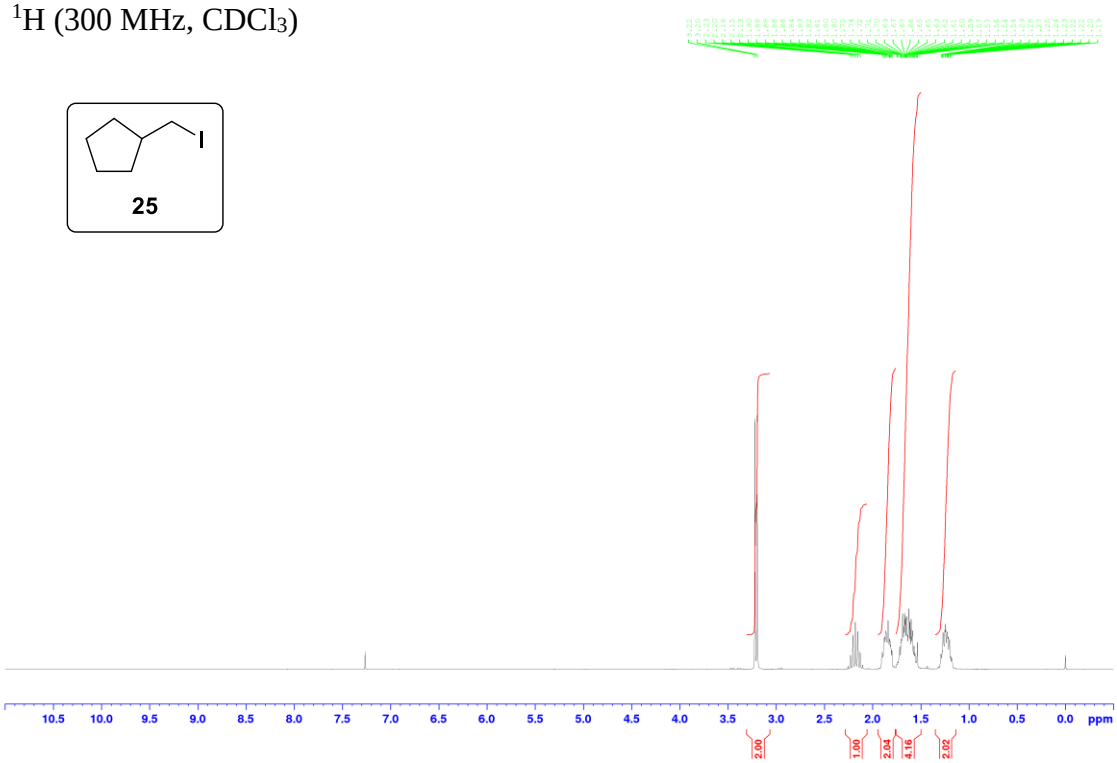

^{13}C (75.5 MHz, $CDCl_3$)

25

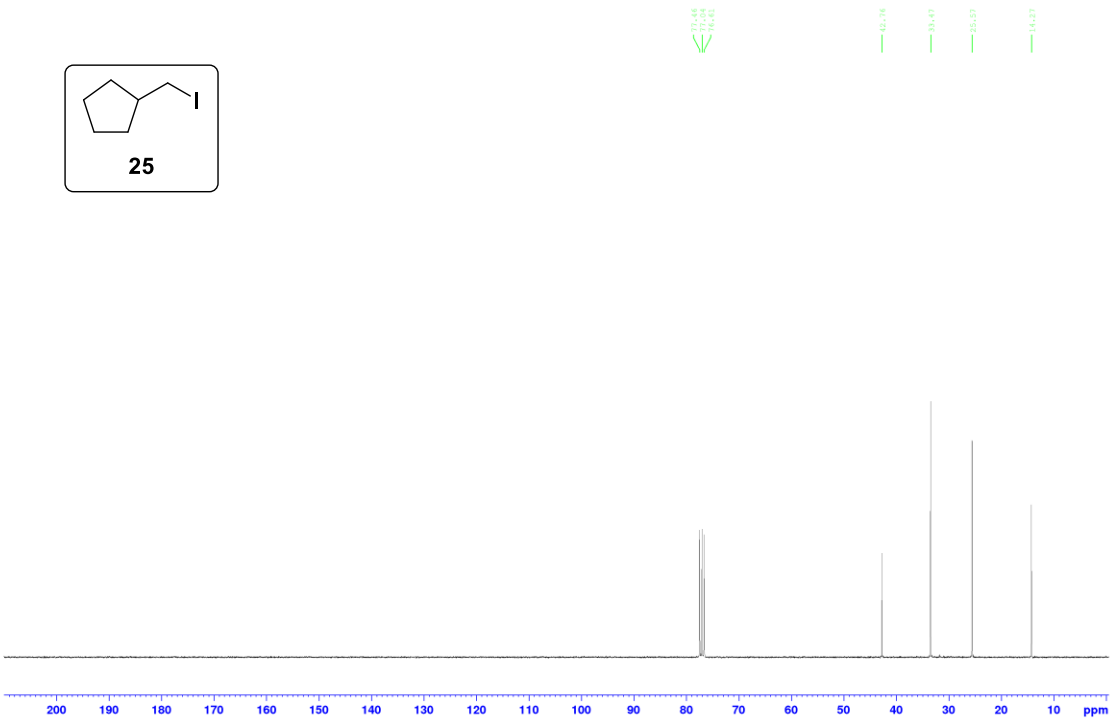

4-(Iodomethyl)heptane (26)

^{1}H (300 MHz, $CDCl_3$)

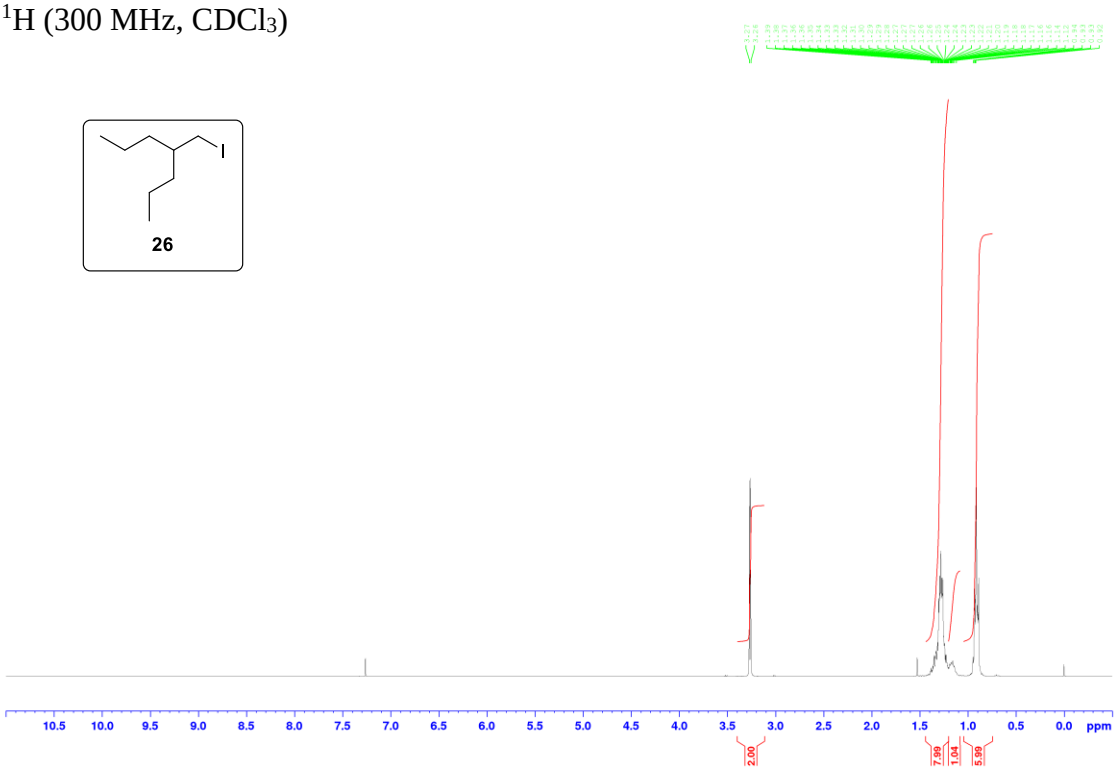

^{13}C (75.5 MHz, $CDCl_3$)

Methyl 2-((2-cyclohexylethyl)sulfonyl)acetate (20)

^{1}H (300 MHz, $CDCl_3$)

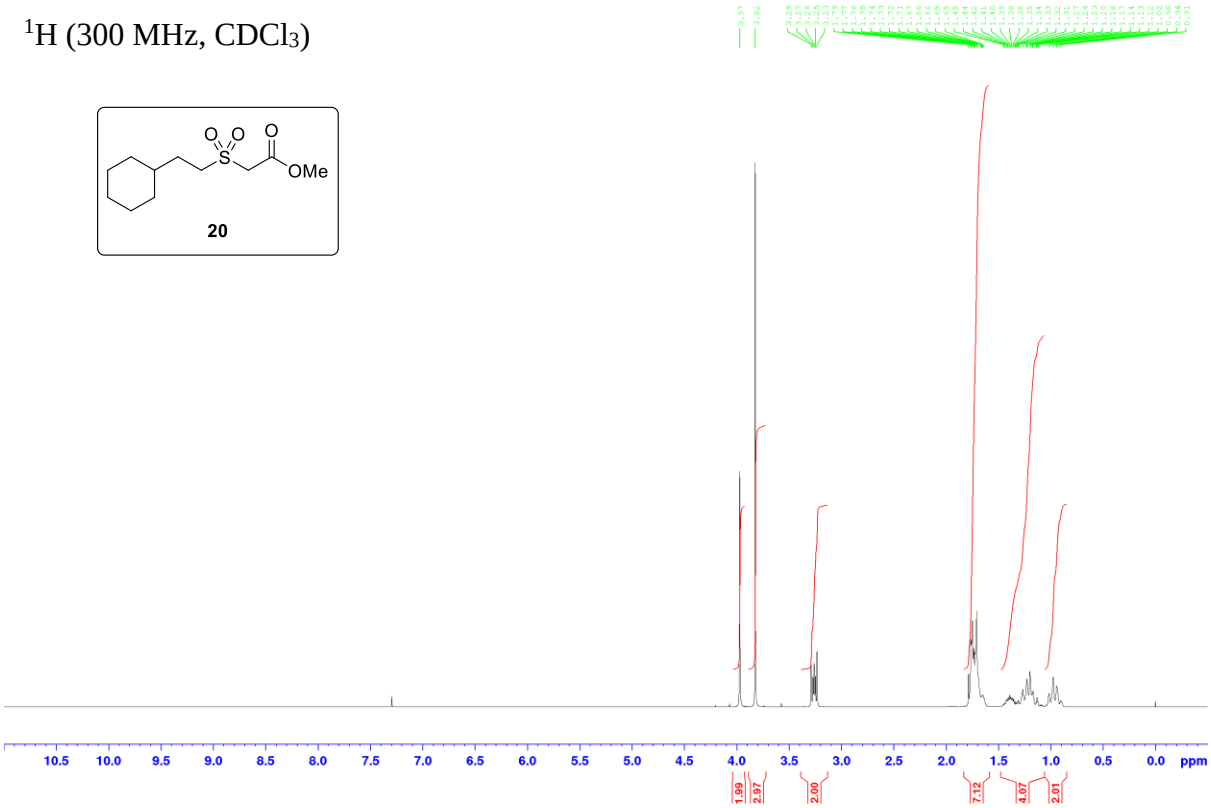

^{13}C (75.5 MHz, $CDCl_3$)

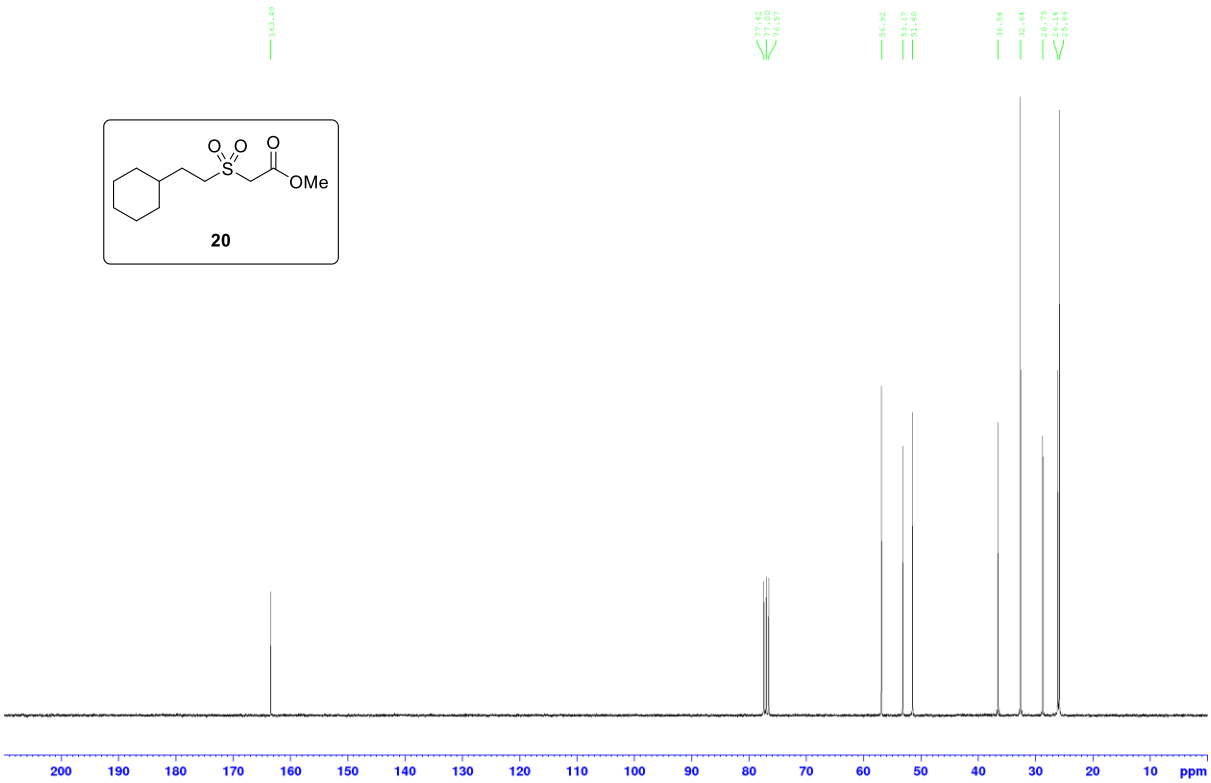

2-((2-Cyclohexylethyl)sulfonyl)-1-acetophenone (21)

^{1}H (300 MHz, $CDCl_3$)

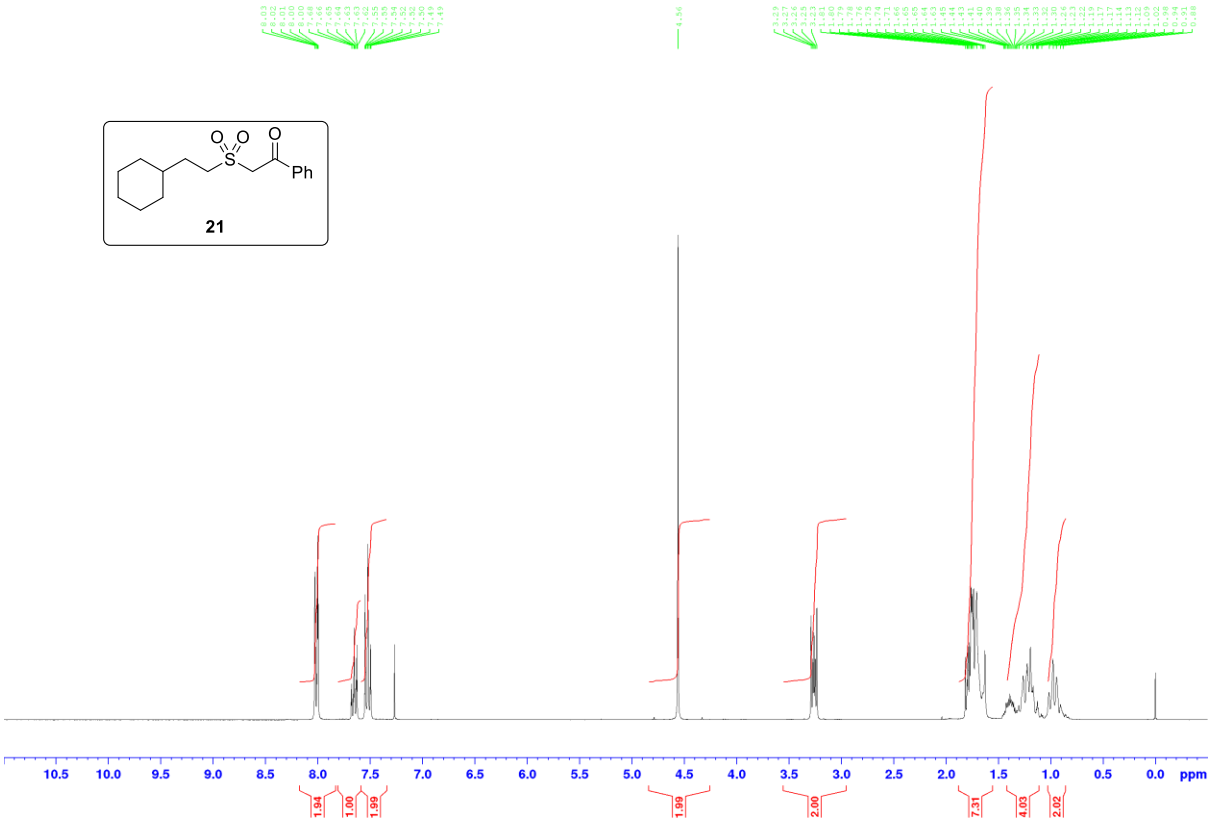

^{13}C (75.5 MHz, $CDCl_3$)

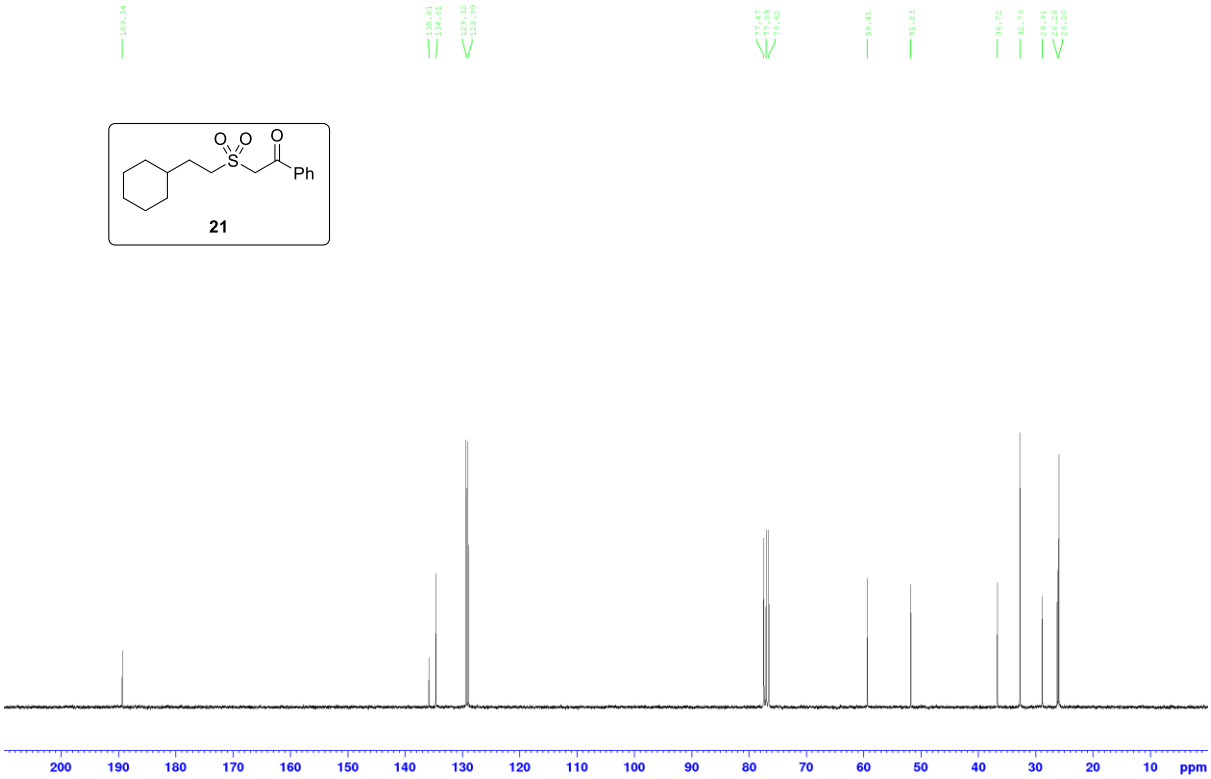

2-((2-Cyclopentylethyl)sulfonyl)-1-acetophenone (22)

^{1}H (300 MHz, $CDCl_3$)

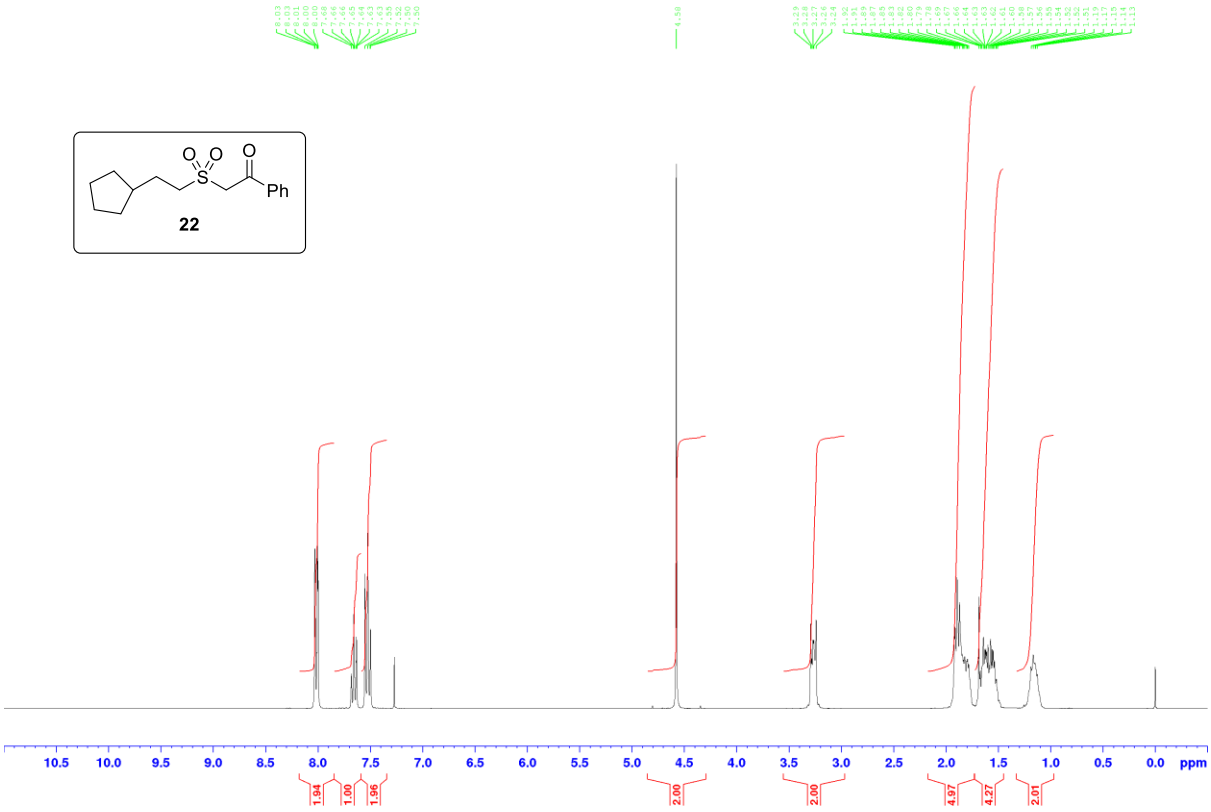

^{13}C (75.5 MHz, $CDCl_3$)

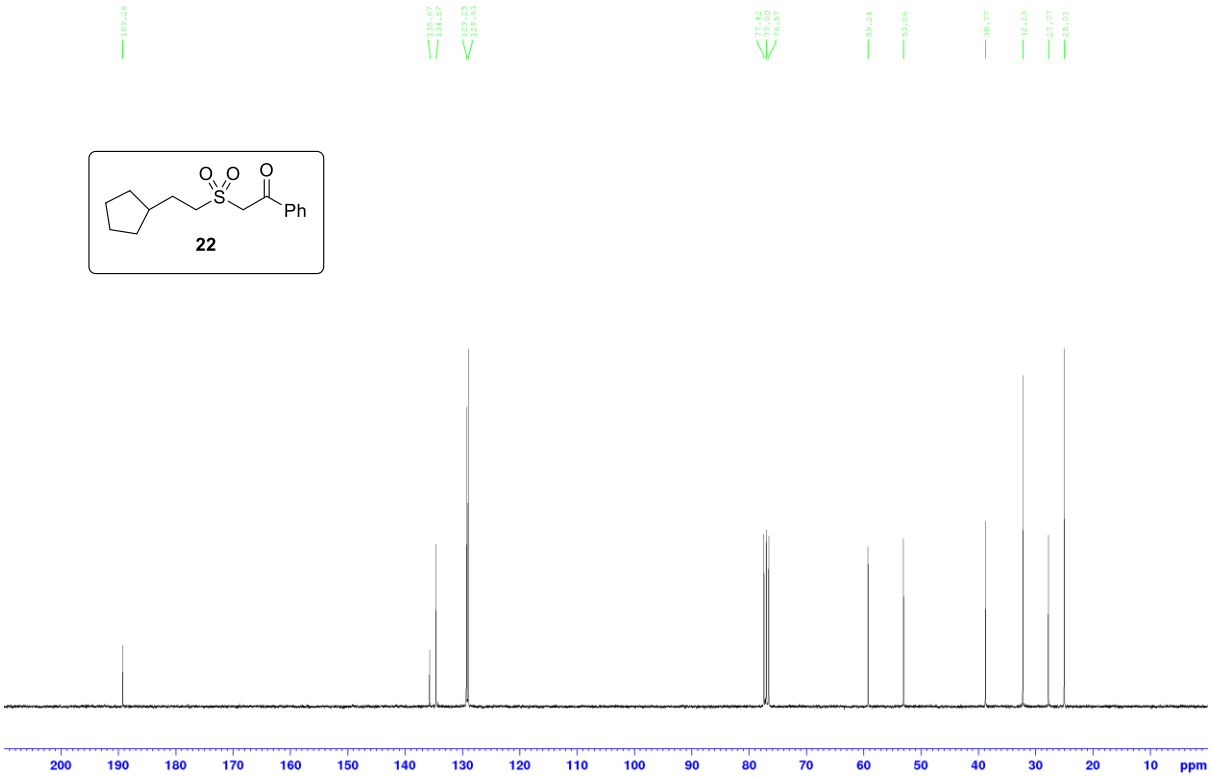

2-((3-Propylhexyl)sulfonyl)-1-acetophenone (23)

^{1}H (75.5 MHz, $CDCl_3$)

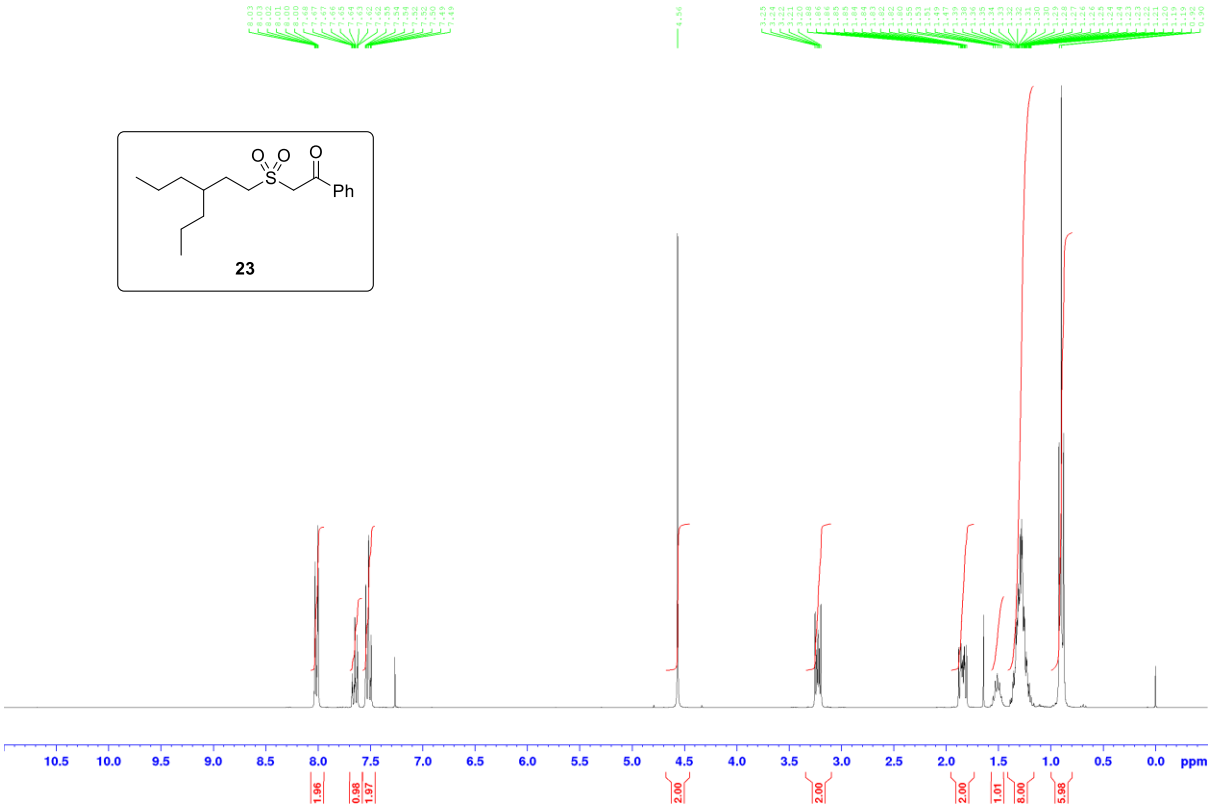

^{13}C (75.5 MHz, $CDCl_3$)

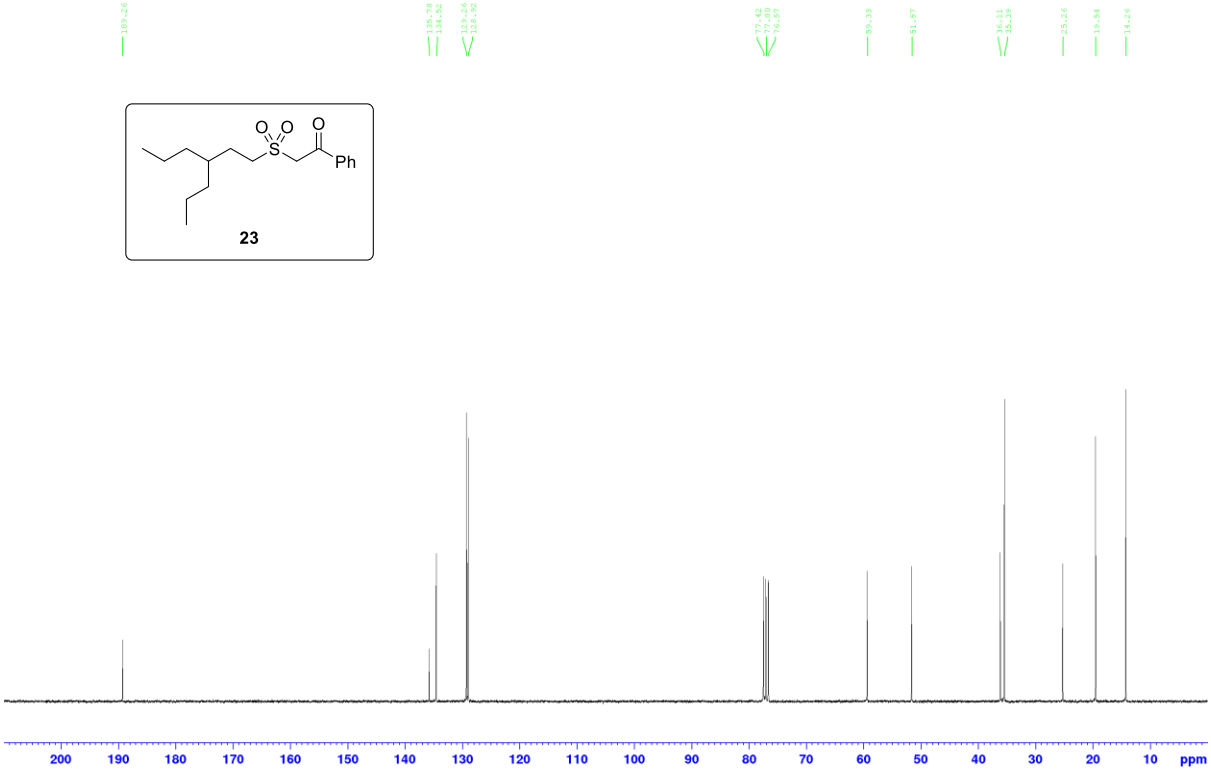

1-Cyclohexyl-3-(phenylsulfonyl)propane-2-one (27)

^{1}H (300 MHz, $CDCl_3$)

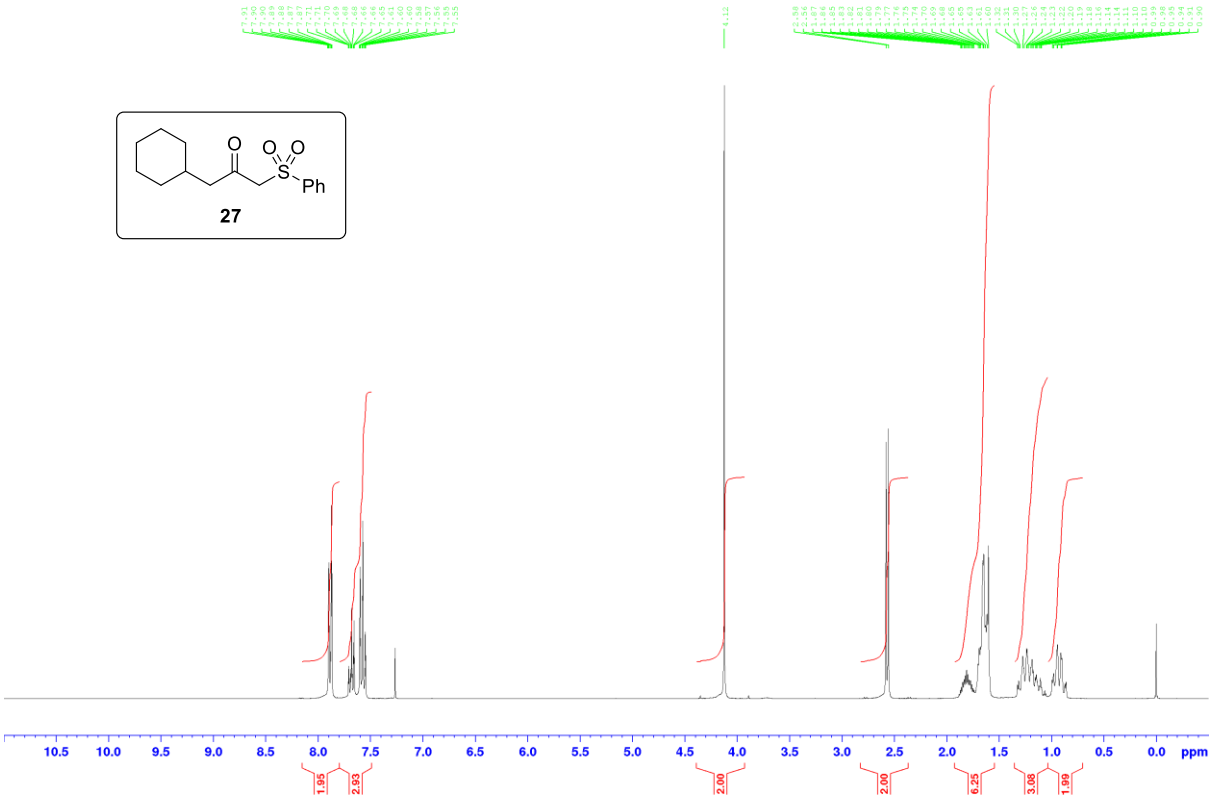

^{13}C (75.5 MHz, $CDCl_3$)

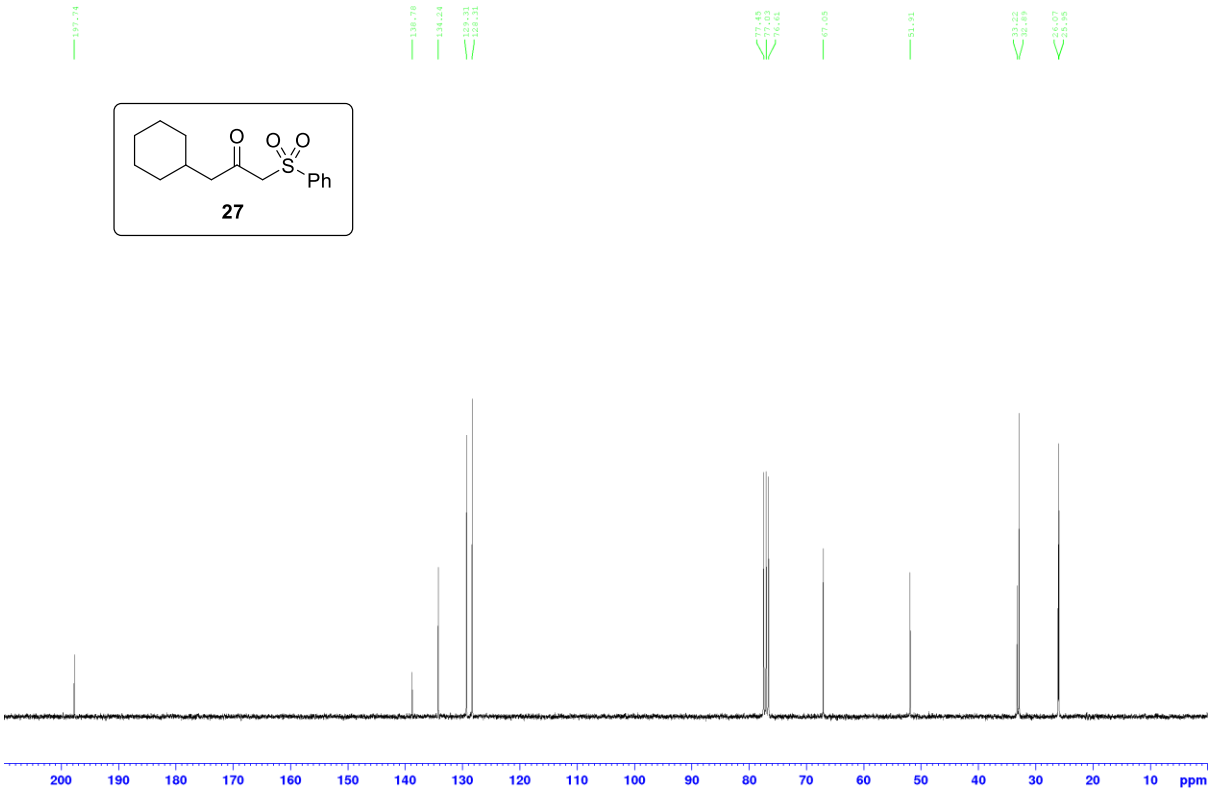

1-(Phenylsulfonyl)-3-propylhexane-2-one (28)

^{1}H (400 MHz, $CDCl_3$)

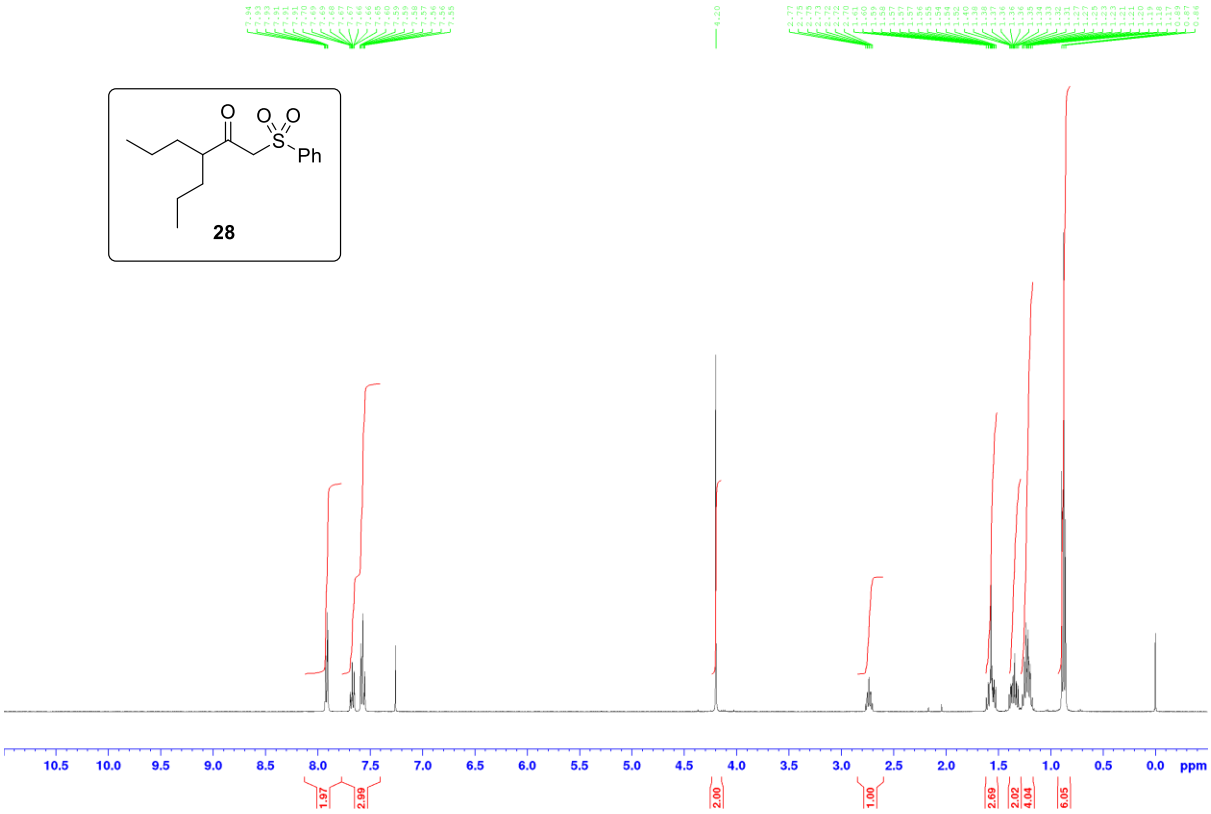

^{13}C (75.5 MHz, $CDCl_3$)

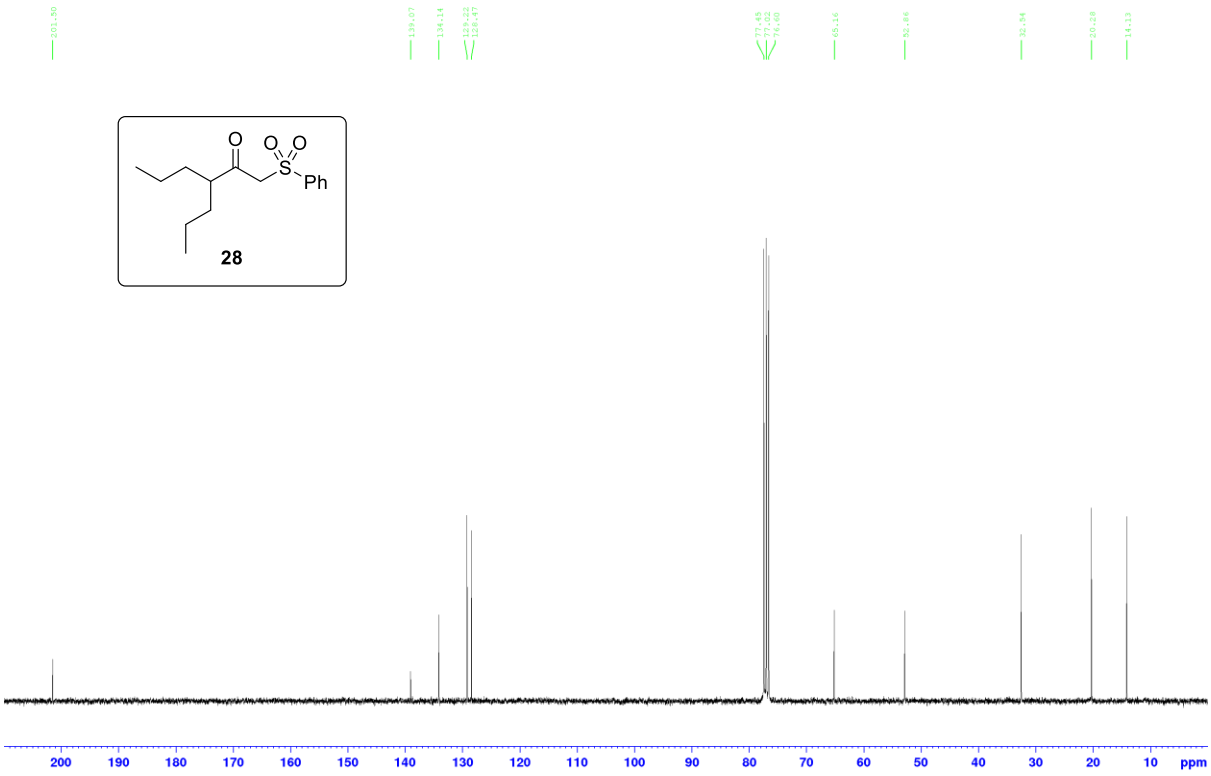

Methyl 2-((2-cyclohexylethyl)sulfonyl)-2-diazoacetate (14)

^{1}H (300 MHz, $CDCl_3$)

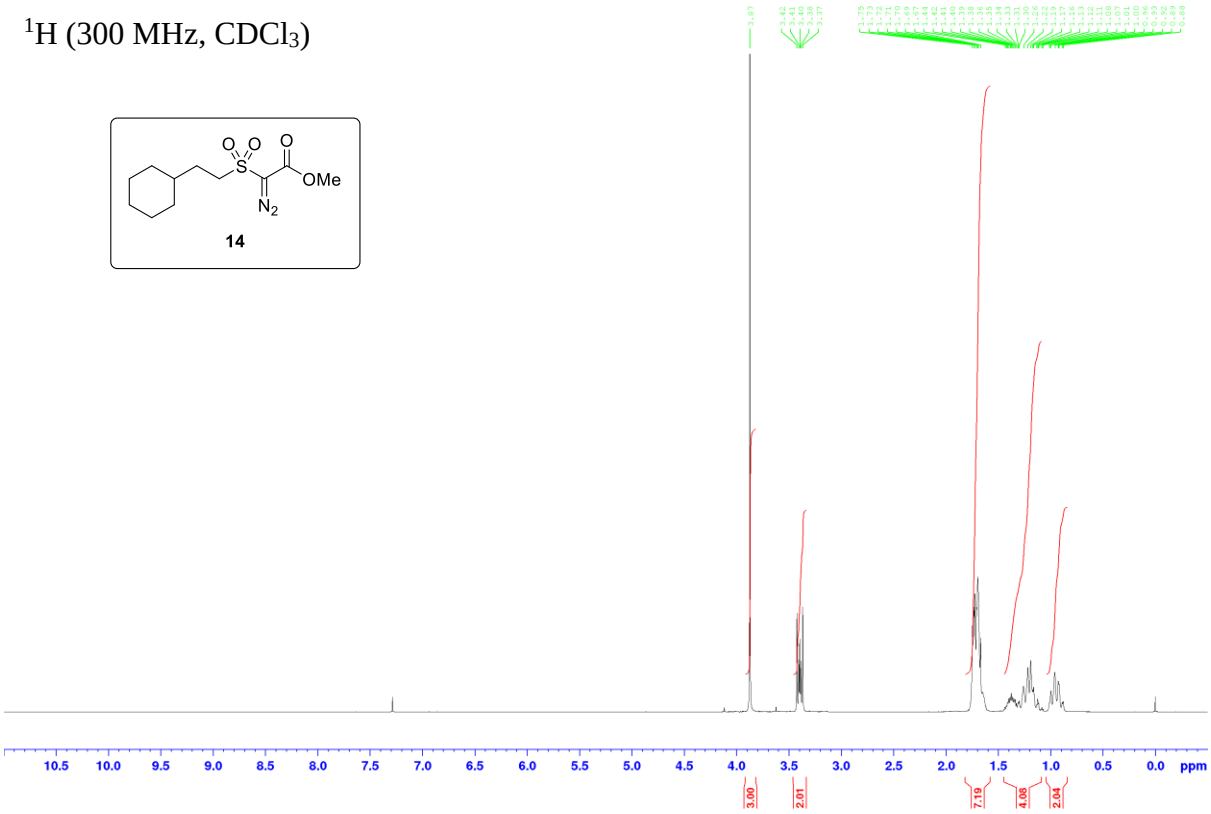

^{13}C (75.5 MHz, $CDCl_3$)

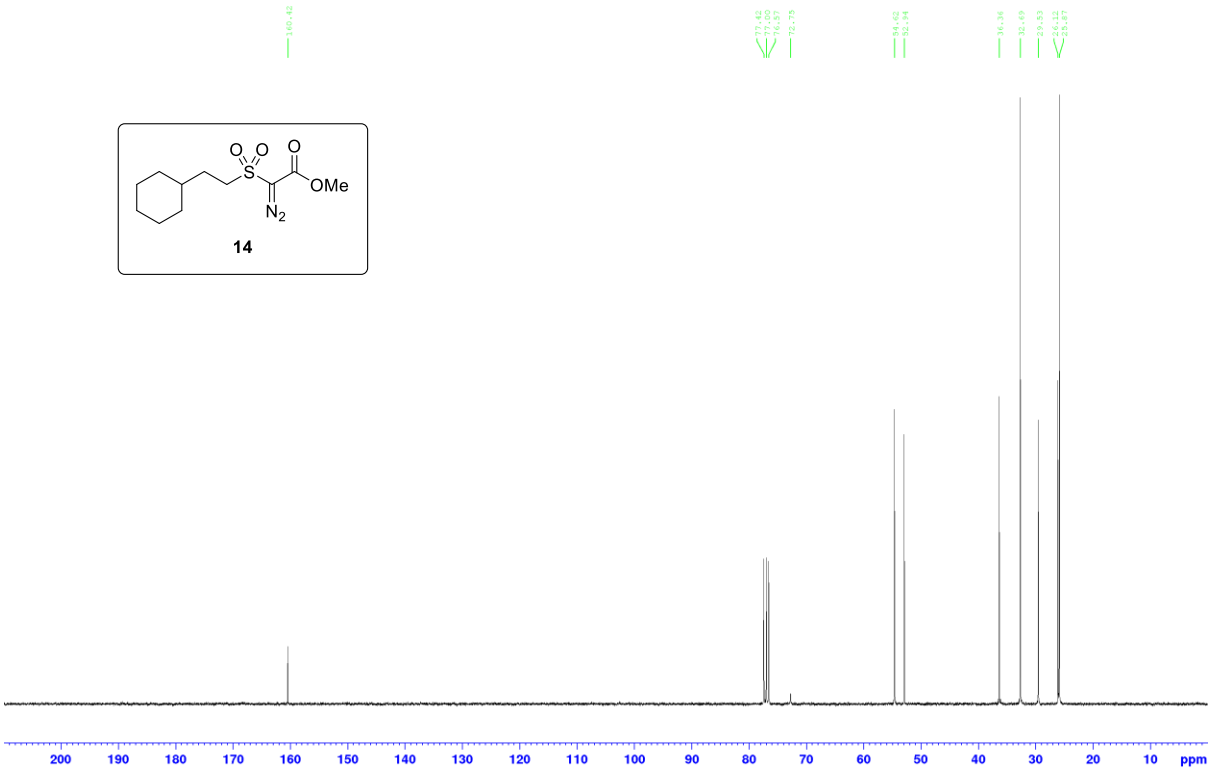

2-((-2-Cyclohexylethyl)sulfonyl-2-diazo-1-acetophenone (15)

^{1}H (300 MHz, $CDCl_3$)

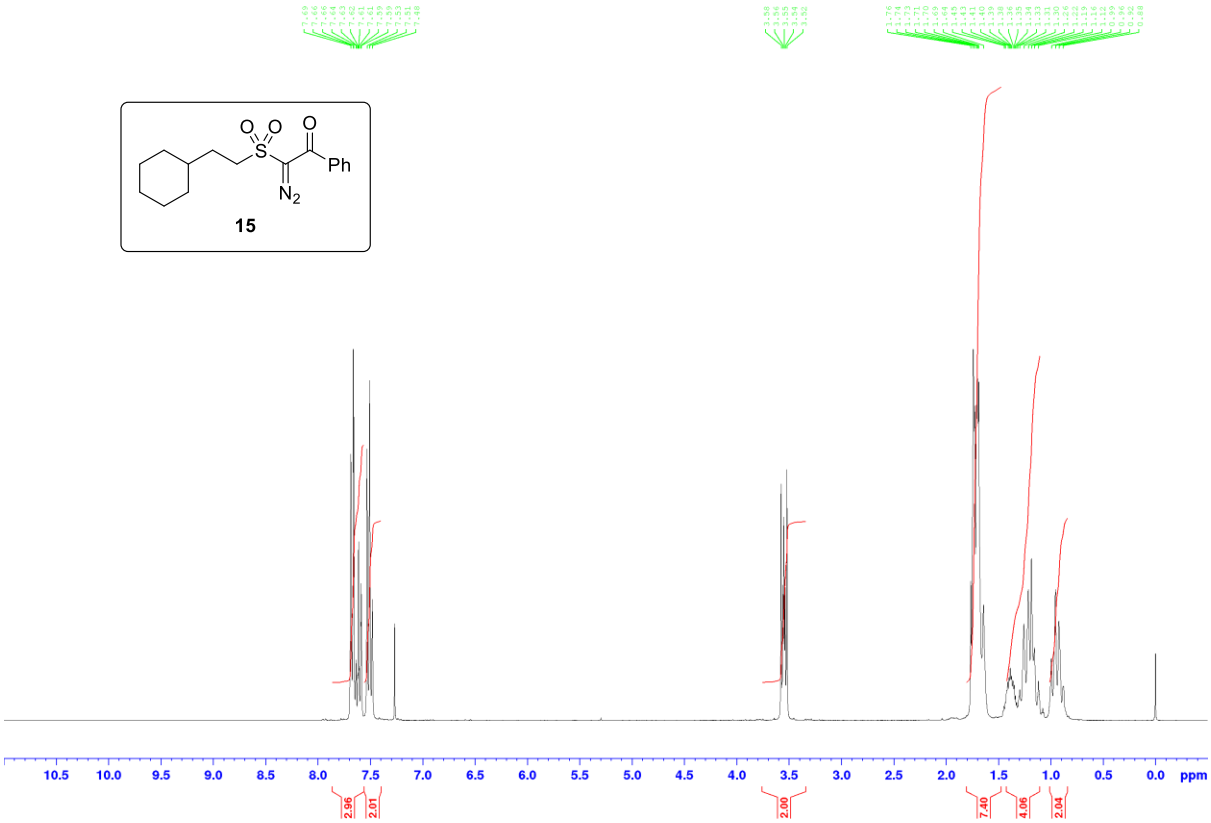

^{13}C (75.5 MHz, $CDCl_3$)

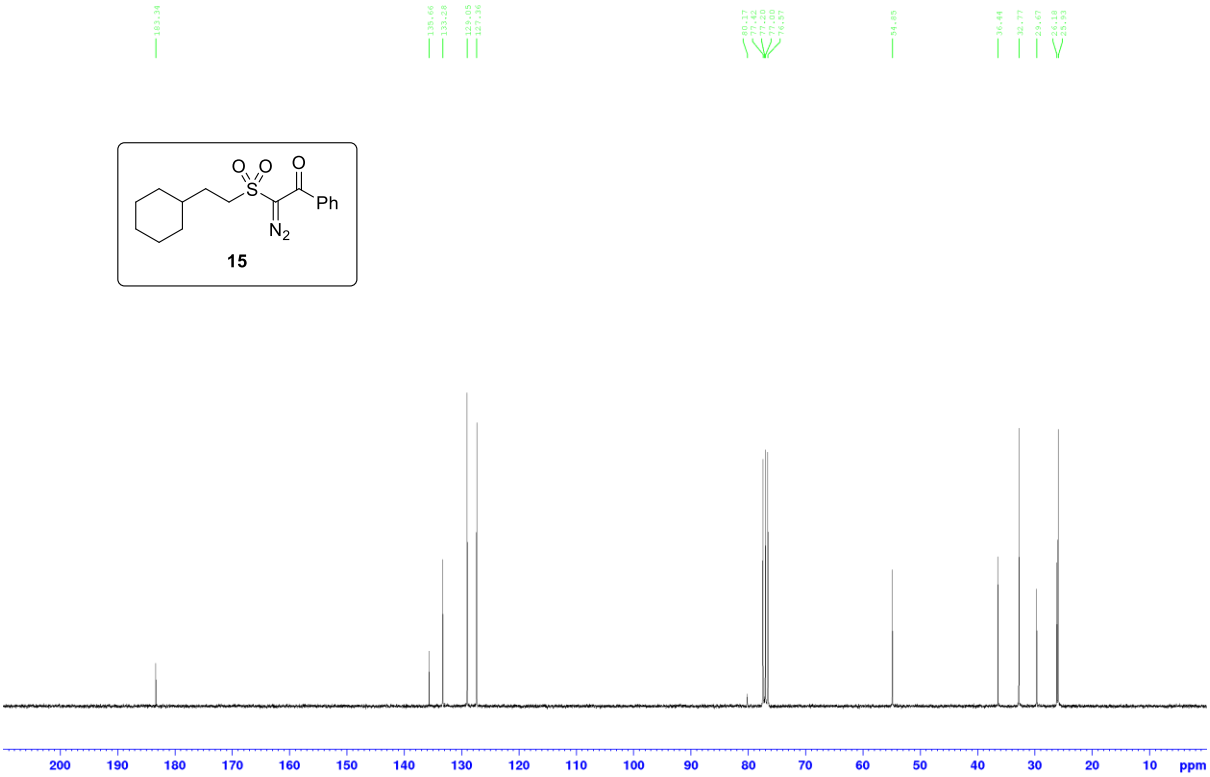

2-((2-Cyclopentylethyl)sulfonyl)-2-diazo-1-acetophenone (16)

^{1}H (300 MHz, $CDCl_3$)

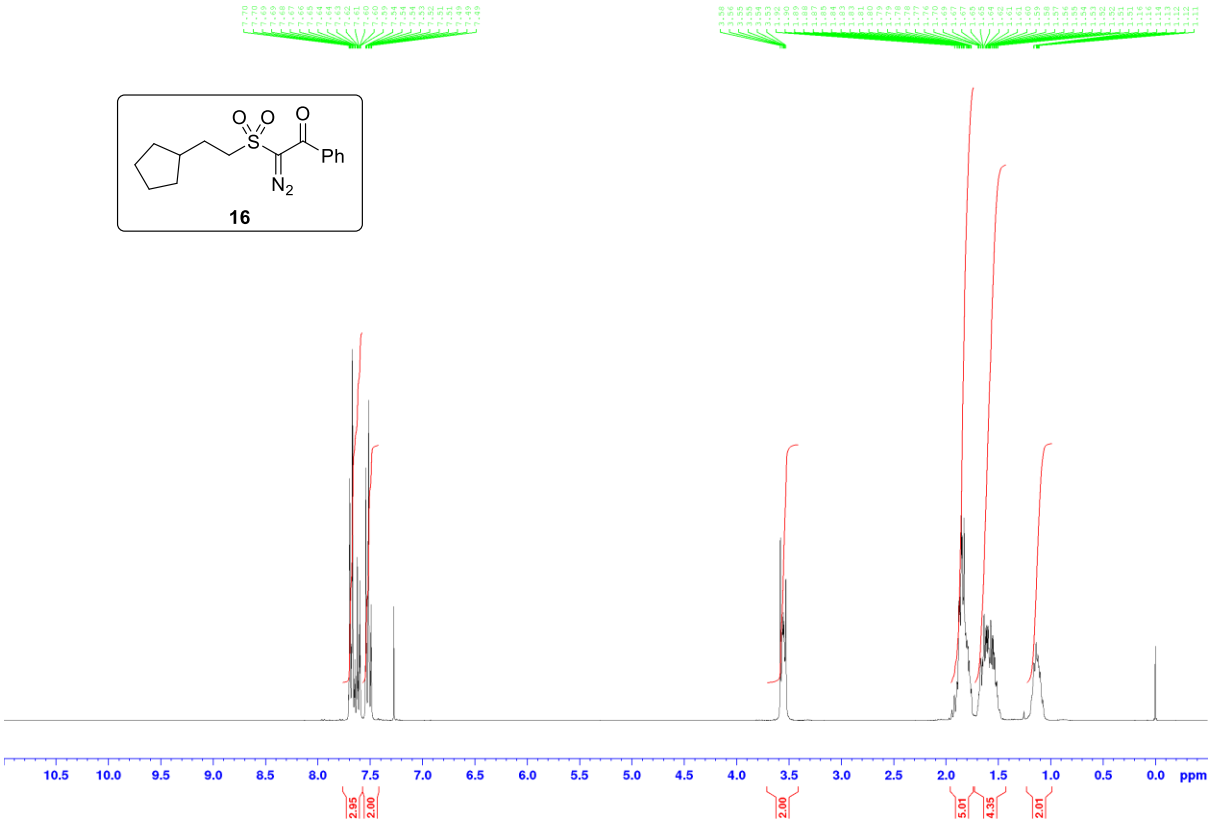

^{13}C (75.5 MHz, $CDCl_3$)

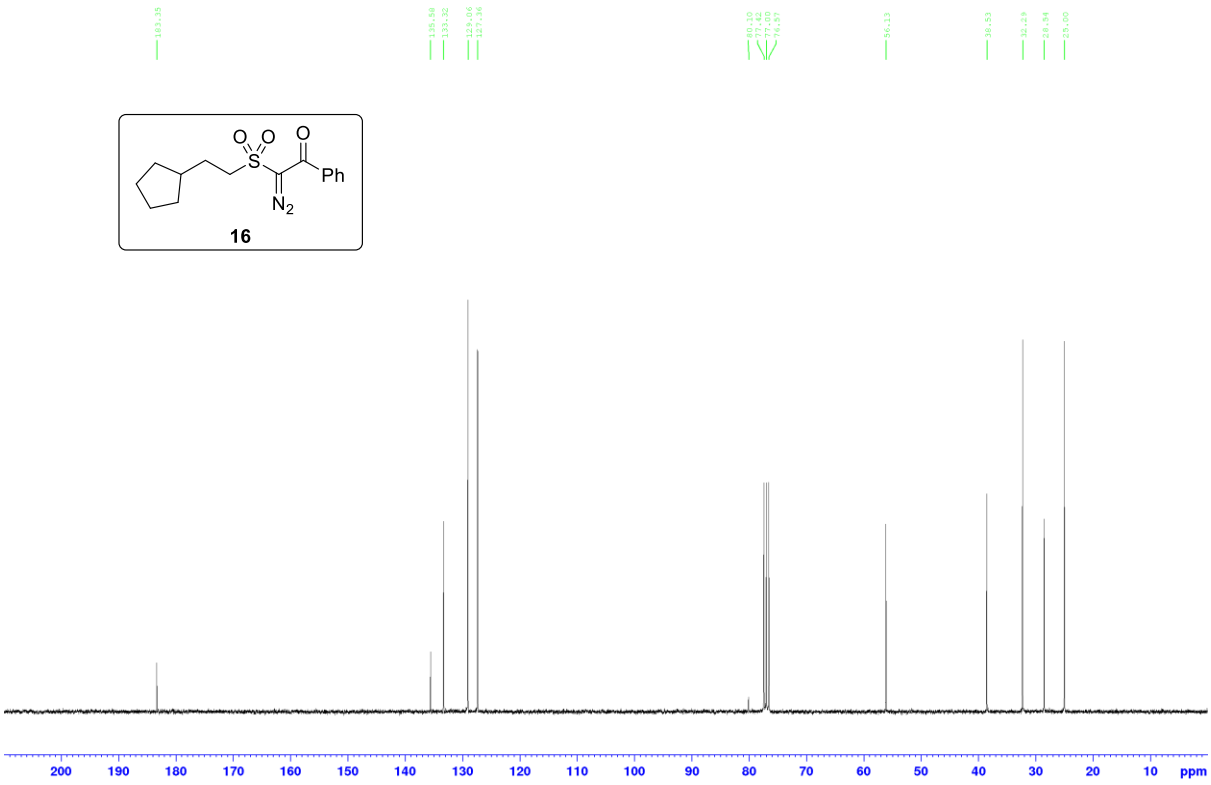

2-Diazo-1-phenyl-2-((3-propylhexyl)sulfonylethan-1-one (17)

^{1}H (300 MHz, $CDCl_3$)

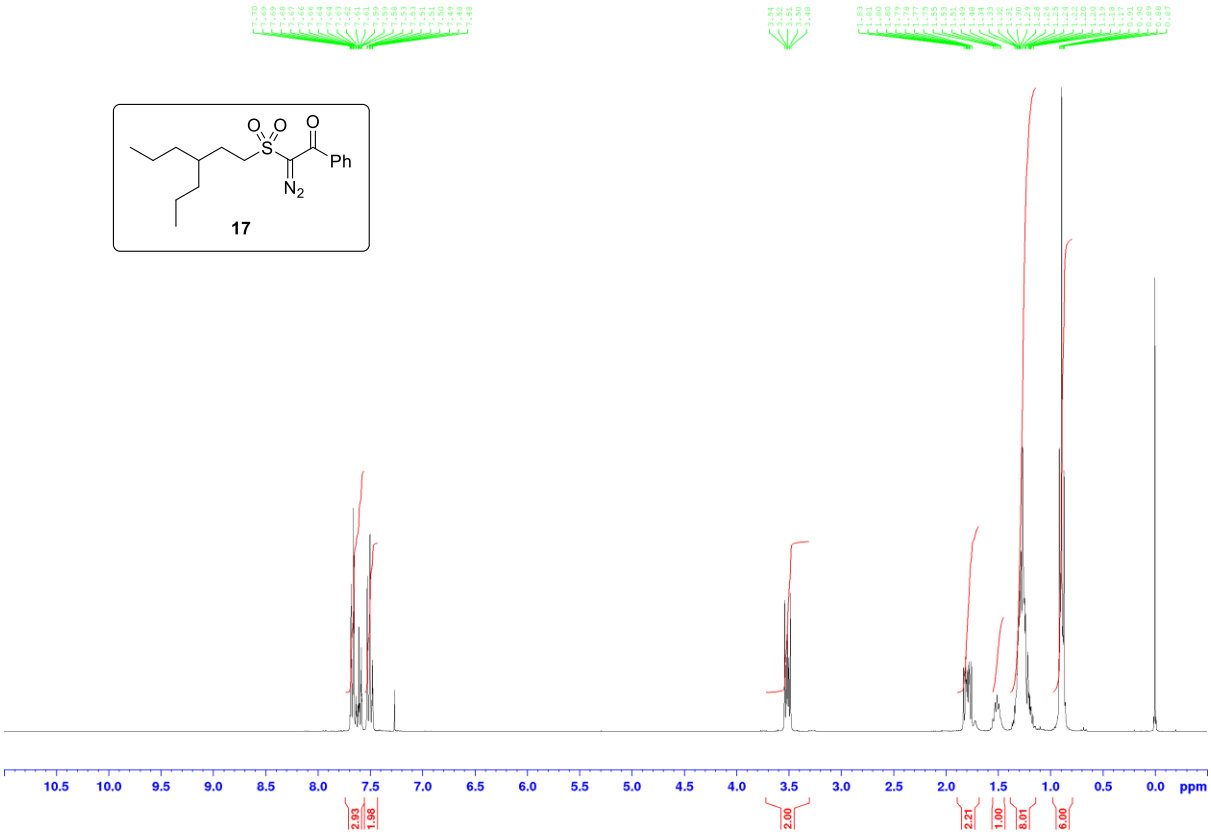

^{13}C (75.5 MHz, $CDCl_3$)

3-Cyclohexyl-1-diazo-1-(phenylsulfonyl)propan-2-one (18)

^{1}H (300 MHz, $CDCl_3$)

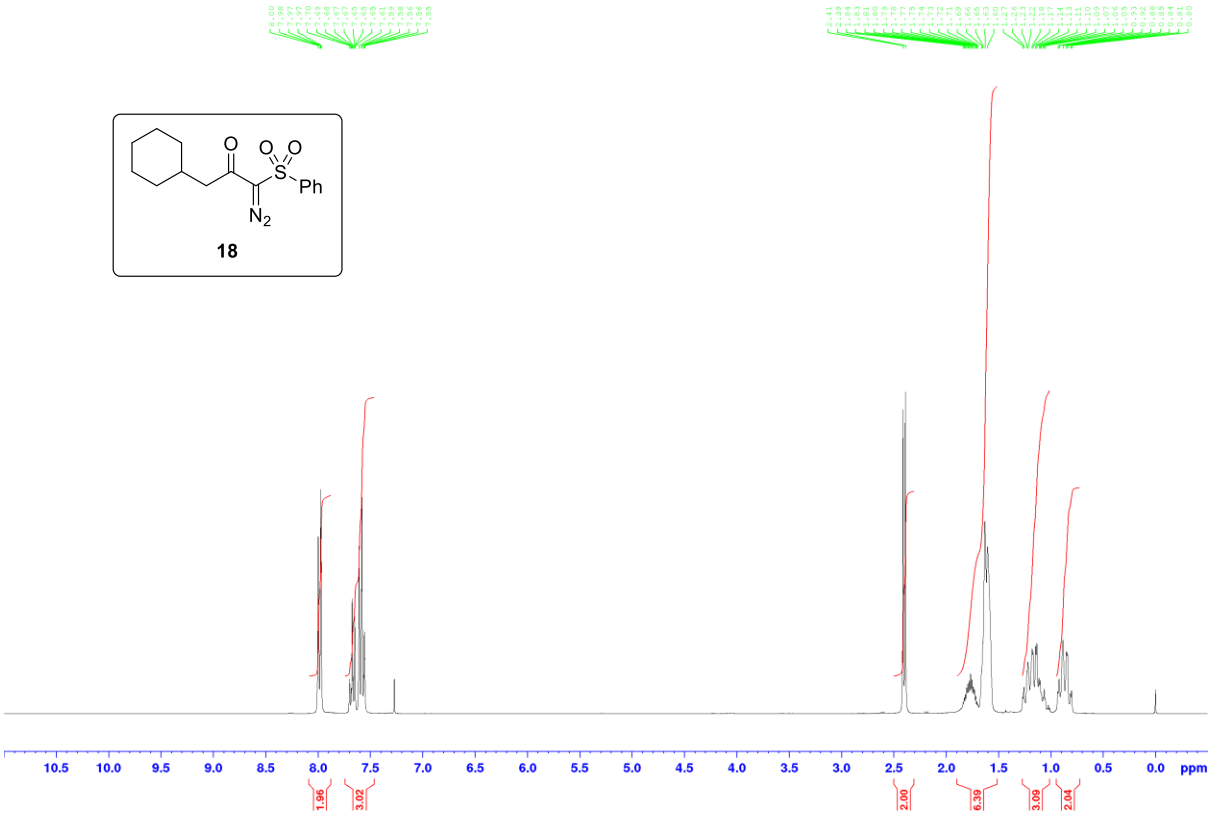

^{13}C (75.5 MHz, $CDCl_3$)

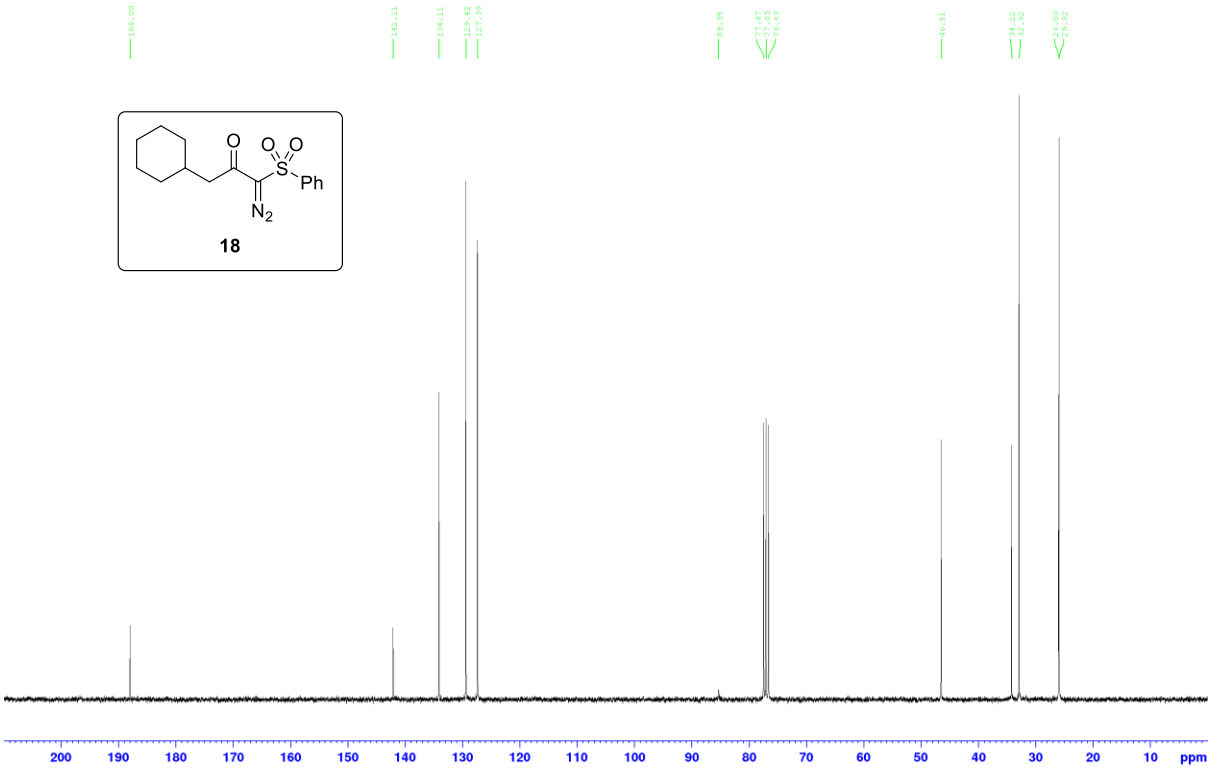

1-Diazo-1-(phenylsulfonyl)-3-propylhexan-2-one (19)

^{1}H (400 MHz, $CDCl_3$)

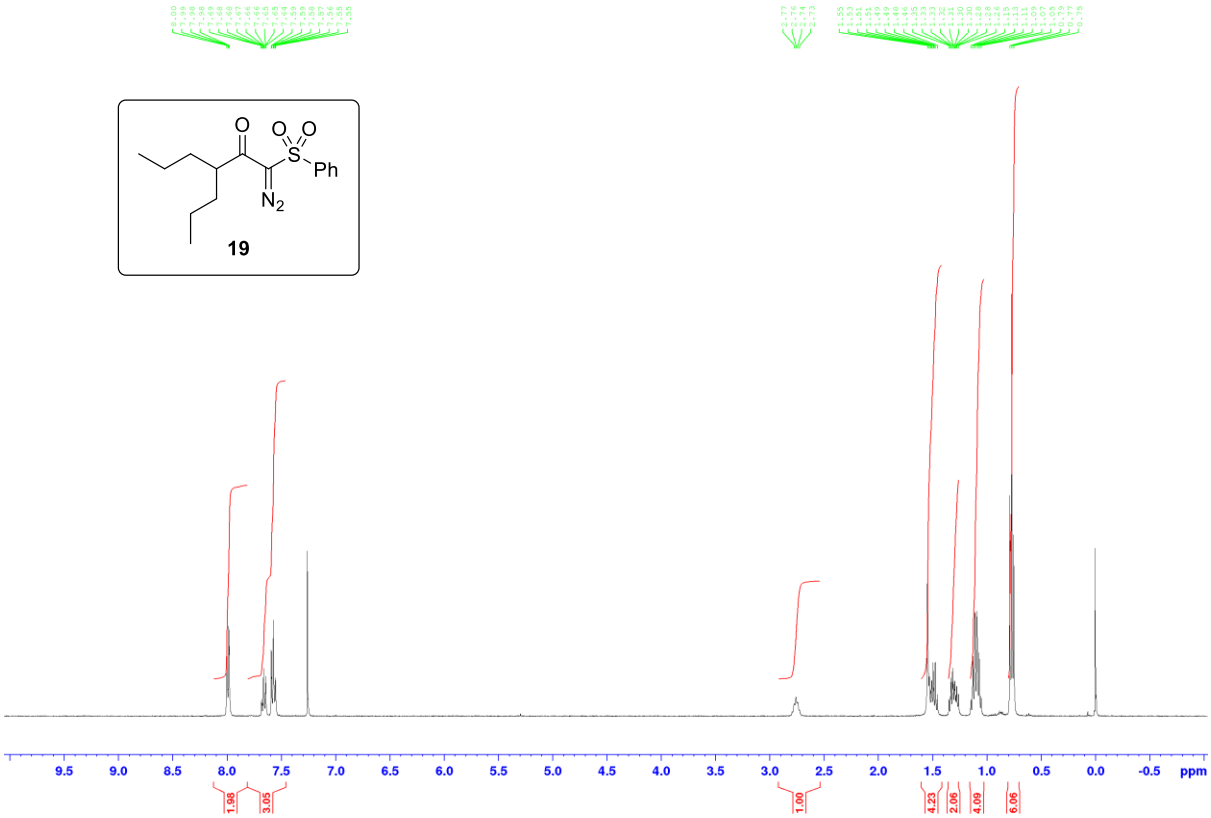

^{13}C (75.5 MHz, $CDCl_3$)

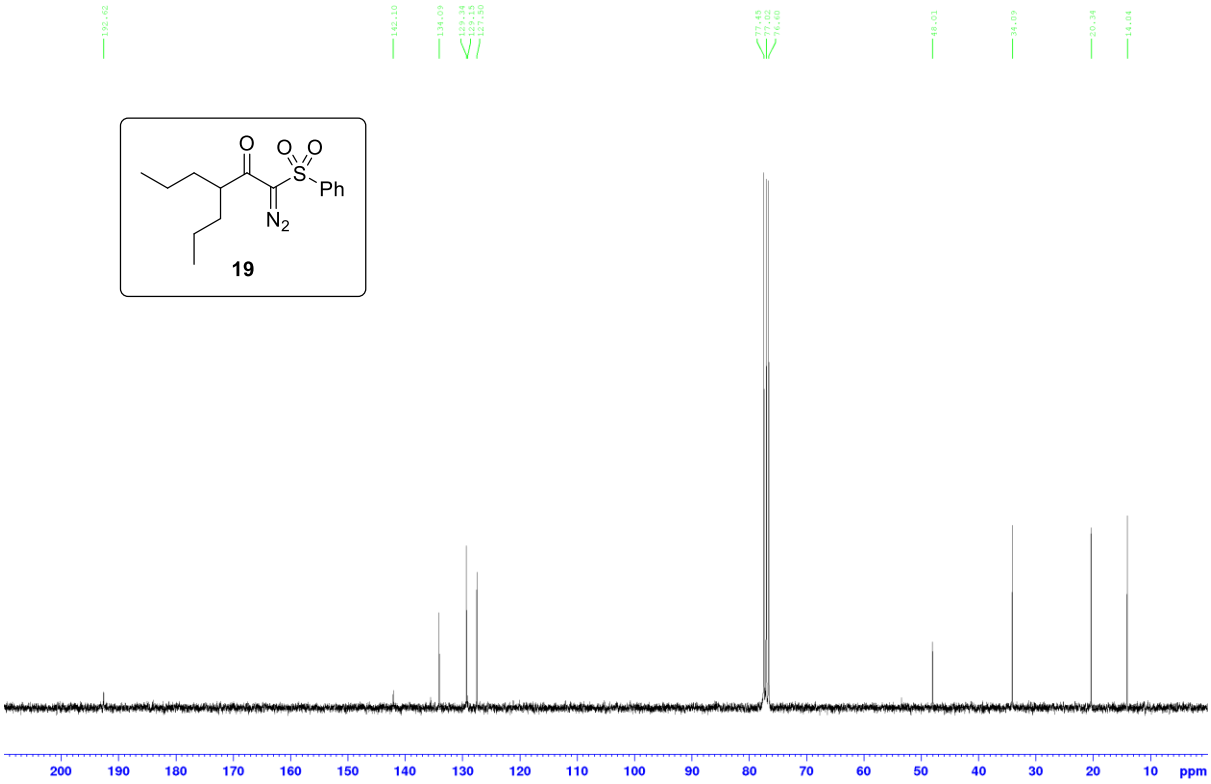

Methyl (1*S,4a*S**,8a*R**)-octahydro-1*H*-isothiochromene-1-carboxylate 2,2-dioxide (29a)**

^{1}H (300 MHz, $CDCl_3$)

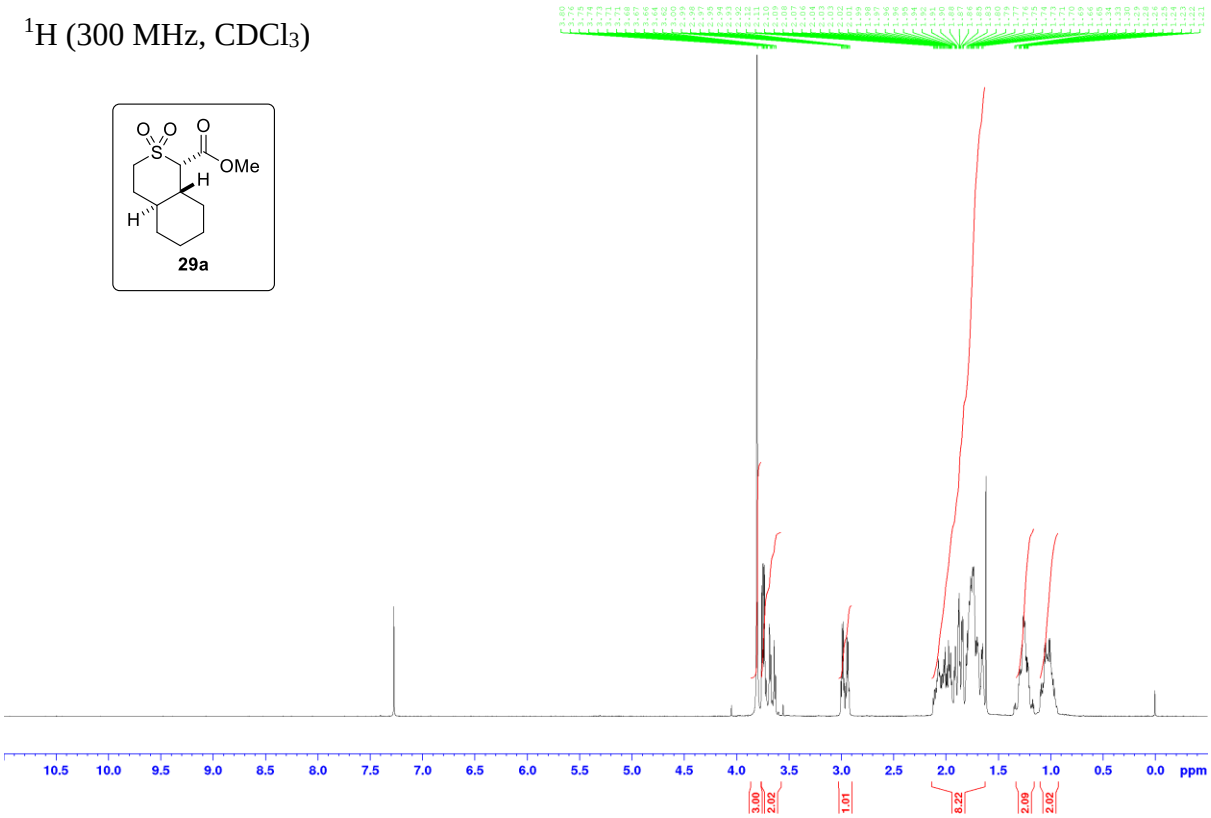

^{13}C (75.5 MHz, $CDCl_3$)

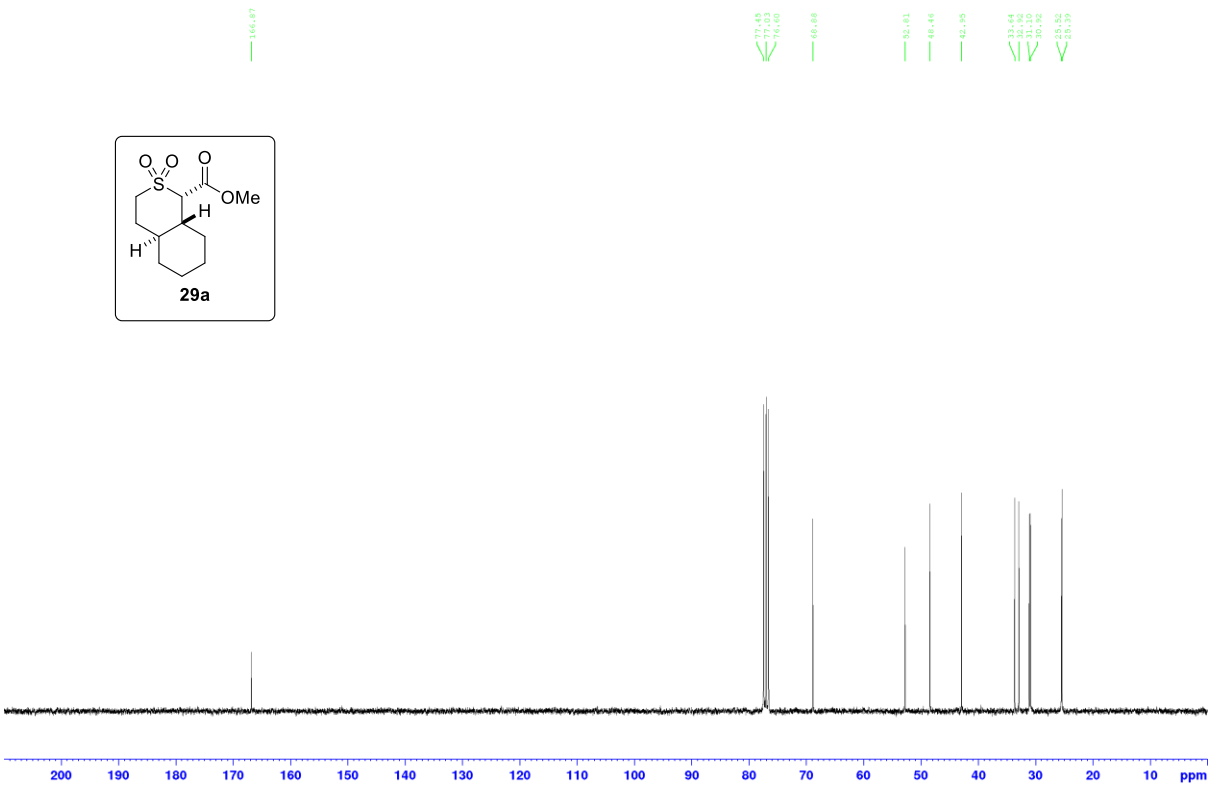

Methyl (1*R,4a*S**,8a*R**)-octahydro-1*H*-isothiochromene-1-carboxylate 2,2-dioxide (29b)**

^{1}H (300 MHz, $CDCl_3$)

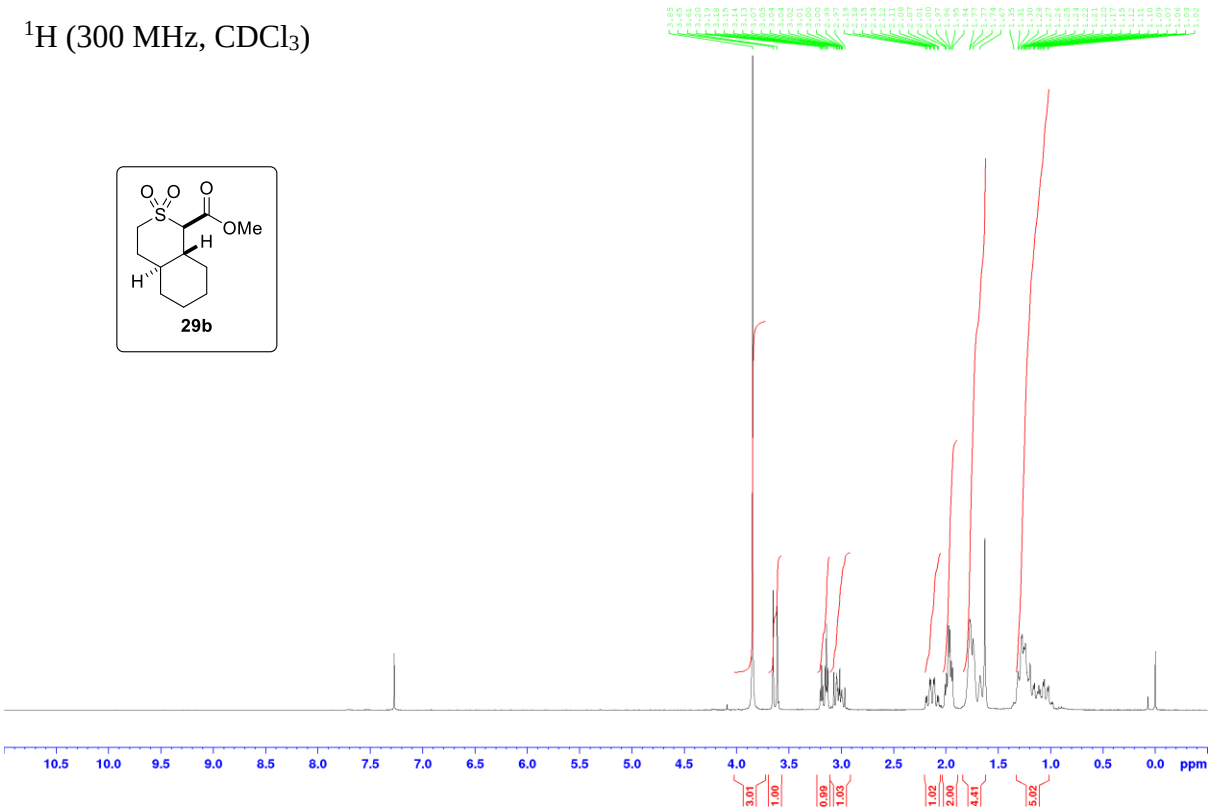

^{13}C (75.5 MHz, $CDCl_3$)

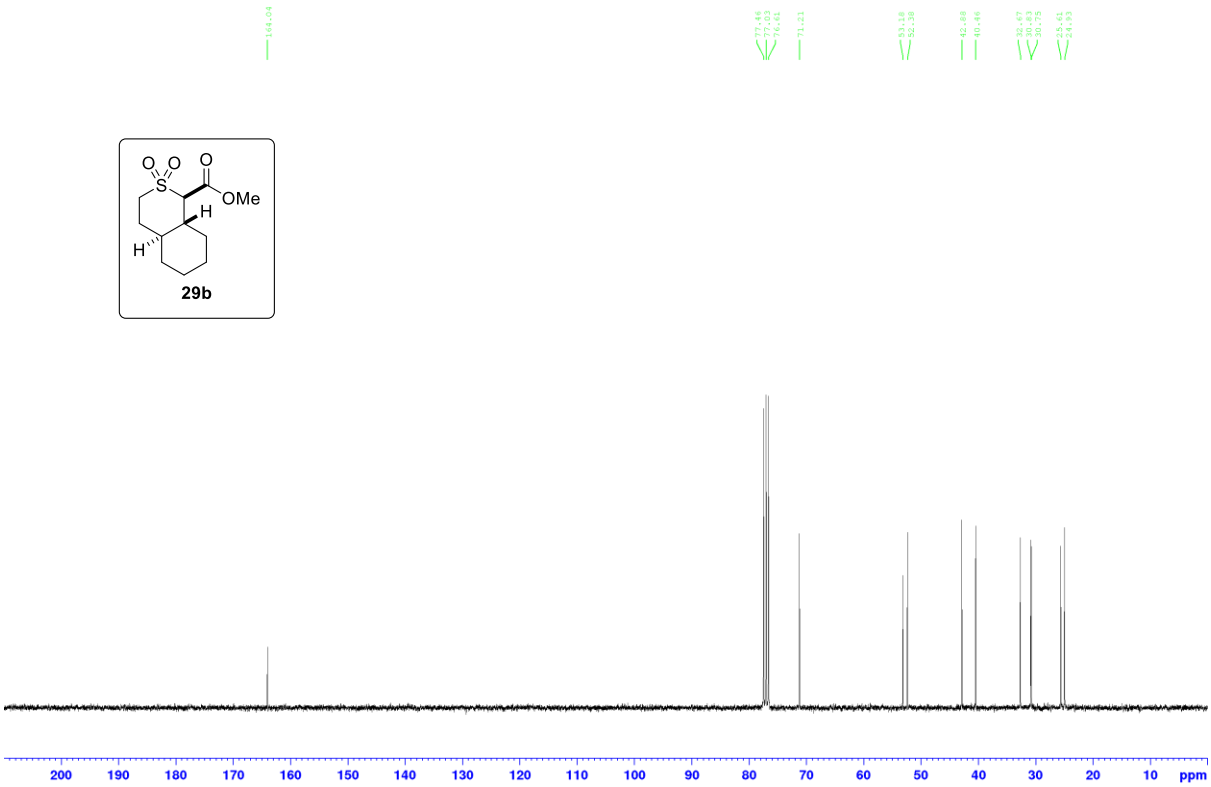

Methyl 2-thiaspiro[4.5]decane-1-carboxylate 2,2-dioxide (30)

^{1}H (300 MHz, $CDCl_3$)

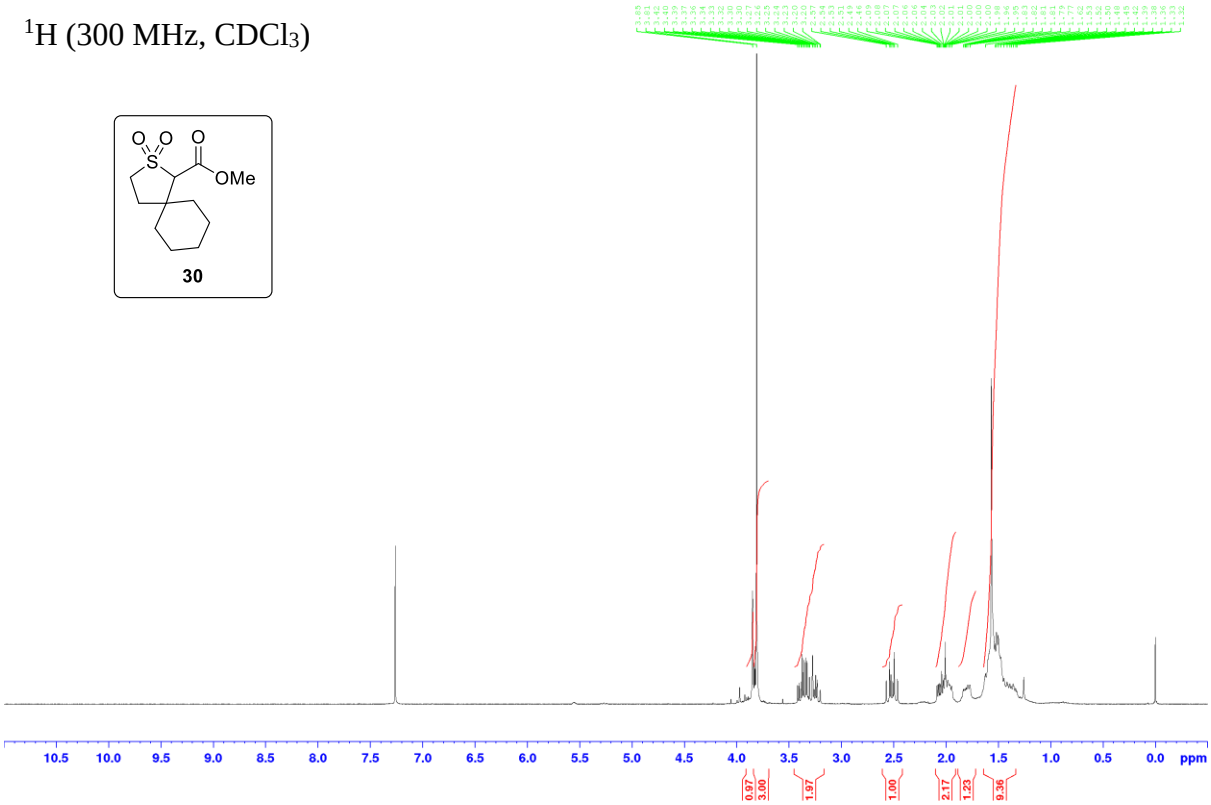

^{13}C (75.5 MHz, $CDCl_3$)

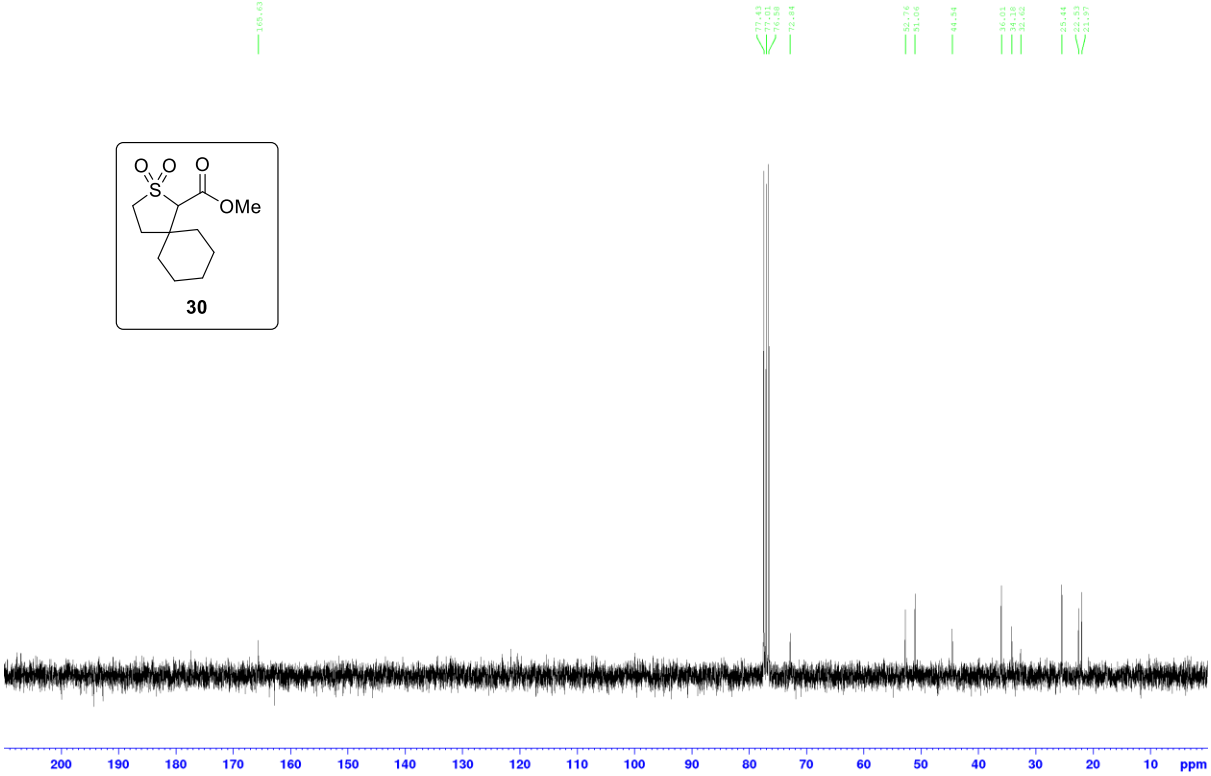

((1*S,4a*S**,8a*R**)-2,2-Dioxidooctahydro-1*H*-isothiochromen-1-yl)(phenyl)methanone (31a)**

^{1}H (300 MHz, $CDCl_3$)

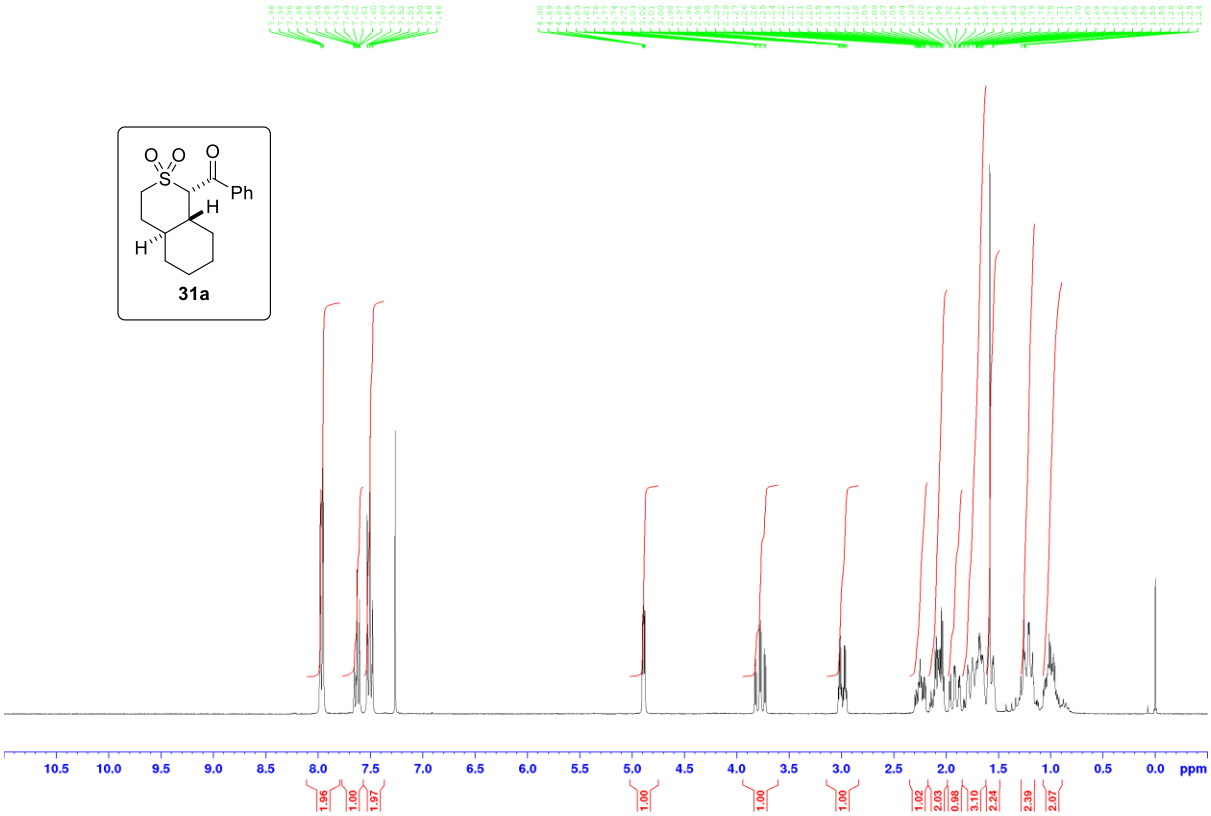

^{13}C (75.5 MHz, $CDCl_3$)

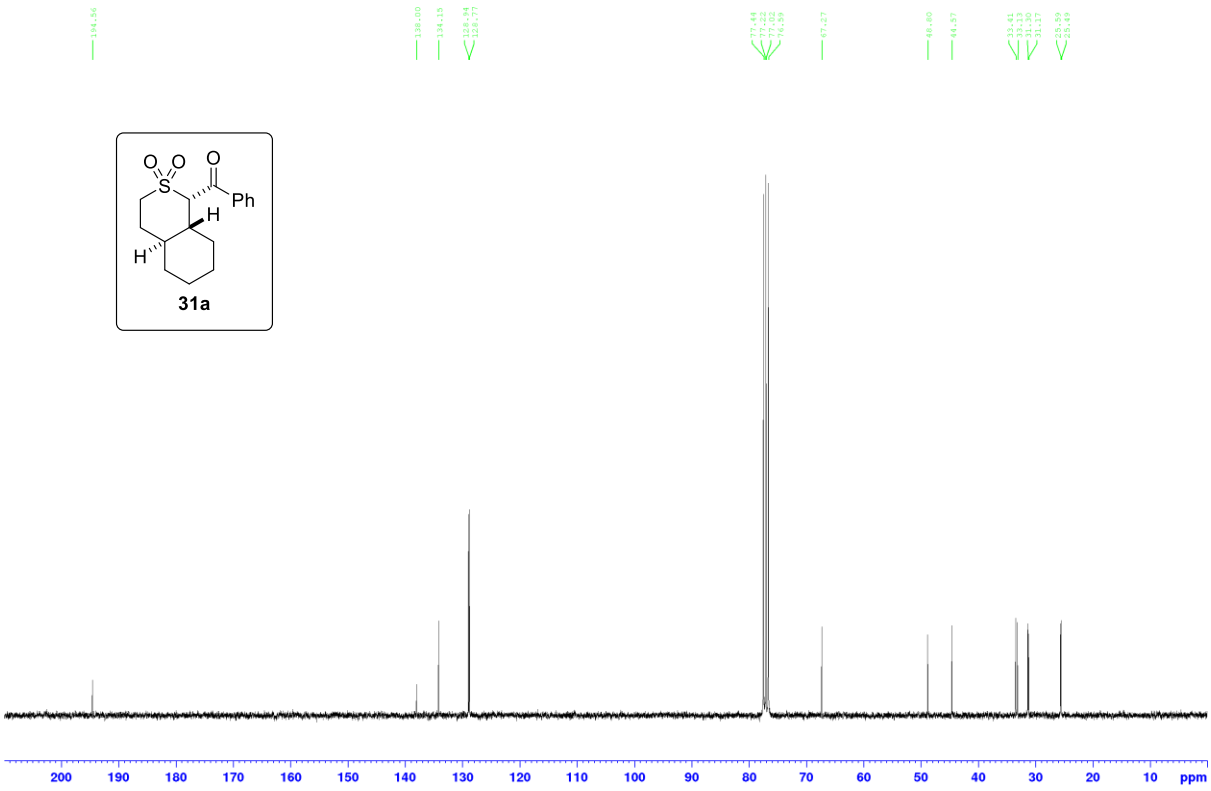

((1*R,4a*S**,8a*R**)-2,2-Dioxidooctahydro-1*H*-isothiochromen-1-yl)(phenyl)methanone (31b)**

^{1}H (300 MHz, $CDCl_3$)

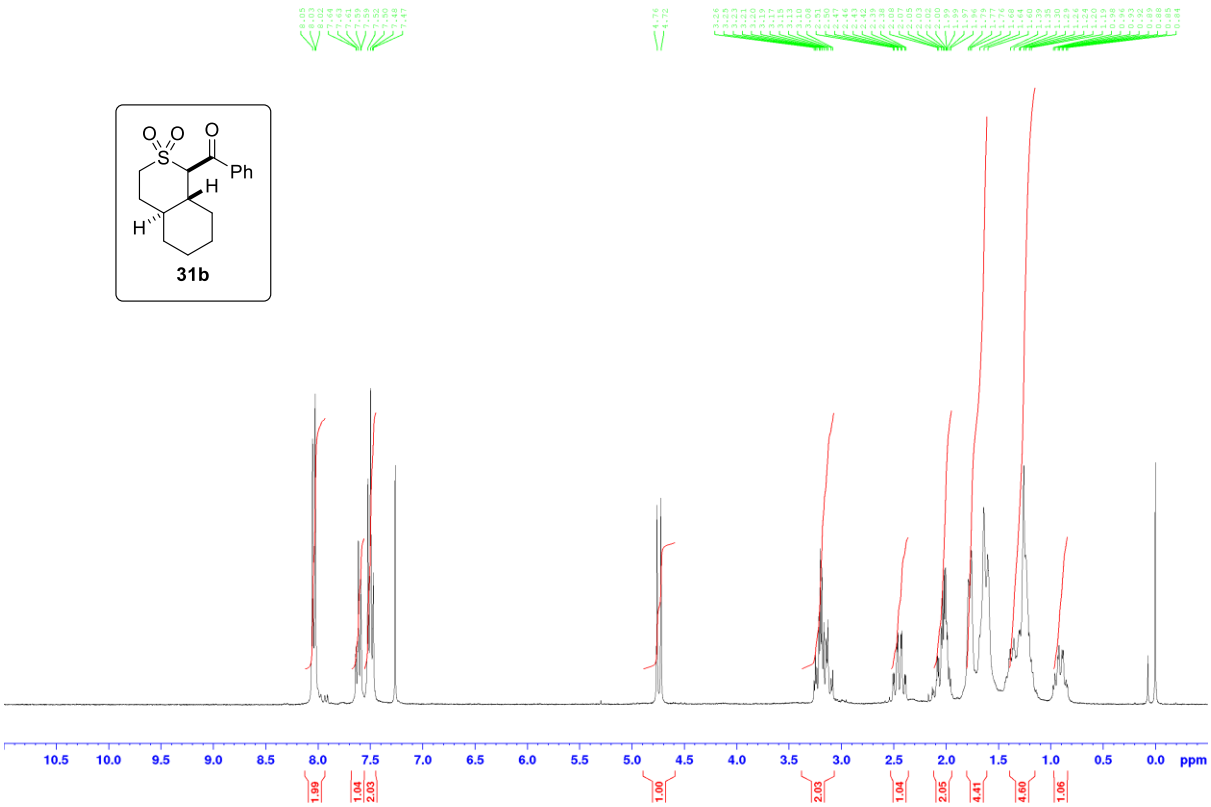

^{13}C (75.5 MHz, $CDCl_3$)

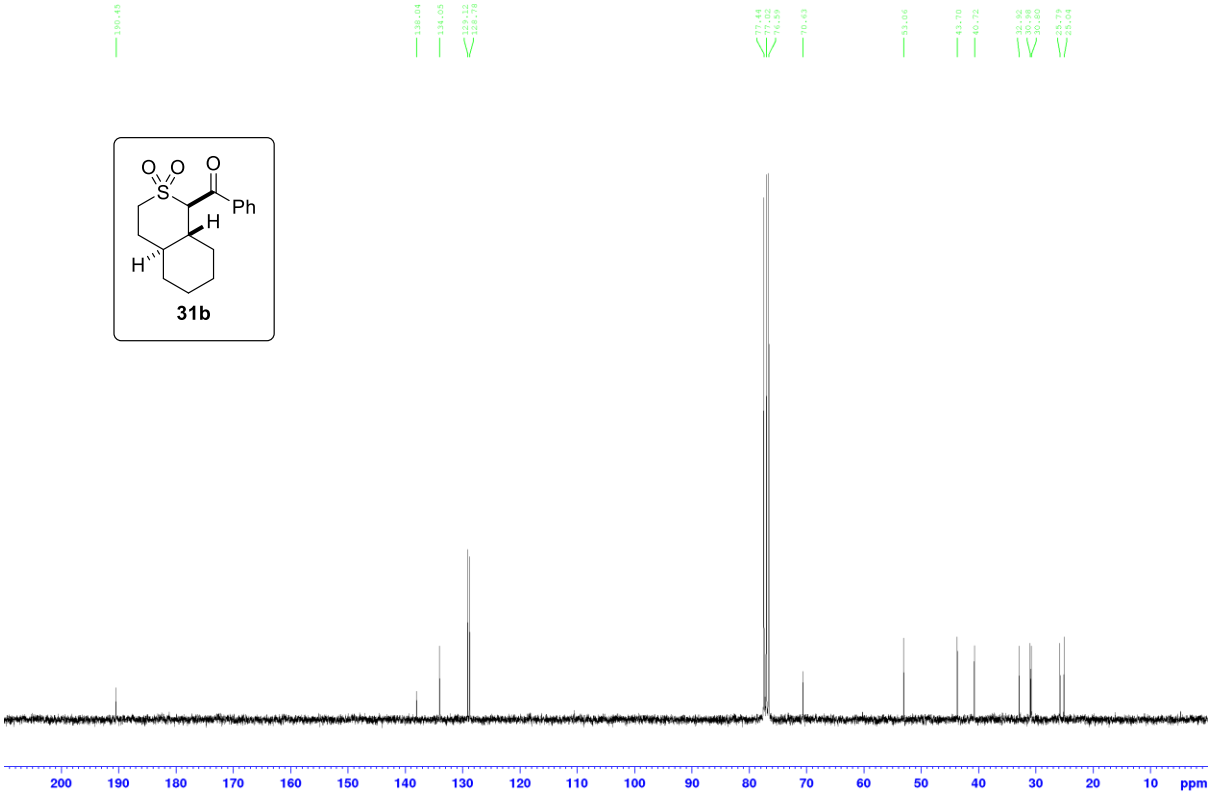

(2,2-Dioxodo-2-thiaspiro[4.5]decan-1-yl)(phenyl)methanone (32)

^{1}H (400 MHz, $CDCl_3$)

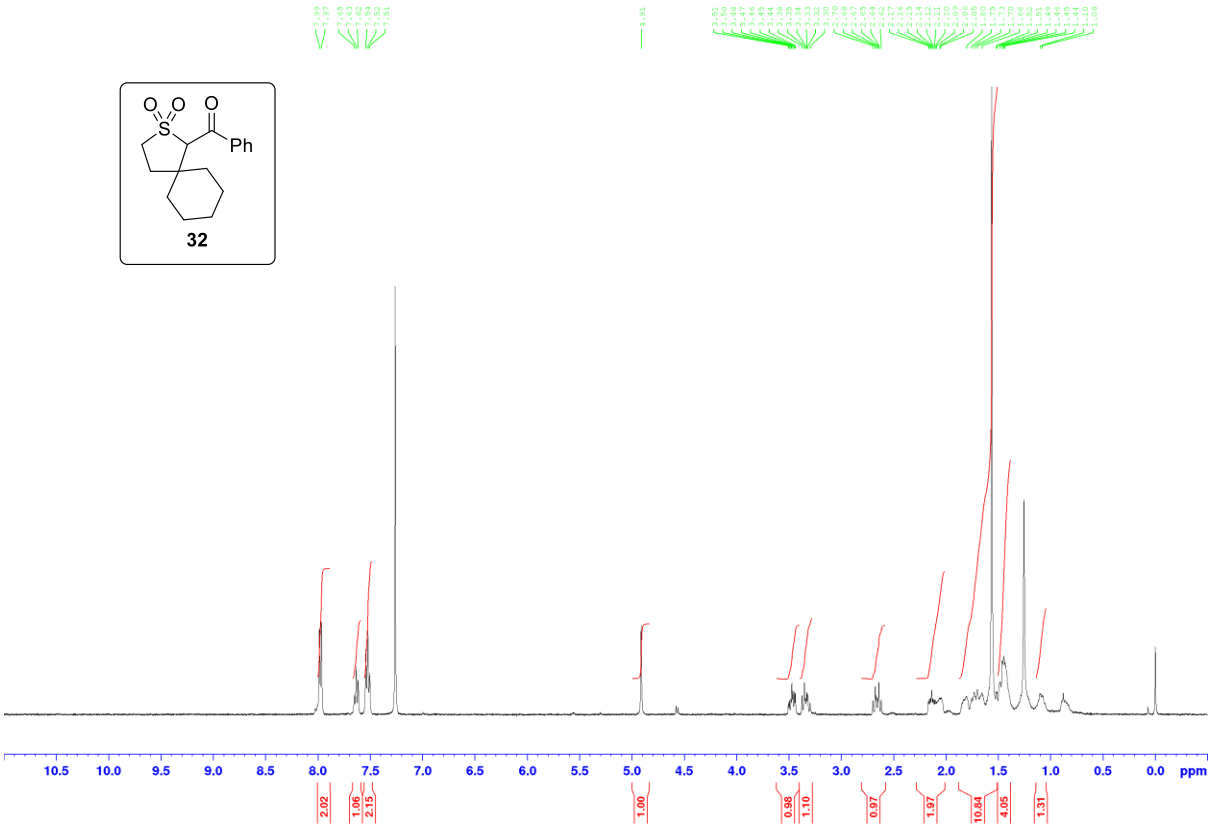

^{13}C (100.6 MHz, $CDCl_3$)

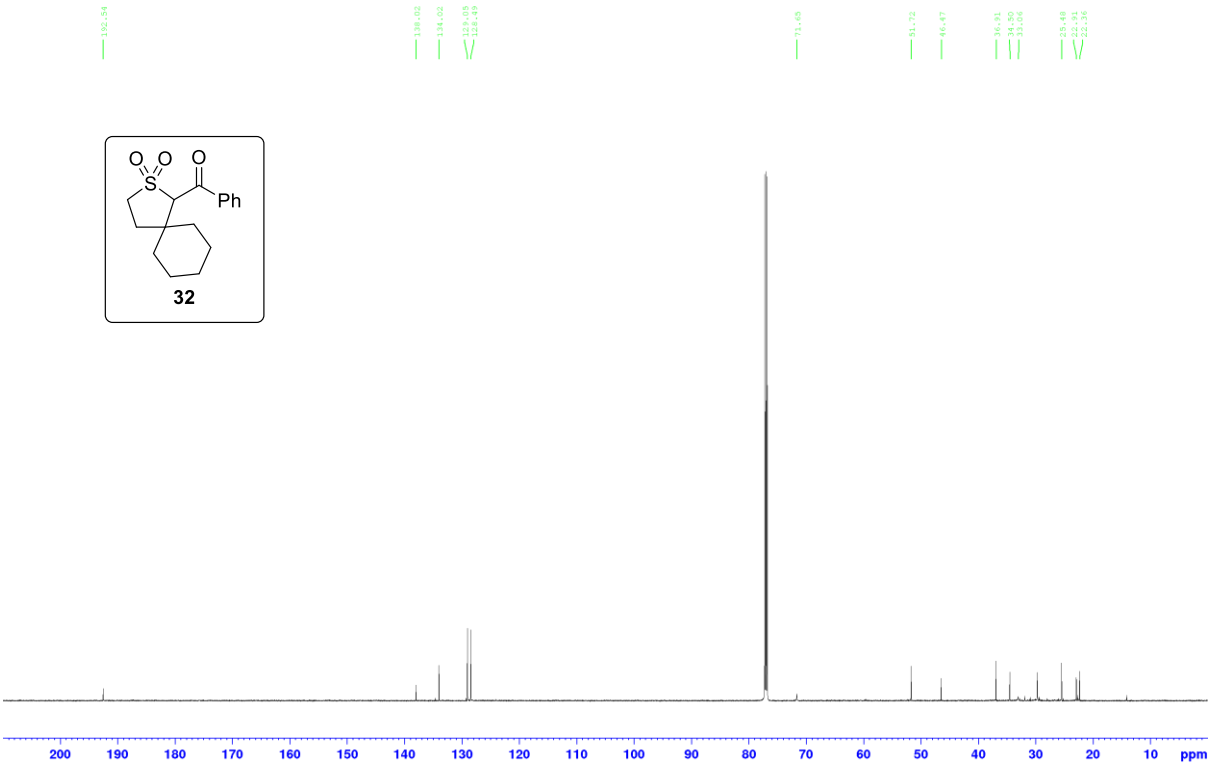

((1*S,4a*S**,7a*R**)-2,2-Dioxodooctahydrocyclopenta[*c*]thiopyran-1yl)(phenyl)methanone (33a)**

^{1}H (300 MHz, $CDCl_3$)

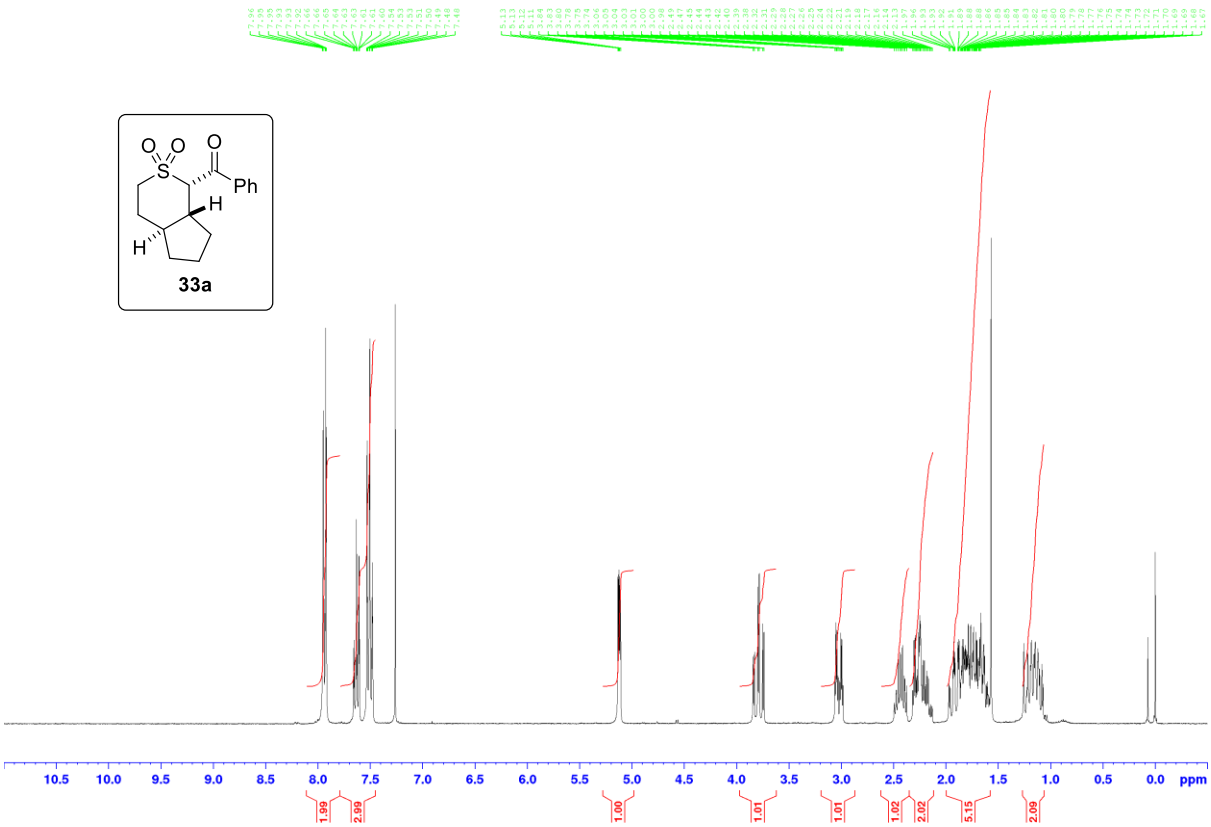

^{13}C (75.5 MHz, $CDCl_3$)

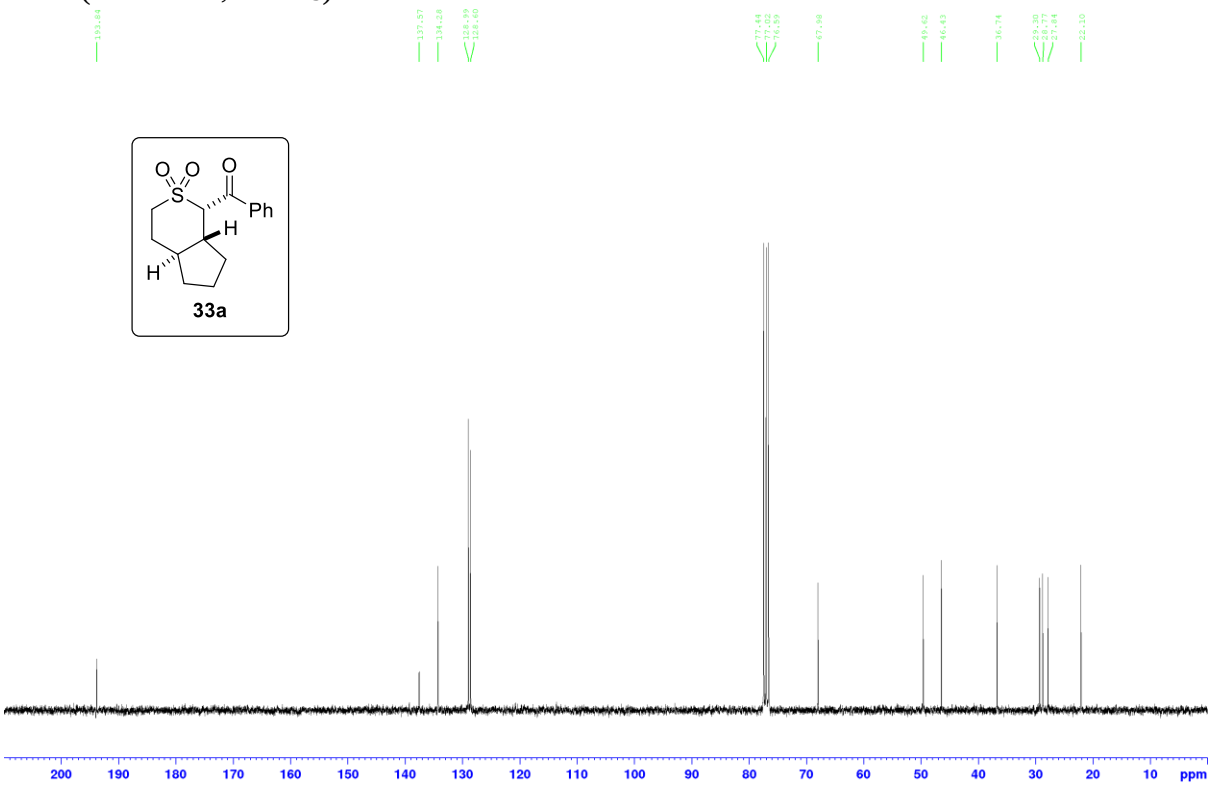

((1*R,4a*S**,7a*R**)-2,2-Dioxodooctahydrocyclopenta[*c*]thiopyran-1-yl)(phenyl)methanone (33b)**

^{1}H (300 MHz, $CDCl_3$)

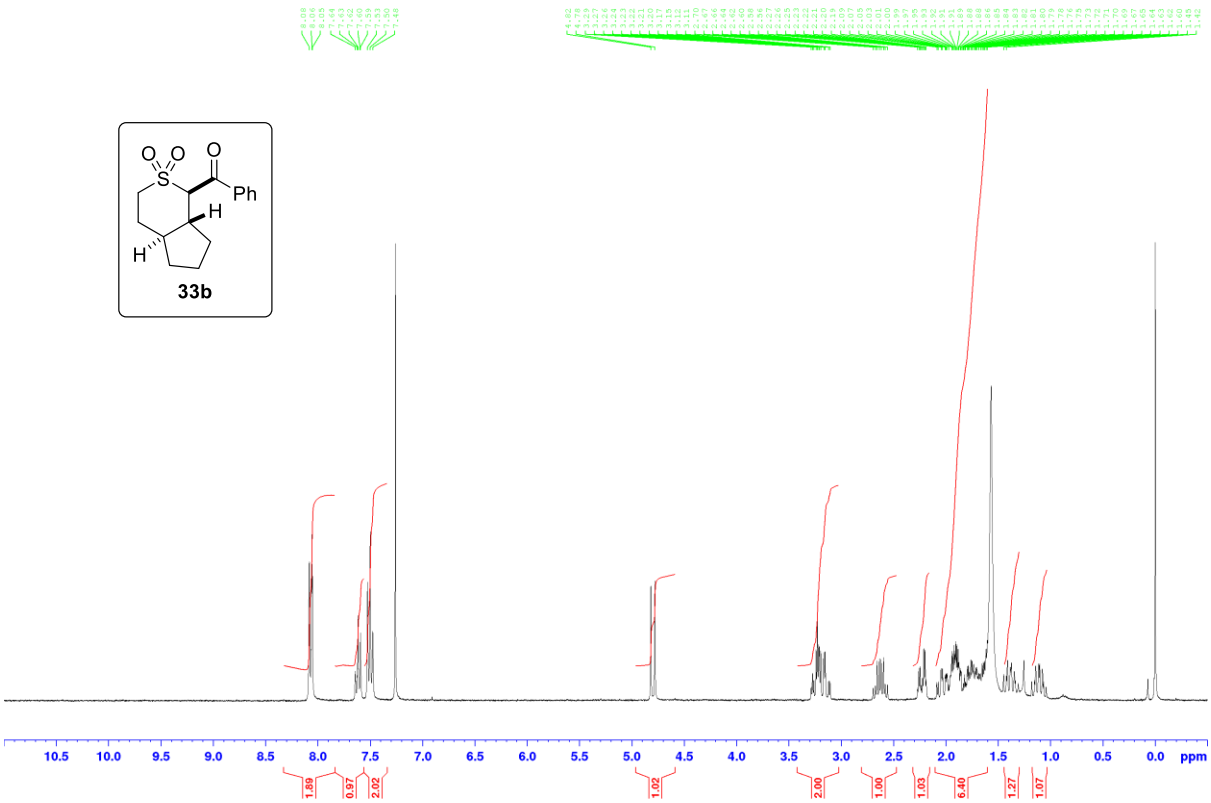

^{13}C (75.5 MHz, $CDCl_3$)

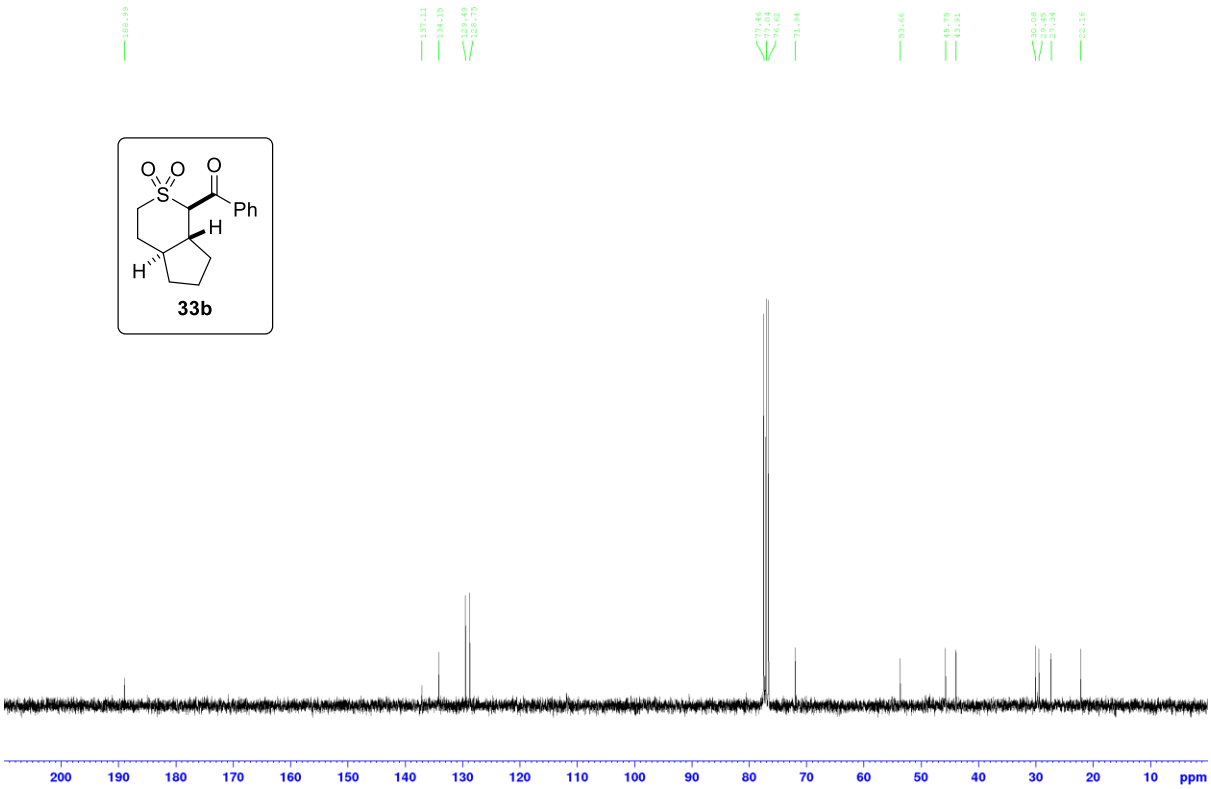

((1*R,4a*R**,7a*R**)-2,2-Dioxodooctahydrocyclopenta[*c*]thiopyran-1-yl)(phenyl)methanone (33c)**

^{1}H (300 MHz, $CDCl_3$)

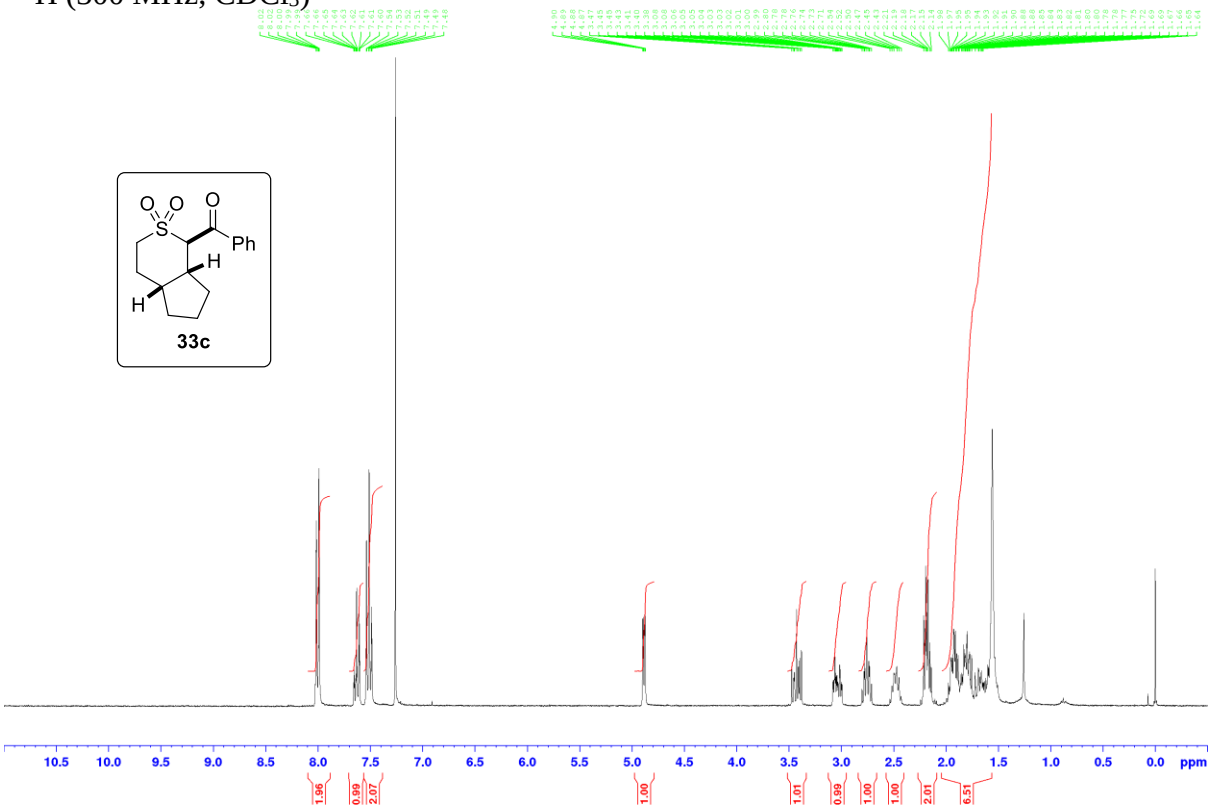

^{13}C (75.5 MHz, $CDCl_3$)

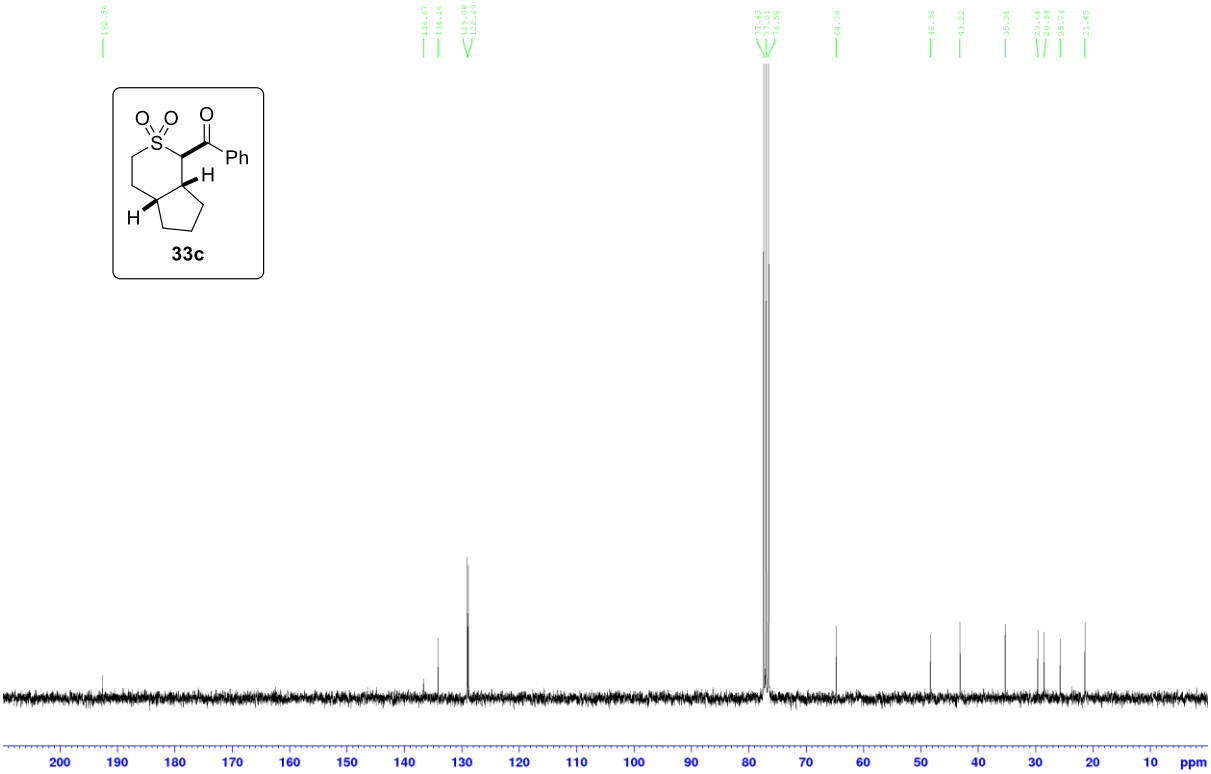

(2,2-Dioxido-2-thiaspiro[4.4]nonan-1-yl)(phenyl)methanone (34)

^{1}H (300 MHz, $CDCl_3$)

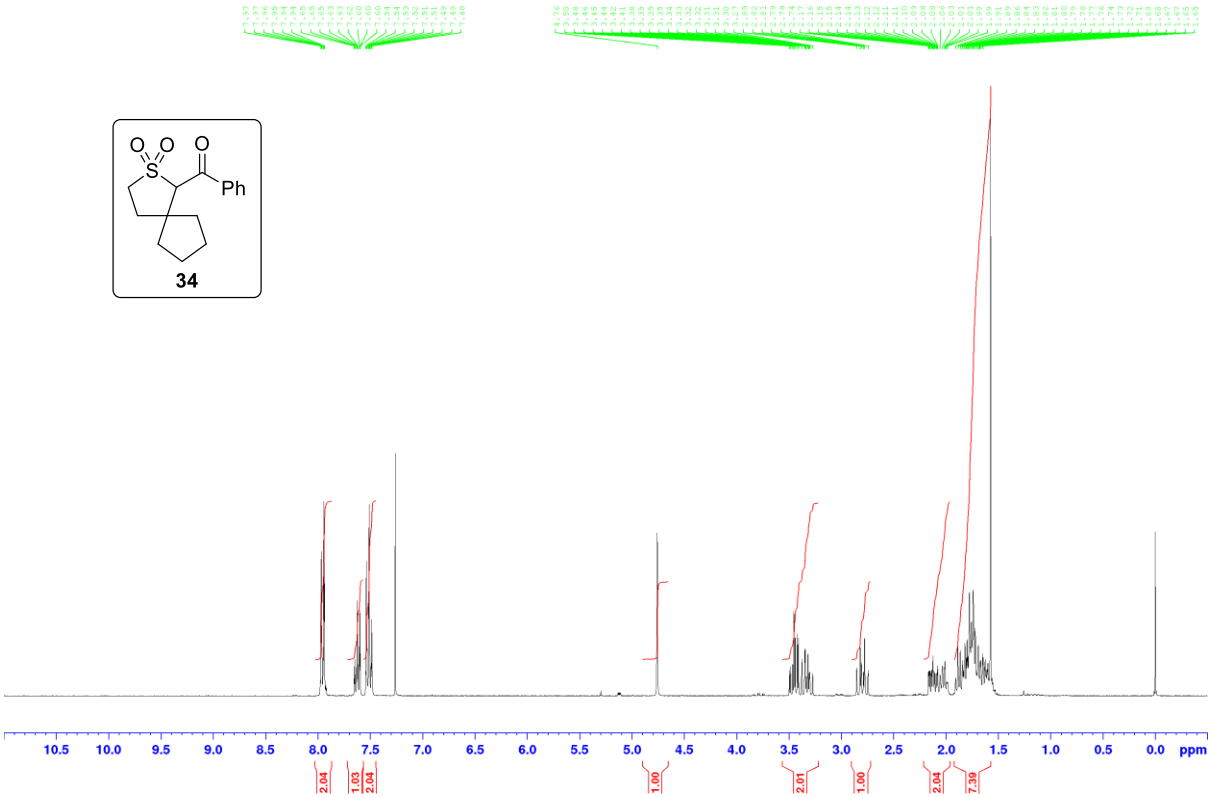

^{13}C (75.5 MHz, $CDCl_3$)

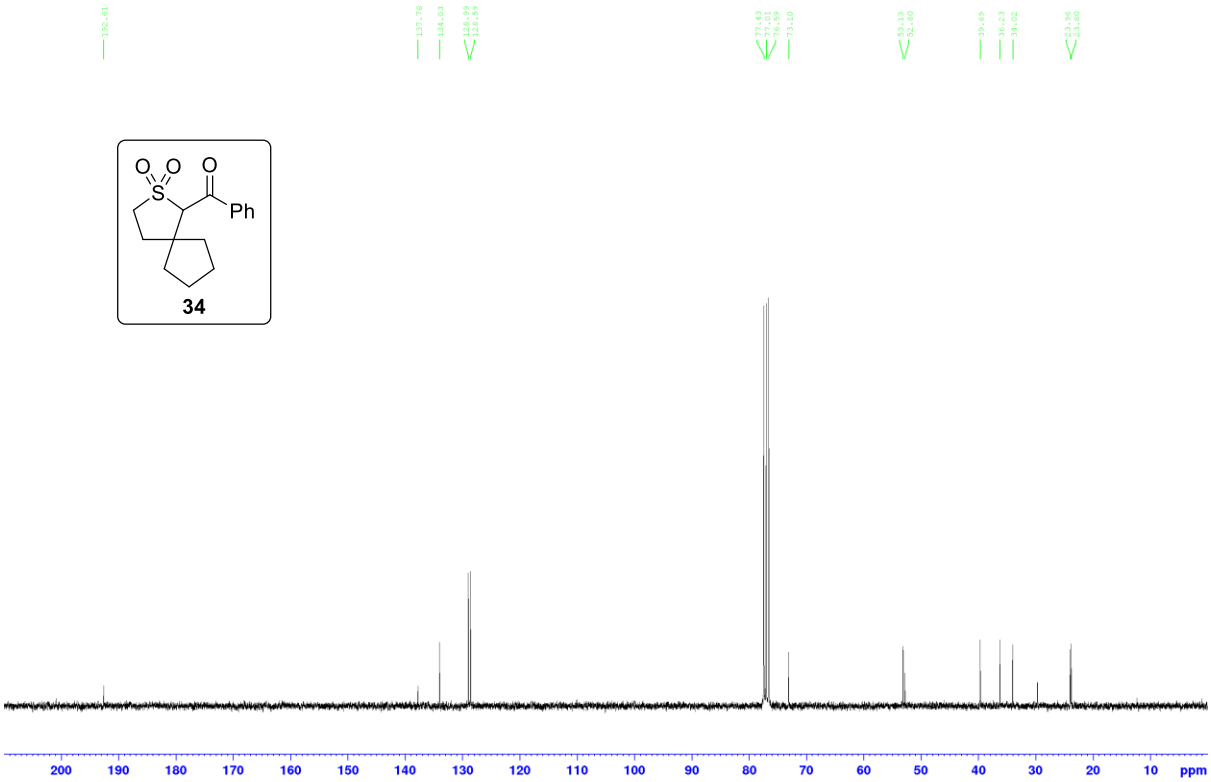

2-((2(Cyclopent-1-en-1-yl)ethyl)sulfonyl)-1-phenylethan-1-one (35)

^{1}H (300 MHz, $CDCl_3$)

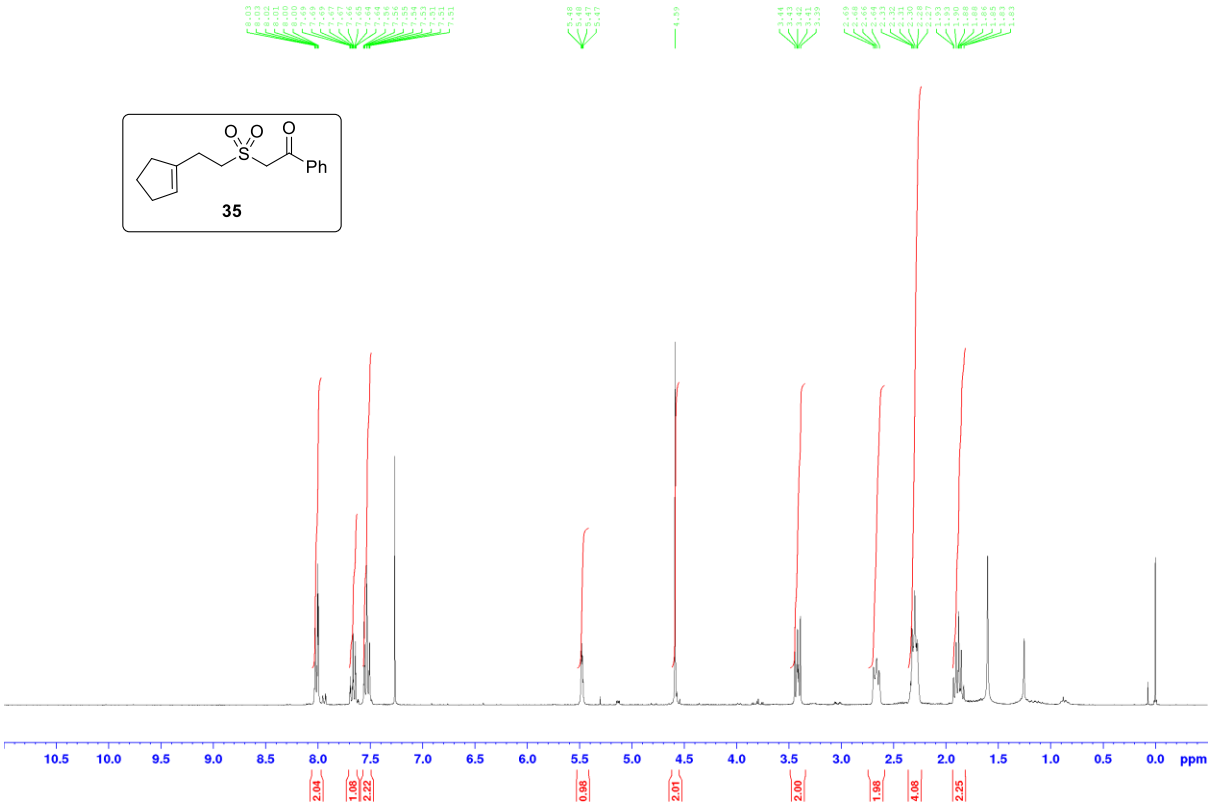

^{13}C (75.5 MHz, $CDCl_3$)

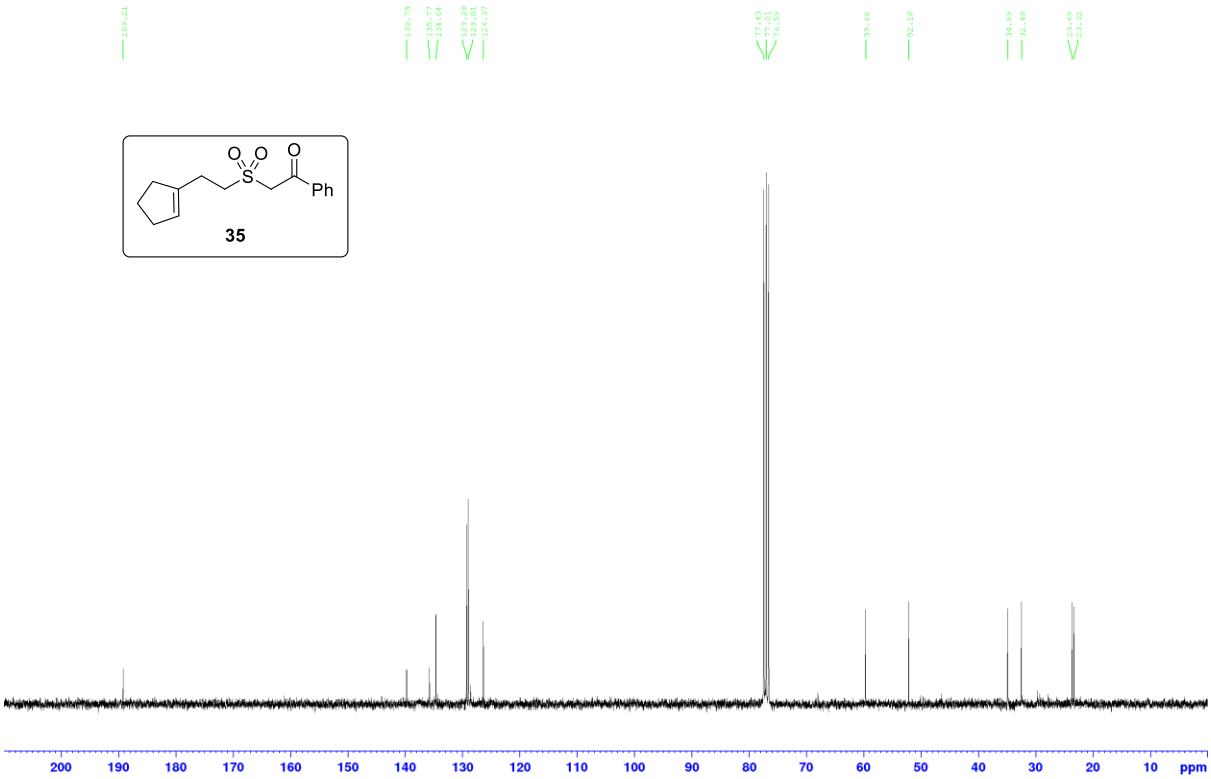

((2*S,3*R**,4*S**)-3-Ethyl-1,1-dioxido-4-propyltetrahydro-2*H*-thiopyran-2-yl)(phenyl)methanone (36a)**

^{1}H (300 MHz, $CDCl_3$)

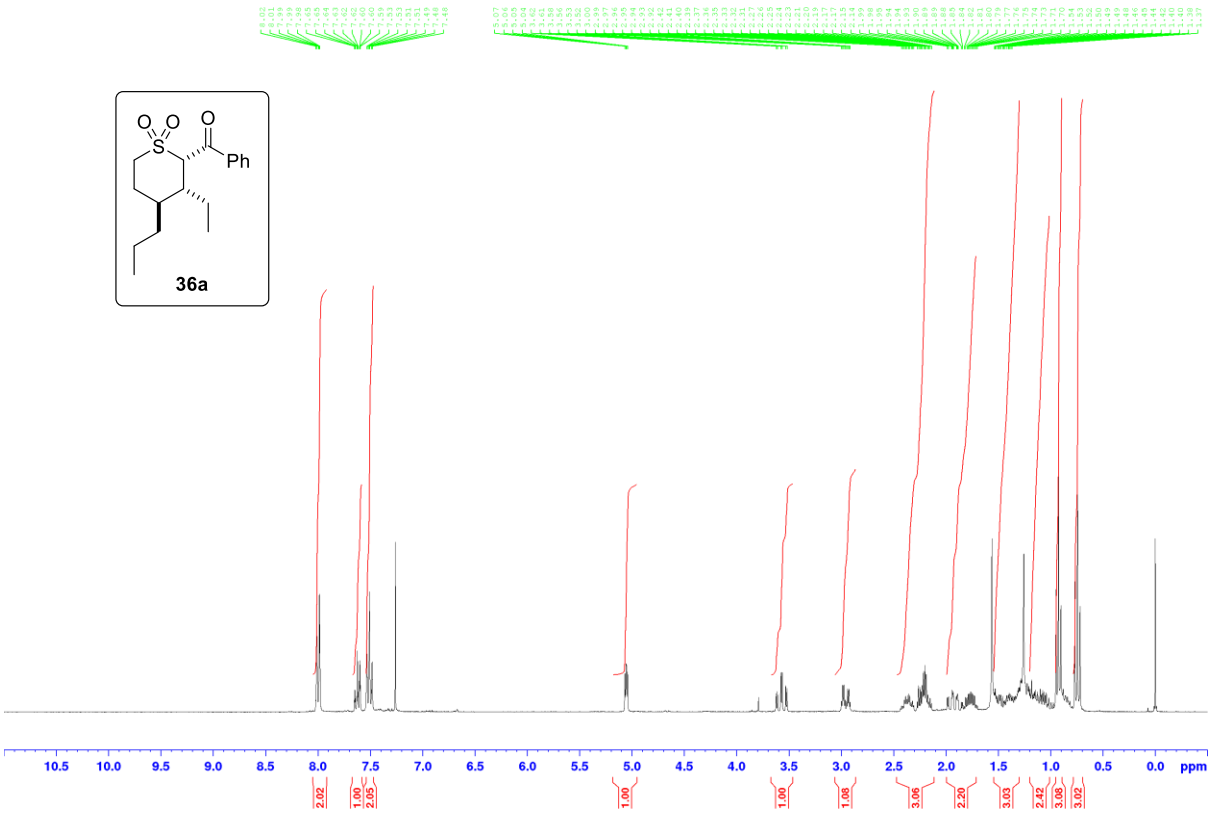

^{13}C (75.5 MHz, $CDCl_3$)

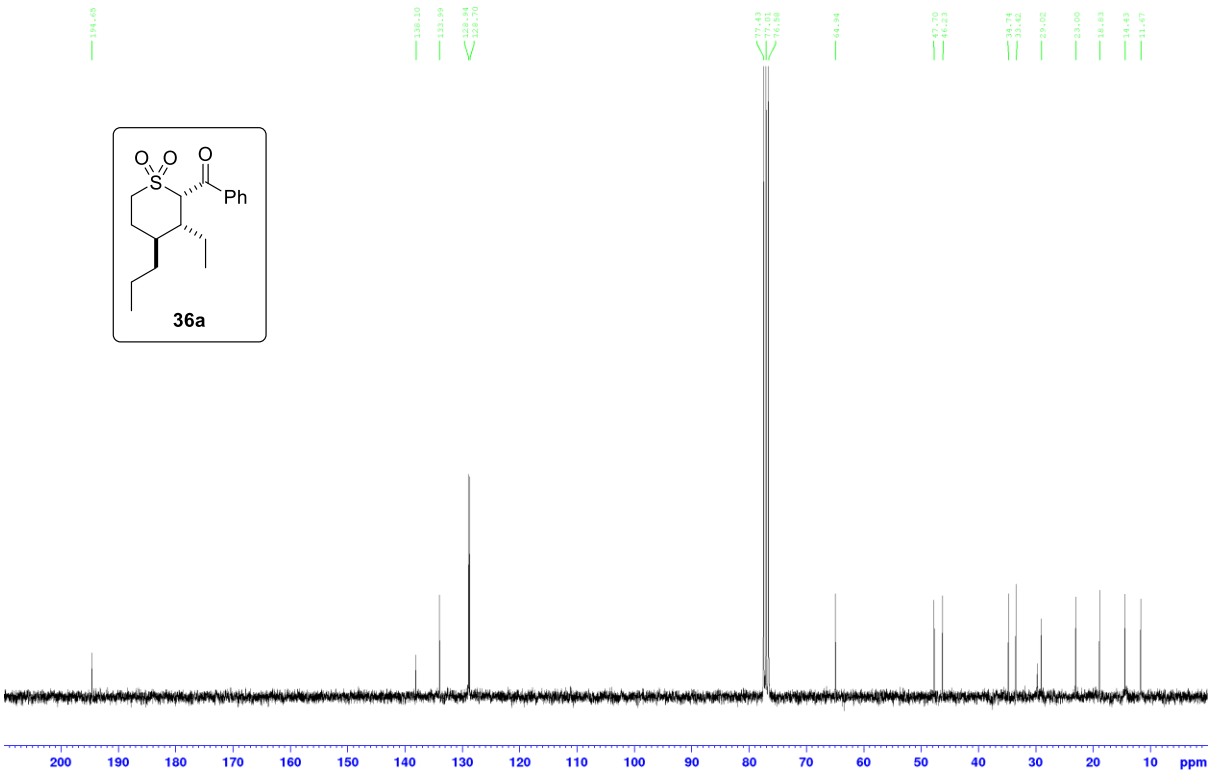

((2*R,3*R**,4*S**)-3-Ethyl-1,1-dioxido-4-propyltetrahydro-2*H*-thiopyran-2-yl)(phenyl)methanone (36b)**

^{1}H (300 MHz, $CDCl_3$)

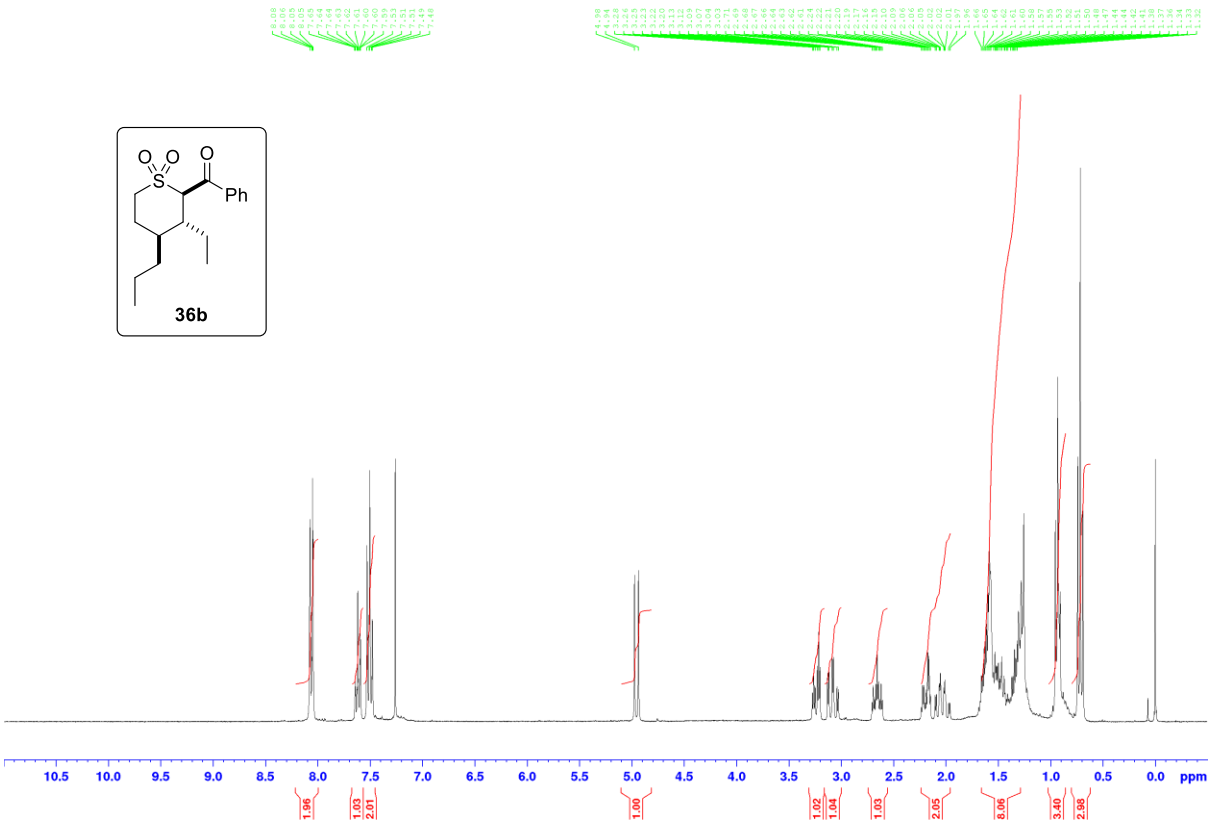

^{13}C (75.5 MHz, $CDCl_3$)

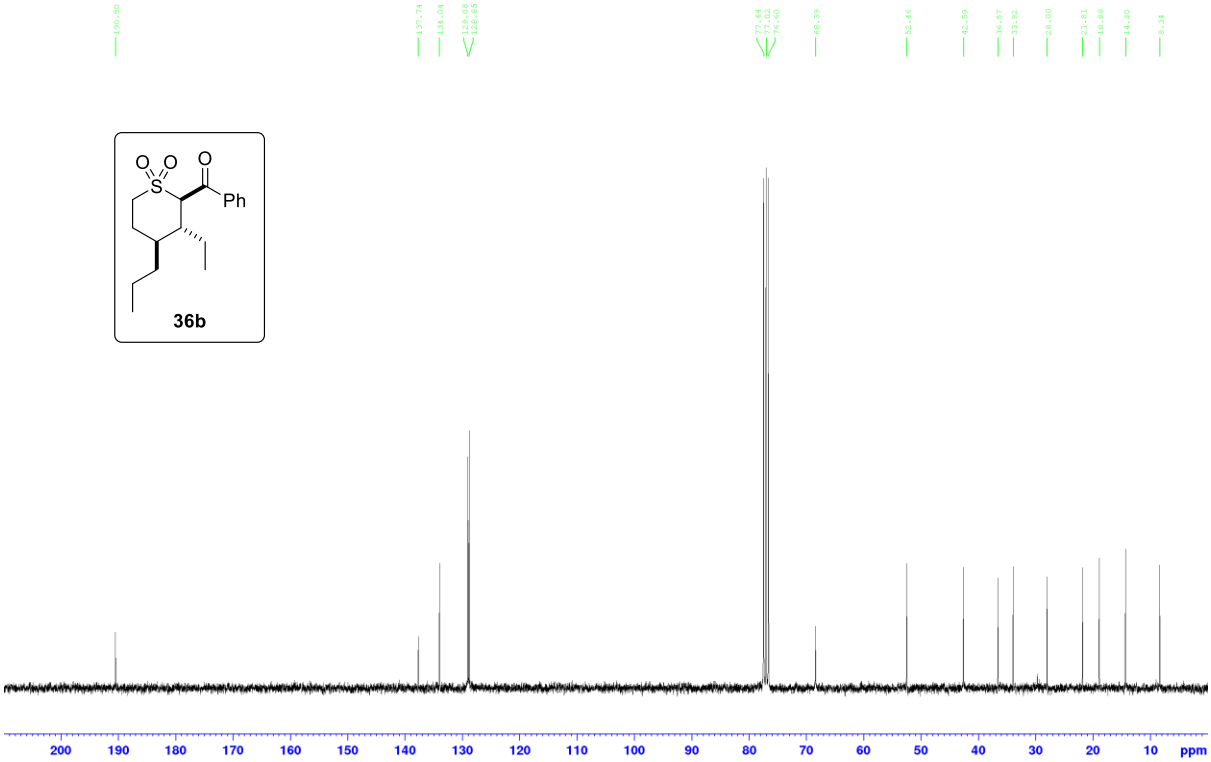

((2*S,3*R**,4*R**)-3-Ethyl-1,1-dioxido-4-propyltetrahydro-2*H*-thiopyran-2-yl)(phenyl)methanone (36d)**

^{1}H (300 MHz, $CDCl_3$)

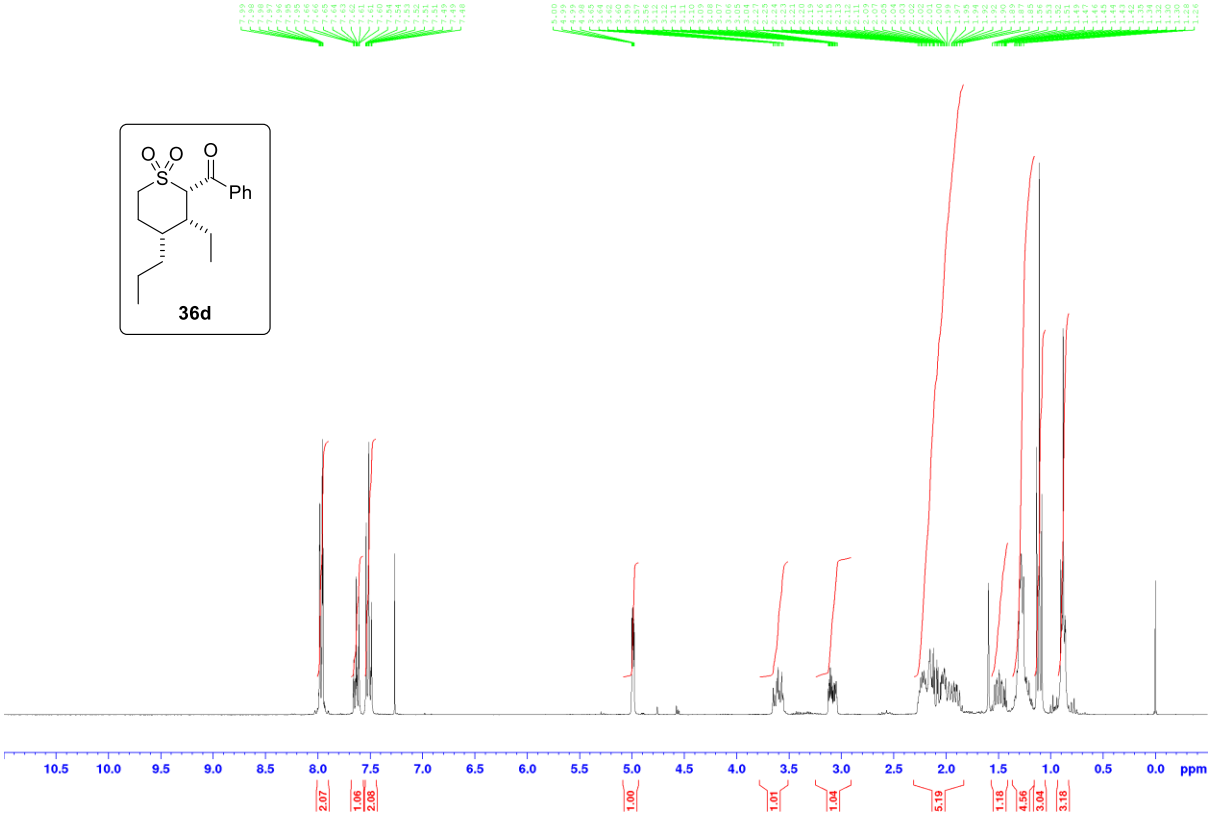

^{13}C (75.5 MHz, $CDCl_3$)

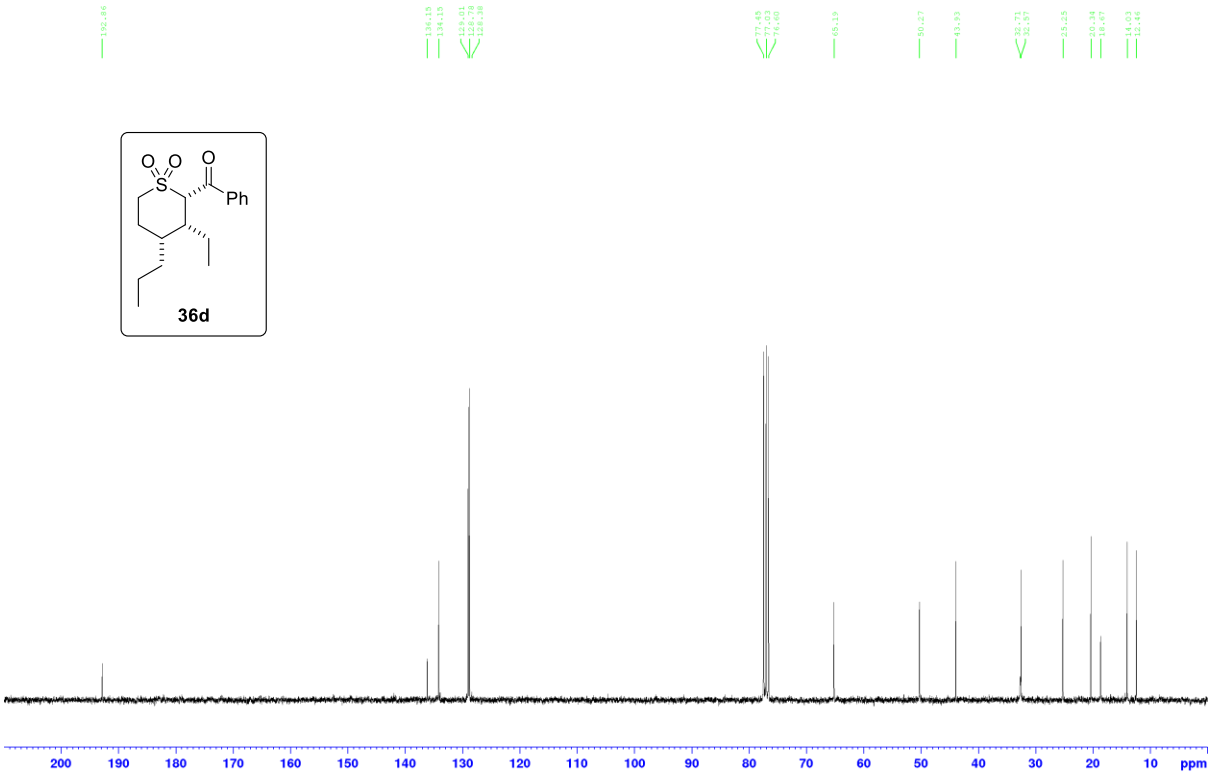

(1,1-Dioxido-3,3-dipropyltetrahydrothiophen-2-yl)(phenyl)methanone (37)

^{1}H (300 MHz, $CDCl_3$)

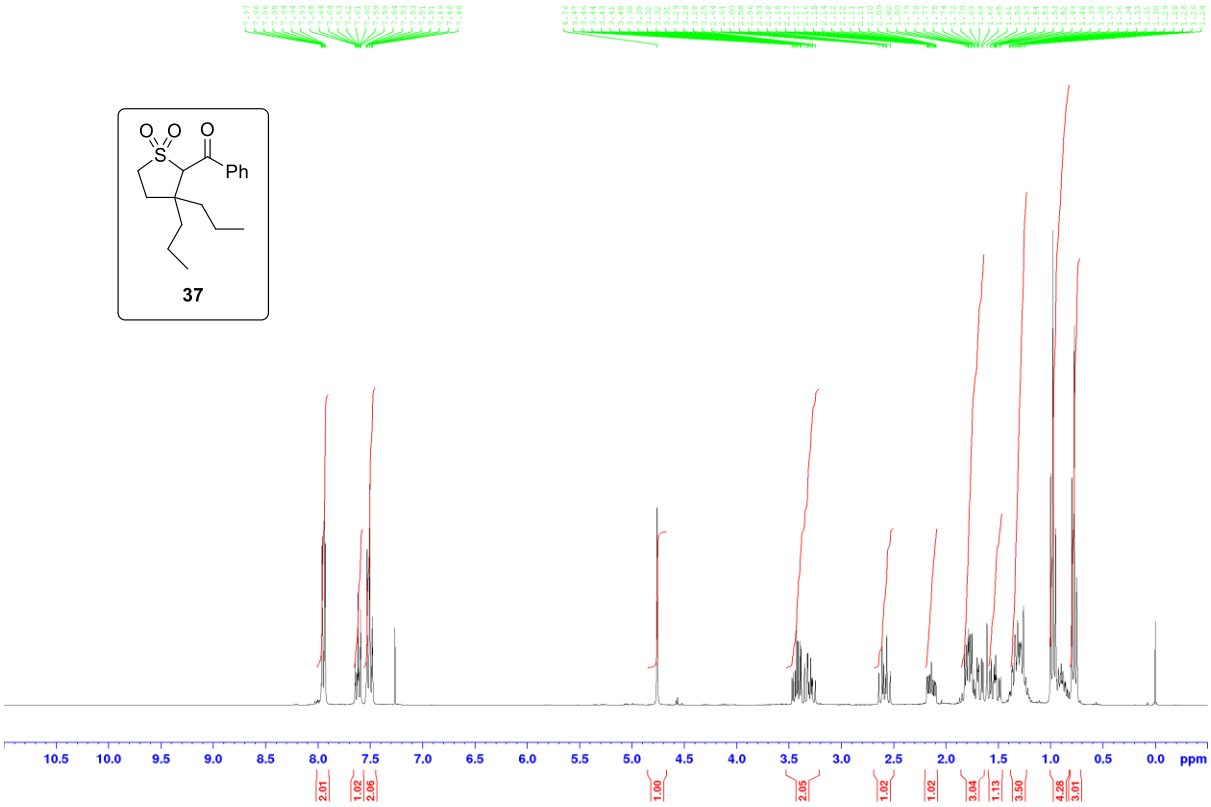

^{13}C (75.5 MHz, $CDCl_3$)

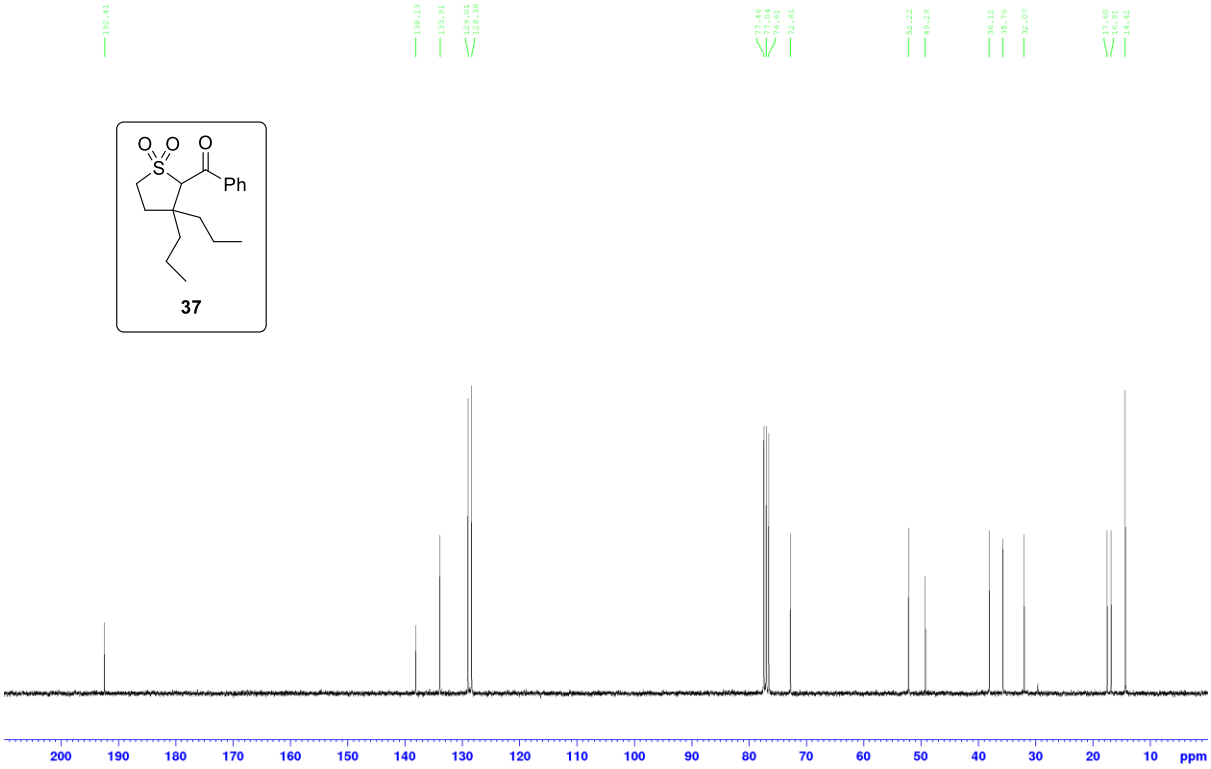

(1*S,3a*S**,7a*R**)1-(Phenylsulfonyl)octahydro-2*H*-inden-2-one (38a)**

^{1}H (300 MHz, $CDCl_3$)

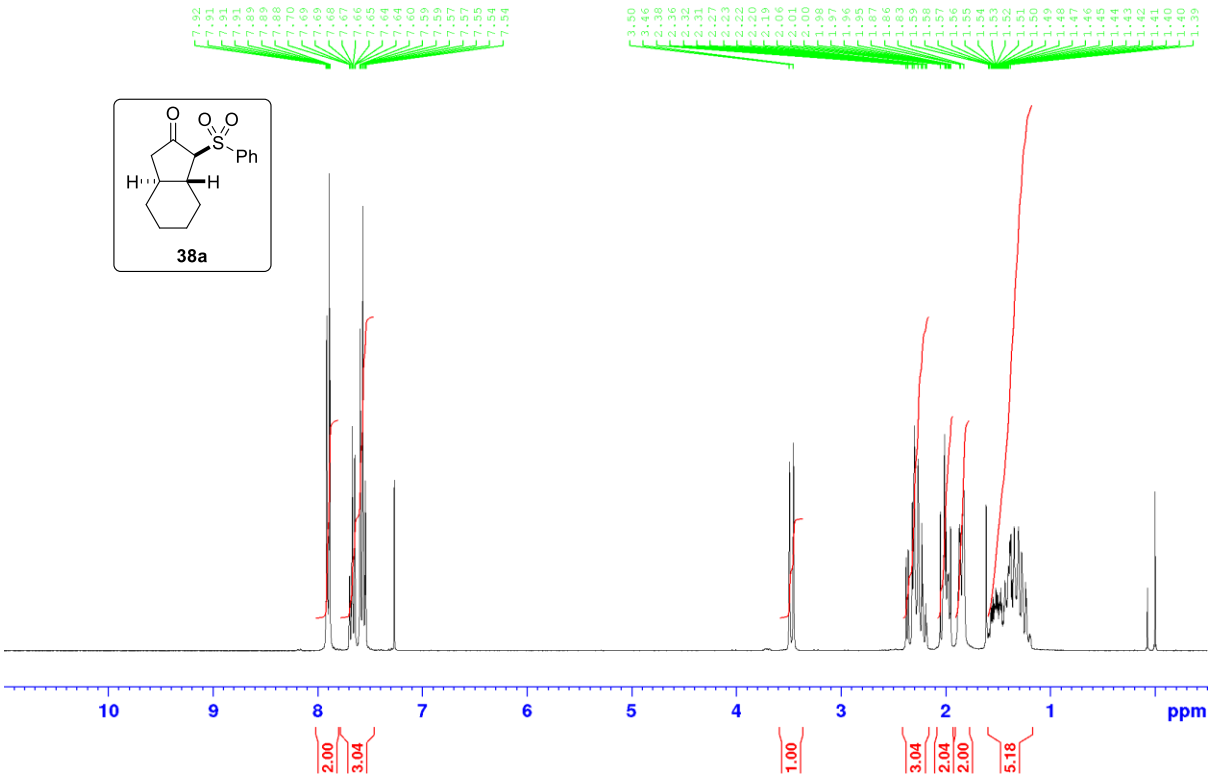

^{13}C (75.5 MHz, $CDCl_3$)

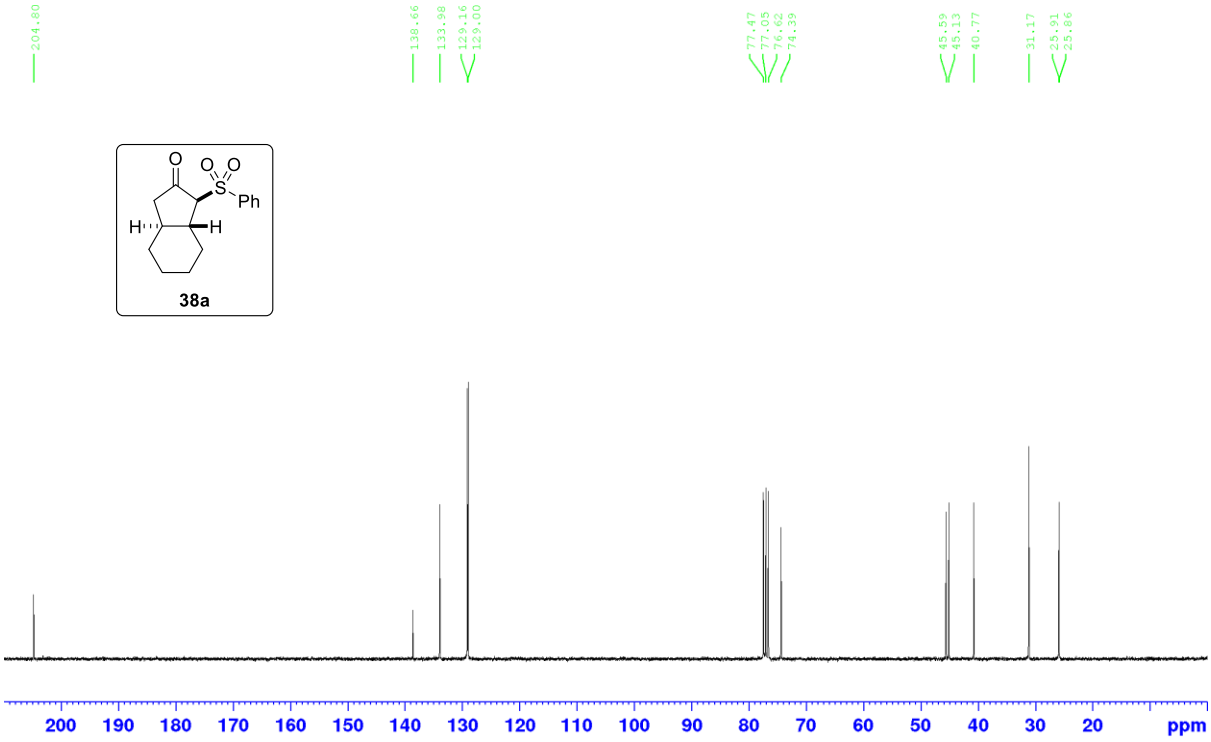

(1*S,3a*R**,7a*R**)1-(Phenylsulfonyl)octahydro-2*H*-inden-2-one (38b)**

^{1}H (300 MHz, $CDCl_3$)

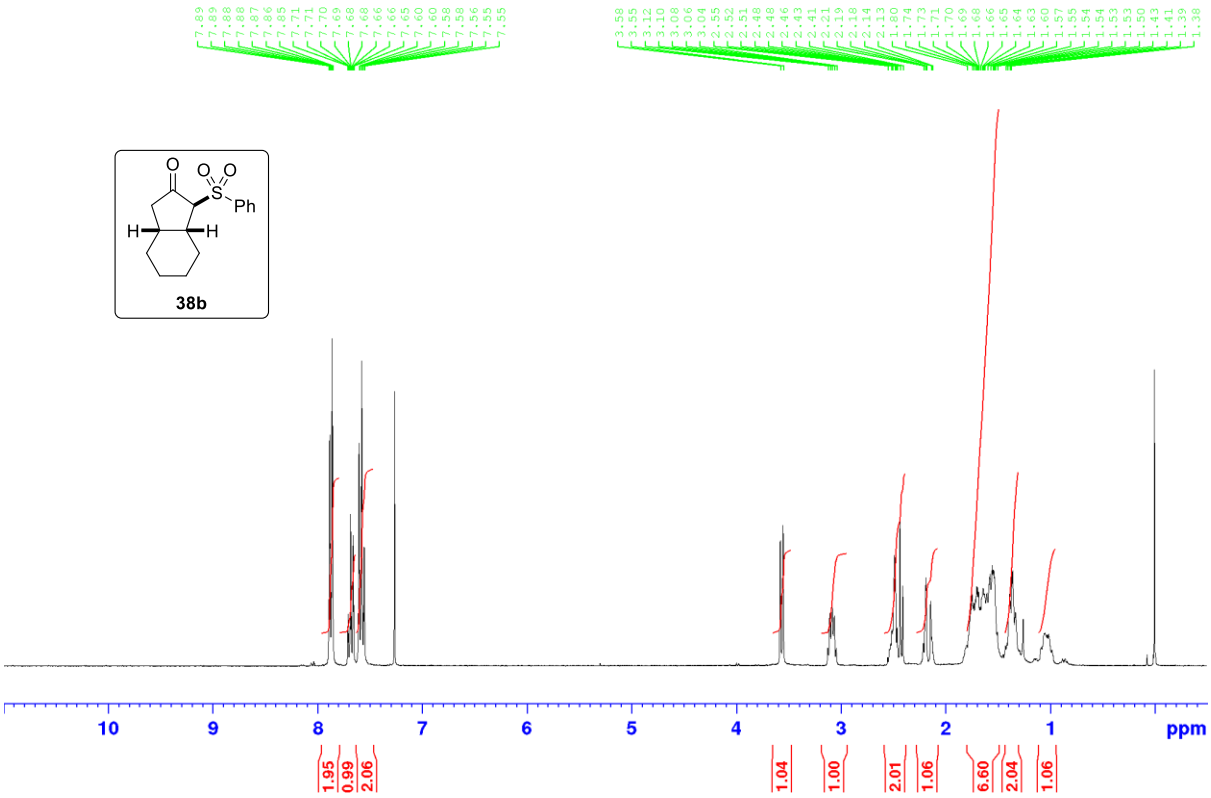

^{13}C (75.5 MHz, $CDCl_3$)

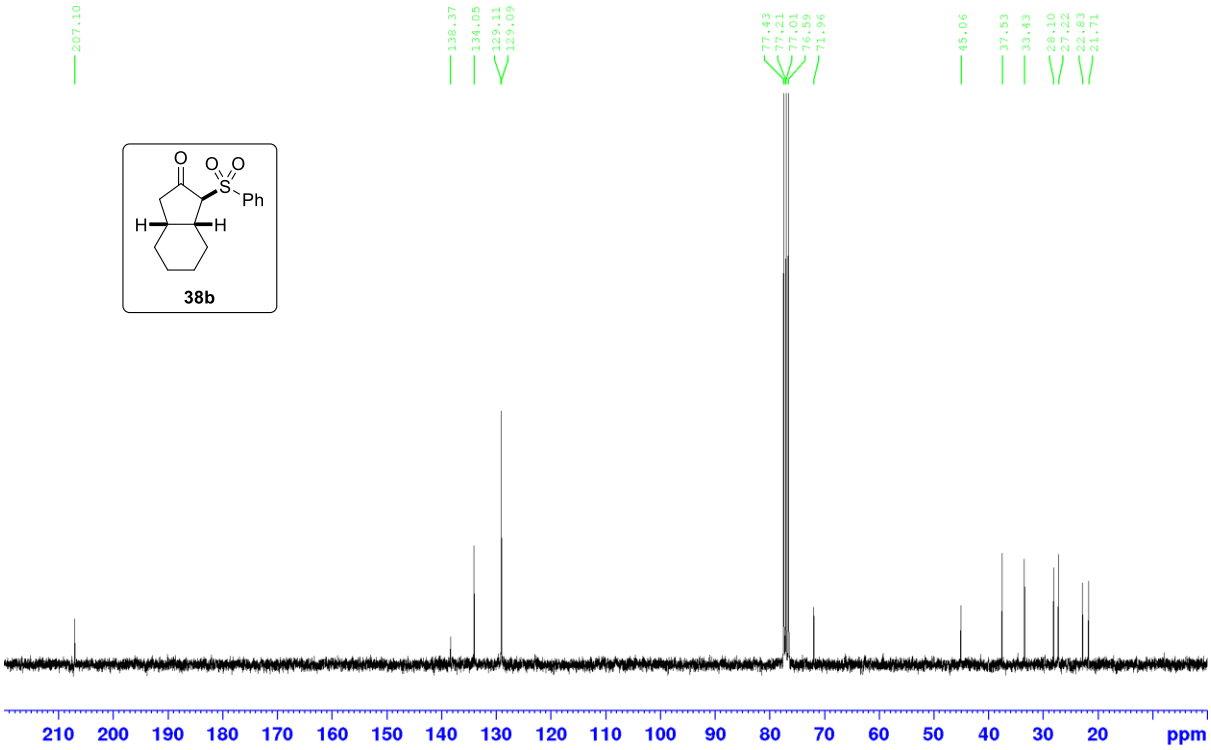

(2*S,3*R**,5*S**)3-Methyl-2-(phenylsulfonyl)-5-propylcyclopentan-1-one (39a)**

^{1}H (400 MHz, $CDCl_3$)

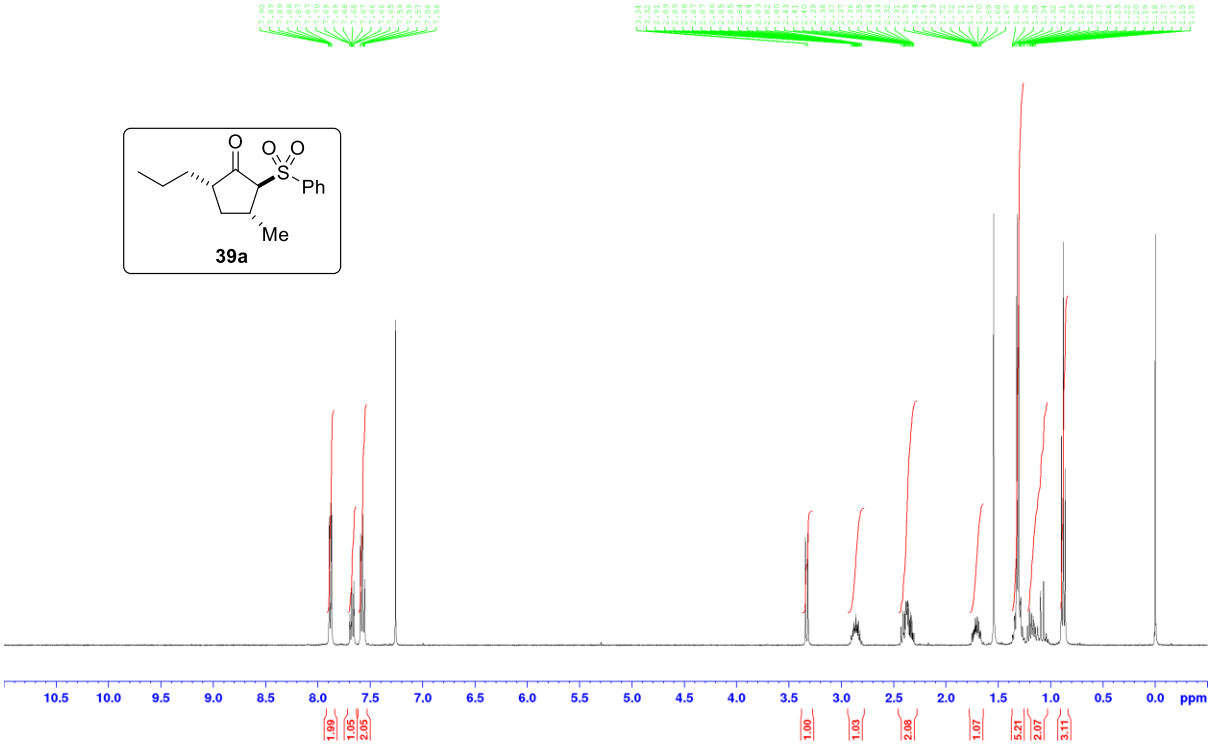

^{13}C (75.5 MHz, $CDCl_3$)

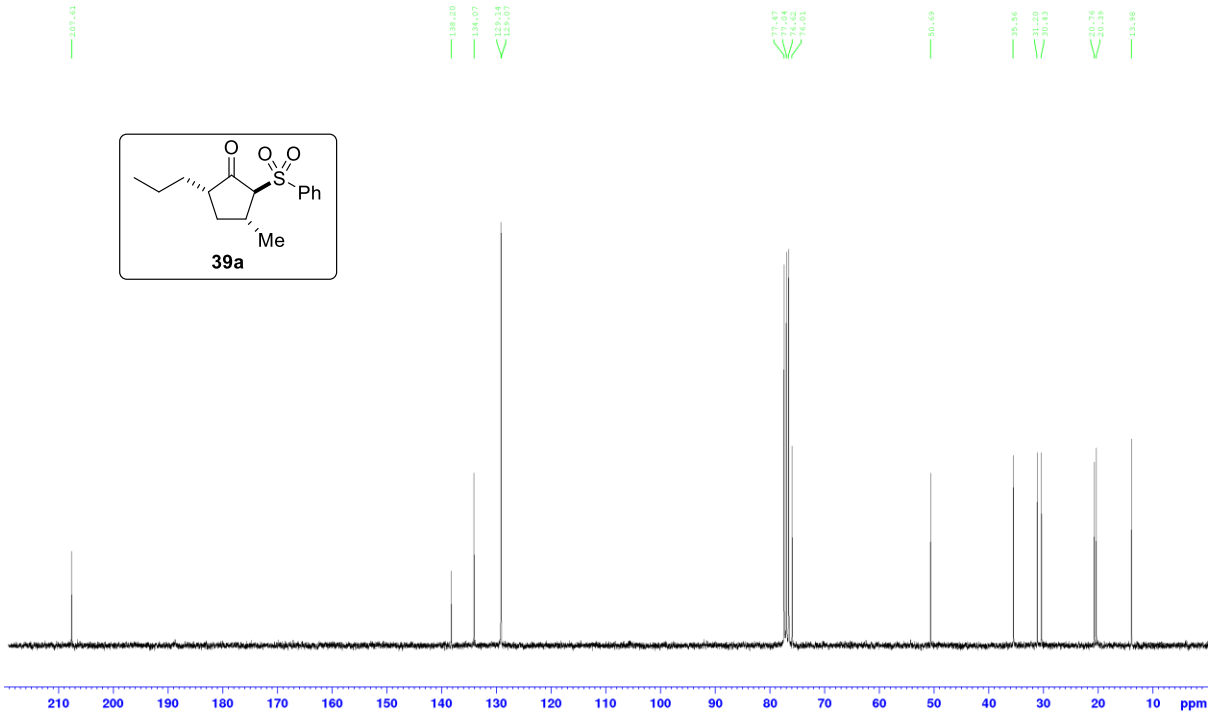

(2*S,3*R**,5*R**)3-Methyl-2-(phenylsulfonyl)-5-propylcyclopentan-1-one (39b)**

^{1}H (400 MHz, $CDCl_3$)

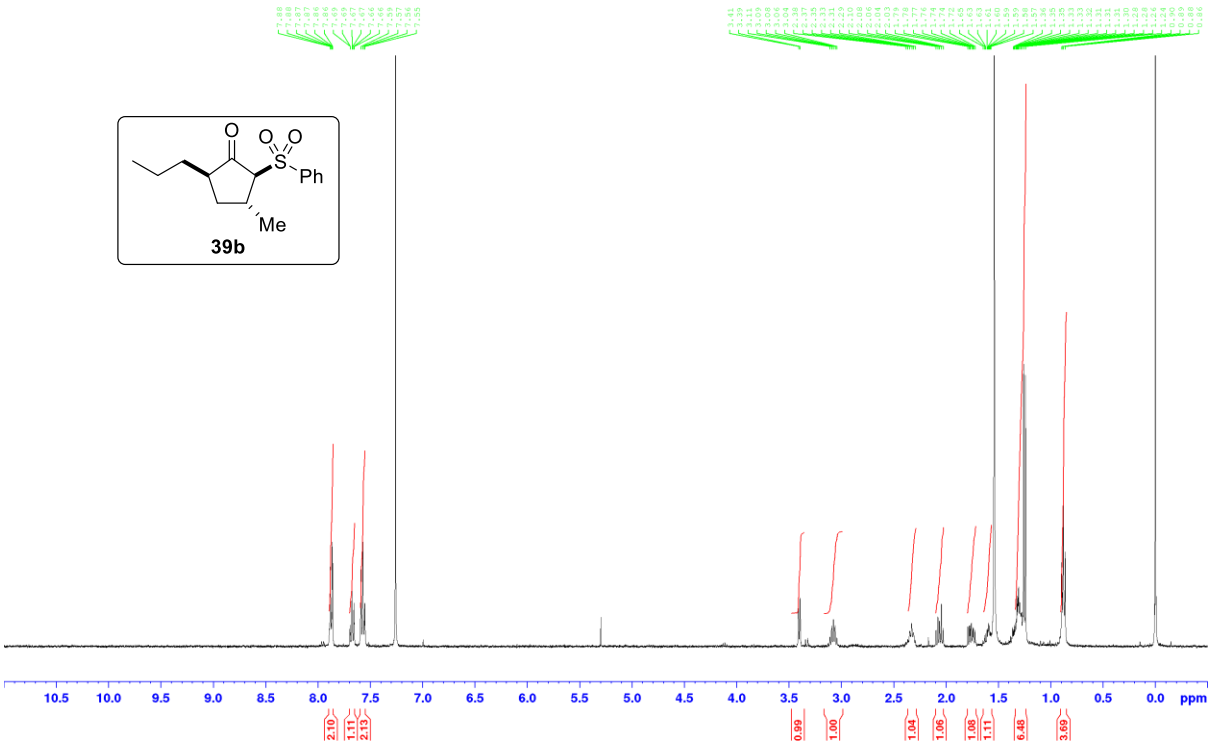
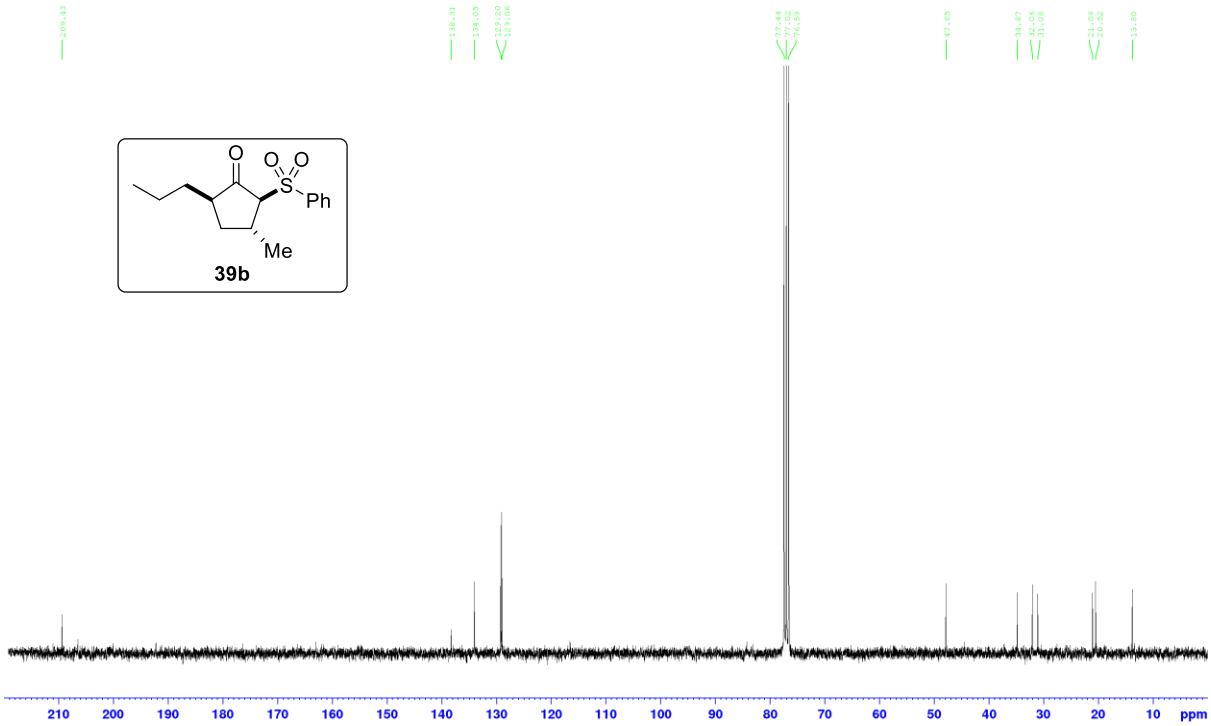
^{13}C (75.5 MHz, $CDCl_3$)